

**A COMPARATIVE STUDY ON THE EFFECT OF INTEGRIN SUBUNITS BETA  
ONE AND BETA THREE ON OSTEOBLAST IMPLANT INTERACTIONS**

IBRAHIM DUQUM, BDS

A thesis submitted to the faculty of the University of North Carolina at Chapel Hill in partial fulfillment of the requirements for the degree of Master in Science in the Department of Prosthodontics, School of Dentistry

Chapel Hill  
2008

Approved by:

Advisor: Dr. Lyndon F Cooper

Reader: Dr. Ingeborg De Kok

Reader: Dr. Zhengyan Wang

## ABSTRACT

IBRAHIM DUQUM: A Comparative study on the effect of Integrin subunits Beta one and Beta 3 on Osteoblast Implant interactions.

(Under the direction of Dr. Lyndon F Cooper, DDS, PHD)

**Background:** Integrin transmembrane receptors has emerged as central regulators of cell biomaterial interactions.

**Aim:** to explore the effects of integrin  $\beta 1$  and  $\beta 3$  receptors on osteoblast implant surface interactions in vitro.

**Materials and methods:** specific monoclonal antibodies were used to functionally perturb the respective integrin receptors before cell plating on CpTi disks of two distinct surface topographies. RT<sup>2</sup>Profiler<sup>TM</sup>PCR Arrays system, quantified the expression of a panel of osteogenesis related genes. Moreover, scanning electron microscopy was used to evaluate the effects of integrin functional perturbation on initial cell adhesion and spreading, in a surface and time dependent manner.

**Results:** data from both morphological and molecular studies showed that functional perturbation of both integrin subunits, significantly affected initial cell adhesion, spreading, and osteogenesis related gene expression, in a surface dependent manner.

**Conclusion:** Integrin  $\beta 1$  and  $\beta 3$  are involved in initial osteoblast adhesion and spreading on implant surface. Moreover, they mediate implant surface specific changes.

## **DEDICATION**

To my wife Lara, who sacrificed a lot for me to continue my graduate education.

To my daughter Selena, who is the joy of my life.

To my parents, who devoted their lives for the happiness and success of their children.

To my sisters, for all of their support and prayers.

## **ACKNOWLEDGEMENTS**

I would like to thank my mentor Dr. Lyndon Cooper for his valuable support and scientific guidance throughout the course of my residency. Also I would like to thank my other committee members, Dr. De Kok and Dr. Wang for their support and friendship. Specially, I would like to thank Dr. Juanli Guo, Dr. Gustavo Mendoca, and Ms. Sara Valencia for their tremendous help in the experimental and analytical part of this study.

This work was partially funded by a research grant from the Academy of Prosthodontics Foundation.

## TABLE OF CONTENTS

LIST OF TABLES.....	viii
LIST OF FIGRUES.....	ix
LIST OF ABBREVIATIONS.....	xi
LIST OF SYMBOLS.....	xiv

### CHAPTER

1. INTRODUCTION.....	1
1.1. Process of Osseointegration.....	3
1.1.1. Definitions.....	3
1.1.2. Peri-implant bone healing.....	4
1.2. Factors affecting Osseointegration.....	9
1.2.1. Dental implant materials and biocompatibility.....	10
1.2.2. Implant surface characteristics and its role in Osseointegration.....	14
1.2.2.1. Chemical composition of the surface of endosseous implants.....	15
1.2.2.2. Surface topography of endosseous implants.....	16
1.3. Models of Osseointegration research.....	19
1.4 The Osteoblast.....	21
1.4.1. Osteoblast cell culture systems.....	23

1.5. Role of cell adhesion in Osseointegration.....	25
1.6. Integrins as central regulators of osteoblast biomaterial interactions.....	27
1.6.1. Integrins and osteoblast implant interactions.....	31
1.7. Goals and specific aims.....	34
1.8. Hypotheses.....	35
2. MATERIALS AND METHODS.....	36
2.1. Commercially pure titanium surface preparation.....	36
2.2. Surface analysis.....	37
2.3. Cells and cell culture.....	38
2.4. Cell treatment with monoclonal antibodies and IgG control.....	38
2.5. Osteogenesis gene expression profiling with RT <sup>2</sup> Profiler™ PCR Arrays experiment.....	39
2.5.1. RNA isolation and first strand cDNA synthesis.....	41
2.5.2. Performing Real-Time PCR using RT <sup>2</sup> Profiler™ PCR Arrays.....	43
2.6. Cell binding experiment using scanning electron microscopy.....	44
2.6.1. SEM preparation.....	45
2.6.2. Quantitative and qualitative evaluation of osteoblast like cell adhesion, spreading and morphology of CP titanium surfaces.....	45
2.7. Statistical analysis.....	46
3. RESULTS.....	48
3.1. Atomic force microscopy surface analysis.....	48
3.2. Initial cell attachment and total cell count.....	49
3.3. Initial cell spreading and spread and round cell counts.....	51
3.4. Subjective evaluation of SEM images at higher magnification.....	57

3.5. RT <sup>2</sup> Profiler™ PCR Arrays results.....	59
3.5.1. Bone morphogenic protein superfamily.....	60
3.5.2. Bone matrix proteins.....	62
3.5.3. Growth factors.....	64
3.5.4. Transcriptional factors.....	67
4. DISCUSSION.....	70
4.1. Experimental model.....	71
4.2. Cell adhesion.....	75
4.3. Cell spreading.....	78
4.4. Relative expression of osteogenesis genes.....	79
4.4.1. Bone morphogenic protein superfamily.....	80
4.4.2. Bone matrix proteins.....	81
4.4.3. Growth factors.....	82
4.4.4. Transcriptional factors.....	83
4.5. Summary of findings and future recommendations.....	84
5. CONCLUSIONS.....	85
APPENDIX A.....	86
REFERENCES.....	88

## LIST OF TABLES

### Table

1.1. Factors affecting Osseointegration.....	9
1.2. Classification of dental implant materials.....	11
1.3. Characteristics of different implant surface scale levels.....	18
1.4. Length range of the different domains of $\alpha$ and $\beta$ chains of the integrin receptors.....	27
3.1. Surface parameter measurements as calculated by atomic force microscopy for smooth and rough surfaces.....	48
3.2. Functional group of genes and genes that presented significant changes among different experimental groups.....	59

## LIST OF FIGURES

### Figure

1.1. Osteoconduction.....	6
1.2. Osteoinduction.....	8
1.3. Schematic representation of integrin subunits and signal transduction.....	29
2.1. A flow chart representing the experimental design for The SEM and the RT <sup>2</sup> Profiler™ PCR Arrays experiments.....	40
3.1. Atomic force microscopy surface topography analyses representative of 50 µm X 50 µm areas of test surfaces.....	49
3.2. Mean number of cells at different time points among the different experimental groups on both smooth and rough surfaces.....	50
3.3. Clustered bar chart showing the mean number of cells among the Different experimental groups on both smooth and rough surfaces.....	51
3.4. Mean number of spread cells at different time points among the Different experimental groups on both smooth and rough surfaces.....	52
3.5. Clustered bar chart showing the mean number of spread cells among the different experimental groups on both smooth and rough surfaces.....	53
3.6. Mean number of round cells at different time points among the different experimental groups on both smooth and rough surfaces.....	54
3.7. Clustered bar chart showing the mean number of round cells among the different experimental groups on both smooth and rough surfaces.....	55
3.8. Examples of SEM images from different experimental groups and different time points that were used for data acquisition.....	56
3.9. SEM images at higher magnification (X 2000).....	58
3.10. Bar graph showing the difference in mRNA expression of Bmp Superfamily genes between anti-β1 and control groups on both smooth and rough surfaces.....	60

3.11. Bar graph showing the difference in mRNA expression of Bmp Superfamily genes between anti- $\beta$ 3 and control groups on both smooth and rough surfaces.....	61
3.12. Bar graph showing the difference in mRNA expression of bone matrix proteins between anti- $\beta$ 1 and control groups on both smooth and rough surfaces.....	63
3.13. Bar graph showing the difference in mRNA expression of bone matrix proteins between anti- $\beta$ 3 and control groups on both smooth and rough surfaces.....	63
3.14. Bar graph showing the difference in mRNA expression of selective growth factors between anti- $\beta$ 1 and control groups on both smooth and rough surfaces.....	65
3.15. Bar graph showing the difference in mRNA expression of selective growth factors between anti- $\beta$ 3 and control groups on both smooth and rough surfaces.....	66
3.16. Bar graph showing the difference in mRNA expression of selective transcriptional factors between anti- $\beta$ 1 and control groups on both smooth and rough surfaces.....	68
3.17. Bar graph showing the difference in mRNA expression of selective transcriptional factors between anti- $\beta$ 3 and control groups on both smooth and rough surfaces.....	69

## LIST OF ABBREVIATIONS

1. Alkaline phosphatase: ALP
2. Alpha-2-HS-glycoprotein: Ahsg
3. Aluminum oxide: Al<sub>2</sub>O<sub>3</sub>
4. Ameloblastin: Ambn
5. Analysis of variance: ANOVA
6. Atomic force microscopy: AFM
7. Average surface roughness: Ra
8. Biglycan: Bgn
9. Bone morphogenic protein: Bmp
10. Bone sialoprotein: BSP
11. Calcium hydroxide: CO<sub>2</sub>
12. Calcium Phosphate: CaP
13. Colony stimulating factor: Csf
14. Commercially pure titanium: cpTi
15. Degree celcius: °C
16. Deionized distilled water: ddH<sub>2</sub>O
17. Deoxyribonucleic acid: DNA
18. Diethylpyrocarbonate water: DEPC water
19. Epidermal growth factor: Egf
20. Extra cellular matrix: ECM
21. Extracellular signal-related kinase: ERK
22. Fgf: Fibroblast growth factor

23. Focal adhesion kinase: FAK
24. Growth differentiation factor 10: Gdf10
25. Hexamethyldisilazane: HDMS
26. Hydroxyapatite: HA
27. Immunoglobulin G: IgG
28. Integrin: Itg
29. Microgram:  $\mu\text{g}$
30. Microliter:  $\mu\text{l}$
31. Micrometer:  $\mu\text{m}$
32. Milliliter: ml
33. Millimeter: mm
34. Mitogen-activated protein kinase: MAPK
35. Msh homebox 1: Msx1
36. Nanometer: nm
37. Phosphate buffered saline: PBS
38. platelet-derived growth factor alpha polypeptide: pdgf $\alpha$
39. Polymerase Chain Reaction: PCR
40. Real Time Polymerase Chain Reaction: RT-PCR
41. Reverse transcriptase: RT
42. Ribonucleic acid: RNA
43. Root mean square roughness: RMS
44. Round per minute: rpm
45. Runt-related transcription factor 2: Runx2

46. Scanning electron microscopy: SEM
47. Sclerostin: Sost
48. SMAD family member 4: Smad4
49. Surface area: Sa
50. Threshold cycle: Ct
51. Titanium oxide: TiO<sub>2</sub>
52. Titanium plasma-sprayed: TPS
53. Transforming growth factor beta 1: Tgfβ1
54. Twist homolog 1: Twist 1
55. University Of North Carolina: UNC
56. Vascular endothelial growth factor: Vegf

## LIST OF SYMBOLS

1. Alpha:  $\alpha$
2. Beta:  $\beta$
3. Difference:  $\Delta$
4. Less:  $<$
5. More:  $>$

## **CHAPTER 1**

### **INTRODUCTION**

The introduction of new medical techniques intended to help patients in overcoming their disabilities and improve their quality of life has always been a priority. However, any novel concept should be based on solid scientific evidence to ensure long term success with minimal side effects. Osseointegration is a concept that was introduced by Branemark and his colleagues in the mid 1960's, and since then it has been a leading topic of interest. Based on this concept many new techniques and materials have evolved and are available to facilitate treatment and rehabilitation of patients.

Branemark placed his first intraoral implant in 1965. Despite having poor clinical results in the following 5 years with a success rate of about 50%, Osseointegration research continued to expand with the introduction of new surgical protocols and implant designs. Indisputable progress was made during the 1970's. This resulted in significant improvement and scrupulous documentation in the field of implantology leading to its general acceptance in Europe. Another important historical event in endosseous implant evolution was their introduction in North America in 1982. The last three decades were marked by expanded Osseointegration research, and tremendous increase in endosseous implants usage (9).

Orthopedics, bone-anchored hearing aids, craniofacial prosthetics, and Prosthodontics are some of the fields that were positively impacted and rejuvenated by the use of endosseous implants. Tissue integrated prostheses are currently a predictable and highly reliable

technique. Endosseous implant markets are growing very rapidly world wide (2, 80, 81). Endosseous implants are used to support and retain all kinds of prostheses in Dentistry and Maxillo-facial prosthetics from single tooth to prosthetic ears and noses. Moreover, they have a wide variety of uses in medicine particularly in the joint replacement field. The impact of those new treatment modalities on patient's life as well as on treatment planning procedures has been tremendous. Implant supported prostheses are the standard of care nowadays to replace missing teeth.

Despite the success, many unanswered questions remain unanswered. Studying the molecular aspects of Osseointegration is an important mode of its research. The tissues that oppose endosseous implants are multidimensional and represent diverse and dynamic living entities. Interfacial tissues include epithelium, soft fibrous connective tissues, and calcified bone (113). These living tissues are regulated at the molecular level. It is important to consider that the clinical success of endosseous implants is associated with the formation and maintenance of bone at implant surfaces (77). This research project aimed to understand some of the fundamentals of Osseointegration, and to reveal the importance of the integrin receptors in the early stages of this process. Integrins are a group of transmembrane proteins that mediate the interaction and cross-talking of the cells with extracellular matrix components and other cells. These receptors particularly integrin beta1 (Itg $\beta$ 1) and integrin beta3 (Itg $\beta$ 3) are thought to play a critical role in Osteoblast interaction with implant surface. Nevertheless, their exact role in this process is yet to be explicitly elucidated.

## **1.1. Process of Osseointegration**

Osseointegration was first described by a Swedish orthopedic surgeon PI Branemark. He discovered that commercially pure titanium (cpTi) when placed in a suitable preparation site in the bone could become fixed in place due to a close contact between the implant and surrounding healthy bone. Furthermore, he discovered that the integrated cpTi implants had the ability to transmit functional loads over an extended period without harmful effects either systemically or in the adjacent tissues.

### **1.1.1. Definitions**

Branemark and his colleagues defined Osseointegration as the direct functional and structural connection between bone and the load carrying implant (19). Another definition that gained popularity was introduced by Albrektsson and collaborators, they defined Osseointegration as the process in which clinically asymptomatic rigid fixation of alloplastic materials is achieved and maintained in bone during functional loading (11). These definitions describe the clinical observation of clinical stability of implants. They verify the success of Osseointegration at the anatomical and histological level. Radiographic and histological examinations can be used to insure the direct bone to implant contact without intervening fibrous connective tissue. However, these definitions do not explain the biological processes controlling bone formation and maintenance at the implant bone interface. Osseointegration is a dynamic process that involves complex cascade of cellular and molecular events. It results in bone formation at the bone implant interface (29). The maximum bone deposition is achieved by 3-4 months after implant placement. Bone

remodelling through constant resorption and new bone apposition is a continuous process that supports the long term functional integration of endosseous implants (77).

### **1.1.2. Peri-implant bone healing**

It is important to understand the cellular and molecular determinants of bone formation at the implant interface. These cellular and molecular activities can be targets for innovative strategies to improve and facilitate implant therapy (29). The process starts immediately after the surgical placement of the endosseous implants. This triggers the bone healing process that results in bone deposition around the implant. The events involved in bone healing at the implant interface recapitulate the events of wound healing. The process is dynamic and time related. After homeostasis, platelet activation, and blood clot formation, fibrinolysis occurs with the formation of loose connective tissue that supports the development of new blood vessels. This is followed by the recruitment, proliferation, and differentiation of osteoblastic cells. Eventually, the formation and the mineralization of a collagen matrix that surrounds the osteoblastic cells are completed, and woven bone is formed. The woven bone will be subsequently transformed to a more organized lamellar bone that is more resistant to physical strain. The time line of these series of events is about 4 months after implant placement. The formed bone is dynamic, vascular, living tissue that will continue to remodel through out life (29, 37).

Bone remodelling reflects the functional adaptation of the bone structure to load by changing the dimension and the orientation of the supporting elements (110). Remodelling starts with osteoclastic resorption, followed by lamellar bone deposition. Resorption and deposition are coupled in space and time. Bone deposition on the implant surface results

from two distinct mechanisms: *Distance Osteogenesis* and *Contact Osteogenesis*. These two mechanisms were described by Osborn and Newesley in 1980 and refer to the general relationship between forming bone and the surface of implanted material. Both involve the formation of new bone “De Novo Bone Formation” (38).

Distance Osteogenesis occurs when new bone is formed on the surfaces of old bone in the peri-implant site. The bone surface provides a population of osteogenic cells that lay down a new matrix that encroaches on the implant. The new bone will not form directly on the implant but on the old bone around the implant until the implant is surrounded by bone. In these circumstances, the implant surface will always be partially obscured from bone by intervening cells. Micro damage that occurs during implant site preparation will stimulate new bone formation. Bone necrosis usually occurs adjacent to osseous wound site despite optimal surgical technique. Distance Osteogenesis can be viewed as a reparative reaction to repair this necrotic bone. Thus this mechanism is expected to occur more in cortical bone healing as the bone is more compact (94).

Contact Osteogenesis occurs when bone is formed directly at the surface of the implant. It relies on the migration of differentiating osteogenic cells. These osteogenic cells are thought to be derived from undifferentiated perivascular connective tissue cells. They migrate through the fibrin matrix and the other structural proteins in the blood clot to the implant surface. The implant surface will be colonized and populated by cells that will differentiate and initiate bone matrix formation and bone deposition (38). Another term that is used to describe this process is *Osteoconduction* that is represented in Figure 1.1.

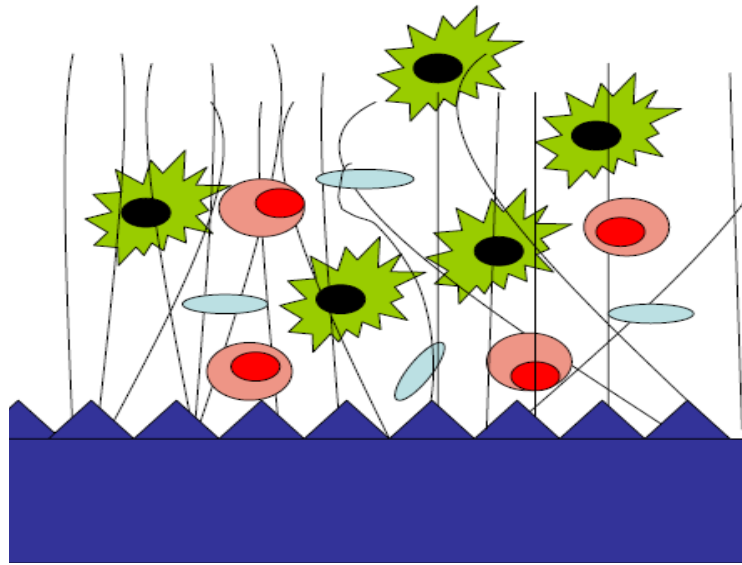


**Figure 1.1: Osteoconduction:** The dark blue area represents the implant and its surface. The black lines represent the fibrin that is adherent to the implant surface before cell migration. The red cells represent the red blood cells. The light blue objects represent the platelets. And the green cells represent the migrating differentiation osteogenic cells that will ultimately differentiate into osteoblasts. The osteoblasts will populate the implant surface and starts the formation of bone matrix and bone deposition.

Osteoconduction relies on the migration of differentiating osteogenic cells, connective tissue cells, blood cells, and platelets to the implant surface. Clearly, the implant design in general and surface in particular has a profound influence on Osteoconduction. It maintains the anchorage of the scaffold that the cells use to reach and populate the implant surface. We can assume that rough implant surface will promote Osteoconduction by both increasing the available surface area for fibrin attachment and by providing surface features with which fibrin could become entangled (38). The metabolic activity of the osteogenic cells is dependent upon an adequate blood supply. Distance and Contact osteogenesis together result in juxtaposition of bone to the implant surface. While they occur concurrently at all implant sites, a favorable result is more likely to be achieved with implant that optimizes contact osteogenesis, hence providing early stability of the implant.

Another important process associated with bone formation at implant surfaces is *Osteoinduction*. It involves the recruitment of mesenchymal stem cells to become osteoblasts. In addition to the differentiated bone cells, like Osteoblasts, Osteoclasts, and Osteocytes, bone and adjacent tissues contain a number of less differentiated cells. These undifferentiated cells are important for proper bone healing and anchorage of an implant. These cells can be recruited to form osteoprogenitor cells, and with time they will develop into differentiated bone cells with the correct inductive signal or stimulus (7). Several cytokines and growth factors work as inductive signals for osteoblast recruitment and differentiation. The undifferentiated mesenchymal cells can be transformed into a preosteoblast, a process which constitutes bone induction (figure 1.2). This process will result in alteration in cell number. Increasing bone formation at the implant surface in an osseous wound requires increased numbers of cells or enhanced biochemical activity (29). Osteoinduction is a basic biological mechanism that occurs regularly as an example in fracture healing and implant incorporation. The injury releases local, biochemical and biophysical messengers that guide the cells to respond in the proper manner. However, these molecular strategies can be a target to enhance osteoblastic proliferation and differentiation in an attempt to improve bone formation at implant surfaces.

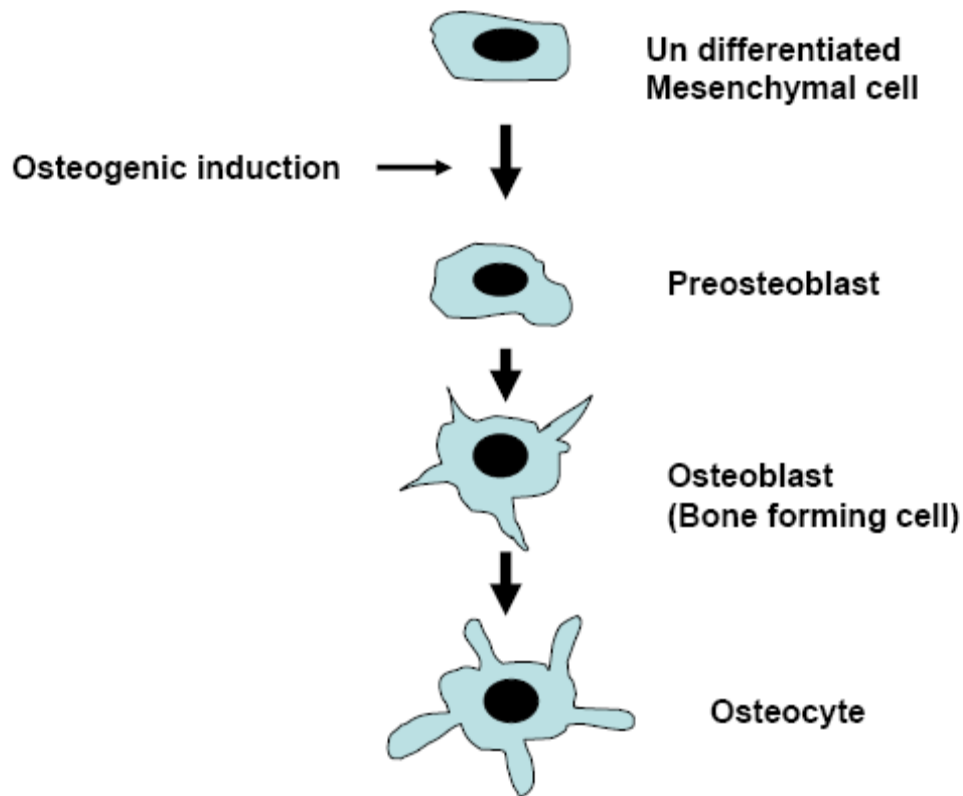


**Figure 1.2: Osteoinduction:** Adequate number of bone forming cells is needed for proper bone healing and repair. Undifferentiated cells are induced to become preosteoblasts that will form the majority of the newly formed bone.

Osteoinduction and Osteoconduction are combined in space and time around endosseous implants and result in new bone formation. This process starts by the deposition of a collagen rich bone matrix. This matrix is deposited by the committed mesenchymal cells in the implant vicinity. It contains large amount of type I and type III collagen, growth factors, and other mediators. It serves as a space filling scaffold for cell migration and osteoblastic differentiation. Simultaneously, endosteal bone formation is activated by committed osteoblastic cells differentiation into secretory osteoblast. This contributes to new bone formation by depositing a complex extracellular matrix that has the potential to support calcium phosphate deposition and matrix mineralization (59, 103). This will eventually result

in the formation of mature mineralized bone around the endosseous implant. Nevertheless, a 20-50 nm electron dense zone was found to separate the implant from the mineralized bone matrix (112).

## 1.2. Factors affecting Osseointegration

Several local and systemic factors can affect and assure the process of osseointegration. Albrektsson and his colleagues proposed six factors that affect osseointegration (6). These factors are presented in table 1.1.

<b>Table 1.1. Factors affecting Osseointegration</b>
<ol style="list-style-type: none"><li>1. Implant material</li><li>2. Implant design</li><li>3. Surface quality</li><li>4. Surgical techniques</li><li>5. Status of the bone</li><li>6. Implant loading conditions</li></ol>

However, other investigators classified these factors into three groups as following:

- A. Clinician related factors: this includes the surgical techniques involved in the implant placement, loading protocols as well as implant stability.
- B. Patient related factors; this includes all the systemic and local factors related to the patient health such as any systemic disease or habits that have an impact on osseointegration or the surgical outcome. Examples include Diabetes mellitus, radiation, and smoking. Furthermore, any local condition that affect osseointegration including bone quality and quantity and local anatomical factors.

C. Implant related factors: These factors include all aspects related to implant design such as implant length, width, and shape. Furthermore they also include implant materials, biocompatibility, and surface characteristic and composition. These factors were and continue being an important area of innovative research and technology to improve and enhance the out come of implant therapy.

Detailed discussions of all the factors that affect osseointegration are beyond the scope of this thesis. However, some of the important factors related to this project will be discussed in details such as, implant materials, biocompatibility, and surfaces.

### **1.2.1. Dental implant materials and biocompatibility**

Multiple biomaterials have been used to fabricate dental implants. These materials can be categorized into two different ways. First they can be classified according to their chemistry into (1) Metals. (2) Ceramics. (3) Polymers. These materials can also be classified according to the biological response they elicit when implanted and their long term interaction with the host tissue. From the biological response point of view, implant materials can be classified into (1) Biotolerant. (2) Bioinert. (3) Bioactive. Table 1.2 summarizes all the dental implant materials and their classification from both chemical and biodynamic point of views, according to classification proposed by Sykaras and collaborates (119).

**Table 1.2: Classification of dental implant materials**

<b>Biodynamic activity</b>	<b>Chemical composition</b>		
	<b>Metals</b>	<b>Ceramics</b>	<b>Polymers</b>
<b>Biotolerant</b>	-Gold -Cobalt-chromium alloys -Stainless steel -Zirconium -Niobium -Tantalum		-Polyethylene -Polyamide -Polymethylmethacrylate -Polytetrafluoroethylene -Polyurethane
<b>Bioinert</b>	- <b>Commercially pure titanium</b>  - <b>Titanium alloy</b>	- <b>Aluminum oxide</b> - <b>Zirconium oxide</b>	
<b>Bioactive</b>		-Hydroxyapatite -Tricalcium phosphate -Tetracalcium phosphate -Calcium pyrophosphate -Fluoroapatite -Brushite -Carbon: vitreous Pyrolytic -Carbon-silicon -Bioglass	

A biocompatible material is defined as the material that has the capability to exist in harmony with the surrounding biological environment (1). The different levels of biocompatibility emphasize the fact that no material is completely accepted by the biologic environment. To optimize biologic performance, artificial structures should be selected to minimize the negative biologic responses while ensuring adequate function. Biotolerant materials are those that are not necessarily rejected when implanted into the living tissue, but are surrounded by a fibrous layer in the form of a capsule. Bioinert materials allow close apposition of bone on their surface (Contact osteogenesis). Bioactive materials allow bone formation on their surface, but ion exchange with the host tissue leads to the formation of a

chemical bond along the interface (bonding osteogenesis). Both the bioinert and the bioactive materials are also called osteoconductive materials as they act as a scaffold allowing bone growth on their surfaces. Biotolerant, bioinert, and bioactive materials are all biocompatible by definition and result in a predictable host response in specific applications (93).

Commercially pure titanium cpTi (99.75%) is the most commonly used material for endosseous implants. This material has various degrees of purity (graded 1 to 4). This purity is characterized by oxygen, carbon and iron content. Currently most dental implants are made from grade 4 cpTi, as it is stronger than other grades (115). Commercially pure titanium has a high corrosion resistance and good biocompatibility. This is attributed to the oxide surface layer (titanium oxide) that forms upon contact with air or tissue fluids (60). Moreover, this oxide layer is rapidly formed with a controlled thickness and has the ability to repair it self instantaneously. The aforementioned features contribute to this material high passivity, making it the material of choice for endosseous implants fabrication. Other important characteristics of this material are its high mechanical strength and low density with a modulus of elasticity that is compatible with bone (119). However, it has low shear strength and wear resistance that renders it unsuitable for the use on articulating surfaces.

Titanium alloy (Ti6AL4V) is another material that is commonly used to fabricate endosseous implants. Titanium is combined with Vanadium and Aluminum to form the alloy. The main purpose is to increase the strength, improve fatigue properties, and to decrease weight of the fixture. Although the general perception was that cpTi and the titanium alloy will perform similarly. Some studies showed that the development of the bony interface is retarded with the alloy compared to the cpTi. Johansson and his colleagues performed a quantitative comparative study in rabbits. They measured the removal torque force needed to

loosen an implant from bone and used microscopic quantification of the amount of bone to implant contact. Although there was no difference after one month, the 6 and 12 month data showed that cpTi implants were more stable with a higher percentage of bone to implant contact in the cpTi group (58).

Other materials used to fabricate endosseous implants are ceramics. These materials can be bioinert or bioactive. The initial motive for the introduction of ceramics in implant dentistry was based upon the relative biological inertness they exhibit in comparison to metals. More emphasis has been given to bioactive and bioresorbable ceramics, materials that show signs of binding with bone and replaced by normal tissue over time. Hydroxyapatite (HA), tricalcium phosphate, and bioglasses are the more commonly used bioactive materials. They can make up the entire implant or applied in the form of coating onto the metallic core. Hydroxyapatite is a calcium phosphate material that has an apatite crystal. It is commonly used as coating to the implants. Being highly bioactive and osteoconductive, calcium phosphate coated implants demonstrated earlier and greater bone bonding at least in the initial stages (14, 22). Some investigators suggested that HA-coated implants may be valuable treatment modalities when placing implants (1) in type IV bone, (2) in fresh extraction sites, (3) in grafted maxillary and/or nasal sinuses, or (4) when using shorter implants (less than or equal to 10 mm)(16). Caulier and coworkers found improved performance with threaded calcium phosphate coated implants placed in less mineralized trabecular bone in goats although, the thickness of the coating decreased overtime(25). Hahn and Vassos showed success of 97.8% at 6 years with HA-coated cylindrical implants after prosthodontic rehabilitation. Their initial data showed a surgical success of 96.4% before prosthetic treatment (52). With all these promising observations there was still some

concerns and controversy regarding the use of calcium phosphate coated implants. Some of these concerns were reviewed by Biesbrock and Edgerton; they include microbial adhesion, osseous breakdown, and coating failure (16). Albrektsson evaluated the published in vitro and short and long term in vivo evidence on HA-coated implants and came out with the following concluding remarks.

1. The long term experimental evidence was very negative.
2. The early positive findings of higher bone to implant contact compared to titanium control either equalized or changed to a lower response with increasing time. (50%-75% more bone around the titanium control after 6 months or more)
3. These findings were not dependant on implant design (5).

From the previous discussion we can conclude that commercially pure titanium is the material of choice for the fabrication of endosseous implants. It has adequate physical and chemical properties, and provide long term efficacy.

### **1.2.2. Implant surface characteristics and its role in Osseointegration**

Implant surface characteristics play a crucial role in the short and long term success of endosseous implants (6). The literature shows that the rate and the quality of Osseointegration in titanium implants are related to their surface properties (68). Two categories of surface characteristics are cited as being important in tissue response to endosseous implants. One category includes the topographic and morphological characteristics that are referred to as surface roughness in many instances. The other category includes the chemical properties which include the chemical composition, charge, and hydrophilicity of the surface. It is hard to practically separate these two different categories,

because methods used to alter surface morphology frequently lead to changes in surface chemistry (91). Massaro and collaborates examined the surfaces of five commercially available titanium implants which are fabricated from cpTi using scanning electron microscopy and X-ray photoelectron spectroscopy. They found out that some surfaces have a variety of elements and chemical compounds not related to the metal composition that might affect the physico-chemical properties of the surface (76). The purpose of surface modification is to retain the key bulk properties of the material while modifying the surface to improve biocompatibility. Typically, this is done by altering the atoms or molecules on the existing surface chemically or physically, or by coating the existing surface with a different material.

#### **1.2.2.1. Chemical composition of the surface of endosseous implants**

Commercially pure titanium and titanium alloy as mentioned earlier are the two most commonly used materials for endosseous implants. These materials dominate because of the combination of mechanical properties and biocompatibility. The biocompatibility is related to the formation of the stable oxide layer, primarily titanium oxide ( $\text{TiO}_2$ ) that spontaneously forms when titanium is exposed to oxygen. Depending on the method of preparation and sterilization cpTi implants can have an oxide thickness of 5-6 nm (76). This oxide layer will determine the chemical properties of the implant rather than the implant material (60). The biomaterial surface interacts with water, ions, and numerous bio-molecules after implantation. The nature of these interactions, such as hydroxylation of the oxide surface by dissociative absorption of water, protein adsorption and denaturation, determine how cells and tissue respond to the implant (91). The composition and charges of the implant surface are critical for protein adsorption and cell attachment. Moreover, the surface chemical

composition also affects the hydrophilicity of the surface. Highly hydrophilic surfaces seem to be more favorable for interactions with cells, tissues, and biological fluids. A recent animal study found out that a more hydrophilic surface gave a higher bone to implant contact (21). Another important aspect of surface chemistry is the ability to manufacture a bioactive surface with chemical modifications of cpTi. These surfaces have the ability to show chemical bonding in addition to biomechanical anchorage (10). Calcium phosphate coated implants have the aforementioned features. However, as discussed in the previous section they have some potential problems that limit their clinical use. Other surfaces that have a bioactive potential include fluoridated OsseoSpeed implant surface by Astra Tech and the NanoTite surface by BIOMET 3i. Several in vitro and in vivo studies showed improved performance of these surfaces compared to controls (33, 43, 49, 88).

#### **1.2.2.2. Surface topography of endosseous implants**

Topographic and morphologic configuration of implant surface is another surface feature linked to implant behavior. The surface topography describes the degree of roughness the surface exhibits, and the orientation of the irregularities of the surface. Several advantages have been attributed to increased surface roughness: increased surface area of the implant adjacent to bone, improved cell attachment to the implant surface, increased bone presence at the implant surface, and increased biomechanical interaction of the implant with the bone. A potential disadvantage of rough surface is inflammation of the peri-implant mucosa if the rough surface is located at the trans-mucosal area (peri-implantitis). Nonetheless, there is no solid clinical evidence to support this (28). A recent meta-analysis by the Cochrane collaboration has not found any clinical evidence demonstrating the superiority of any particular implant surface or system. Moreover, it didn't identify any significant correlation

between surface roughness and periimplantitis (44). On the other hand, there are multiple other reviews that showed a paramount evidence of improved performance of rough surfaces both from in vitro and in vivo investigations (27, 28, 106). Surfaces are simply described as rough or smooth. This categorization is intended to segregate machined surfaces from others. This dichotomous categorization is not sufficient, it misrepresents the fact that machined surfaces are not smooth or polished and that rough surfaces can vary considerably in their features (28, 91). Several guide lines were proposed by Wennerberg and Albrektsson for the evaluation of surface topographies (123). Detailed descriptions of these parameters are beyond the scope of this discussion. However, surface roughness can simply be divided into different levels depending on the scale of the features. Table 1.3 summarizes the different roughness scale levels of endosseous implant surfaces with their advantages and potential risks (10, 68).

**Table 1.3: Characteristics of different implant surface scale levels**

<b>Roughness scale</b>	<b>Roughness (Sa)</b>	<b>Advantages</b>	<b>Potential risks and problems</b>	<b>Clinical usage and examples</b>
Macro-Rough	Millimeters to tens of microns	Mechanical interlocking between implant surface and bone ingrowth	Periimplantitis, ionic leakage	Threaded screws and macroporous surface treatment
Rough	> 2.0 $\mu\text{m}$	Improved bone to implant contact over turned implants. But weaker response than moderately rough implants	Periimplantitis	Plasma sprayed and HA-Coated implants
Micro-Rough (Minimally and moderately rough)	0.5-2 $\mu\text{m}$	Improved bone response with good clinical documentation		Most implants used today ( SLA, Tioblast, TiUnite...etc)
Nano-Rough (nano-scale)	Nanometers to millimeters	Protein adsorption and adhesion of osteoblastic cells	Reproducible surface roughness is difficult	Nanosclae implants (NanoTite, Osseospeed )
Machined (turned)	0.5-1 $\mu\text{m}$	Longest clinical documentation	Longer time for integration and higher failure rate in low bone quality	Turned implants mostly before 1995, Osseotite

By careful interpretation of the information provided in table 1.3 we can conclude that moderately rough surfaces with microtopographic features have some clinical advantages compared to smoother turned and rougher plasma-sprayed surfaces(10). Moreover, nano-rough surfaces seem to positively impact Osseointegration and look very promising. Although the clinical advantage of micro-rough surface is evident, the exact mechanisms behind its role in Osseointegration are still not clear especially at the cellular and molecular levels. Multiple theories were proposed to explain the enhanced performance of microtopographic surfaces on how they increase the rate or early Osseointegration. Some

investigators highlighted the ability of micro- textured surfaces in promoting early bone healing and their effectiveness in retaining fibrin during the critical osteogenic cell migration stage of Osteoconduction (38). Another important effect of the micro-textured surfaces on the early events of endosseous bone healing was attributed to its ability to promote blood clot retention. These observations emphasize the importance of implant surface microtopography in orchestrating the biological cascades of early peri-implant endosseous healing (38). The effect of implant surface on cellular attachment and osteoblastic proliferation and differentiation is another step in the early events that orchestrate peri implant healing. There is growing evidence to support the use of micron-scale cp titanium implant surfaces. Several studies showed that micro- rough surfaces produce the topography and the morphology that is favored by the cells to enhance cell adhesion, osteoblastic differentiation, and matrix mineralization (65, 75, 100, 101). Nevertheless, the exact mechanisms and pathways that govern cells interaction with surfaces of different topographies remain unknown.

### **1.3. Models of Osseointegration research**

The initial concept of Osseointegration stemmed from vital microscopic studies of the bone and marrow response to blood flow through titanium chambers (18). These microscopic in vivo studies that were performed by Branemark and his collaborates in the early 1960s are considered the standard by which all other clinical implant research is compared (111). Following the development of this concept, new basic and clinical research efforts have emerged to reexamine this paradigm. Osseointegration research developed very rapidly during the last 3 decades to cover all clinical and scientific aspects of this phenomenon. Different research models were used in the endosseous implant research. These models can be simply classified into two categories; in vivo and in vitro models.

1. **In vivo models:** these models include randomized human clinical trials as well as prospective and retrospective human cohort studies. Implant survival and success rates, patient satisfaction, complications, tissue response, loading protocols are some of the aspects that can be evaluated in such studies. Another integral part of the in vivo models includes the animal studies. This in vivo module is an essential step in the testing of endosseous implants prior to their clinical use in humans. Any new implant material or surface has to be tested in animal to ensure its biocompatibility, mechanical stability and safety (89). A clear advantage of the in vivo models, is the ability to mechanically tests and evaluate the osseointegration process. A number of biomechanically applied tests were utilized to compare and contrast the strength and integrity of the bone to implant contact on different implant materials, designs, surfaces. The pull or push out test and removal torque test are examples of those in vivo models of osseointegration (77). In vivo animal studies are also beneficial in the evaluation of the bone tissue interface, particularly at the microscopic level and the molecular levels. These will provide important information to answer some of the fundamental question about Osseointegration, and extrapolate results from in vitro studies to the in vivo situation (87).
2. **In Vitro Models:** in vitro tests cover a wide range of endosseous implant research. Biomaterial testing, biomechanical tests as well as cell culture model are examples of in vitro models of Osseointegration research. An important aim of in vitro models of biomaterial research is to investigate biological responses to biomaterials. And materials used for implantology are no exception. There are two broad categories of use for in vitro systems in investigating cell responses to biomaterials:

(1) fundamental studies on the mechanisms of cell response, and (2) modeling physiological function in vivo (20). The value of using cell cultures to model physiological function in vivo is controversial. Cells must surely experience different environments in vitro and in vivo, which open critics that they may well be irrelevant to cell responses in vivo. Nevertheless, cell culture models offer unique opportunities to investigate biological responses to biomaterials. They provide a useful tool for investigating cell and matrix interaction with alloplastic materials and their surfaces. Processes, such as cell attachment, motility, proliferation, differentiation, and protein synthesis can be investigated (31, 30). Culture models have the advantage of allowing more controlled conditions especially at the cellular level and help reducing animal experiments. The osteoblast cell culture model is the most widely used cell culture mode in osseointegration research. This model proved to be very successful in investigating the aspects of bone formation and osteoblast implant interactions. Different osteoblastic cell lines with different state of phenotypic maturation have been utilized to study osteoblastic response to different implant material and surfaces (31, 17). The following section will review the characteristics of the osteoblast, its functions, and the various cell lines and culture systems available, with particular emphasis on the osteoblast-like mouse non-transformed MC3T3-E1 cell line.

#### **1.4. The Osteoblast**

Bone is a mineralized tissue that confers multiple mechanical and metabolic functions to the skeleton. Bone is composed by cells and an extracellular matrix which becomes

mineralized by the deposition of calcium hydroxyapatite, giving the bone rigidity and strength. Bone has three distinct cell types: the osteoblasts, or bone-forming cells, the osteoclasts, or bone-resorbing cells, whose functions are intimately linked, and the osteocytes, which are osteoblasts entrapped within lacunae. In order to balance bone formation and resorption in healthy individuals, osteoblasts secrete factors that regulate the differentiation of osteoclasts and osteocytes secrete factors regulating the activity of both osteoblasts and osteoclasts. Bone is constantly being resorbed by osteoclasts and then replaced by osteoblasts in a process called bone remodelling, which is tightly synchronized by local and endocrine factors (42). It is apparent that any imbalance in this process will lead to problems. In endosseous implant therapy the clinical success is related to the formation and maintenance of bone at the bone implant interface (77). The formation of bone at the implant surface is associated with the osteoblast metabolic and secretory activities (39). Nevertheless, the maintenance of bone at the interface is related to the long term balance between bone resorption and reformation.

Osteoblasts are mononuclear, not terminally differentiated, specialized cells that form bone. They arise from osteoprogenitor cells of mesenchymal origin and terminally differentiate to osteocytes. These cells have a set of distinctive characteristics that include the capability of forming a collagen rich matrix (osteoid) and mineralizing it, which results in the formation of calcified bone. When they are active they have a large Golgi apparatus and an abundant rough endoplasmic reticulum. In addition, they form tight junctions with adjacent osteoblasts and have regions of plasma membrane specialized in vesicular trafficking and secretion (23). Moreover, osteoblasts are autocrine regulatory cells that synthesize and deposit growth factors into the bone matrix and respond to these factors when they are

released during bone resorption phases of repair and remodelling. Moreover, osteoblast commitment, differentiation, and function are governed by several transcription factors, resulting in expression of phenotypic genes and acquisition of osteoblast phenotype (29, 73).

Several ways can be considered to control osteoblastic activity at implants, such as; osteoblast recruitment, attachment, proliferation, and differentiation. These aspects of osteoblast physiology are interrelated represent potential targets for clinical improvement of bone formation at implant surface (29).

#### **1.4.1. Osteoblast cell culture systems**

Osteoblast cell culture model is widely used in osseointegration research. As mentioned earlier this model provides an invaluable opportunity to investigate aspects of bone formation and cell biology in the laboratory. Several cell lines and culture systems have been developed and utilized in investigating the osteoblast activity and interaction at implant surface. Cooper and his collaborates categorized these cells according to their origin into

1. Primary cultures such as bone marrow stromal cells, intramembranous bone, or trabecular long bone.
2. Nontransformed clonal cell lines such as the mouse osteoblast like cells MC3T3-E1.
3. Osteosarcoma cell lines such as, the human osteosarcoma MG63 cells and the rat osteosarcoma ROS 17/2.8 cells.
4. Intentionally immortalized cell lines such as the rat calvarial cell line RCT-1(31).

This classification reflects the origin of cell lines, but not the characteristics of each model. These different cell lines represent different states of phenotypic maturation in the osteoblast lineage and have substantially different levels of homogeneity (17). Nevertheless, in cell culture studies the significance and validity of each system depends on the question to be

addressed, and the biochemical and molecular properties of the system (31). The osteoblast cell lines most commonly used to study the interaction of cells with implant surface include; the human osteosarcoma MG63 cells, the mouse osteoblast like MC3T3-E1 cells, the rat osteosarcoma osteoblast like ROS 17/2.8 cells, and the fetal rat calvaria FRC cells (17).

In the present investigation the mouse osteoblast like MC3Ts-E1 cells were used. These cells were originally cultured from newborn mouse calvaria. They have unique features that make them a good model to study the mechanisms of biological calcification, osteoblast differentiation, and matrix mineralization. The cells have a low alkaline phosphatase (ALP) activity in the growing state; however, the enzyme activity will increase in the confluent state. This osteogenic cell line has the capacity to differentiate into osteoblasts, osteocytes, and deposit minerals in vitro. The cells are capable of showing different stages of growth and development under cell culture conditions (79). The pattern of osteogenesis that this cell showed in vitro is similar to intramembranous ossification pattern in vivo. The cell morphology in the growing state resembles a fibroblast. Nevertheless, when the cells grow they start to resemble the osteoblasts in morphology and they can grow in layers (117). In intramembranous ossification the process is triggered by the aggregation of undifferentiated mesenchymal cells into layers or membranes. These cells synthesize and secrete a loose organic matrix that regularly contains blood vessels, fibroblasts, and osteoprogenitor cells. The osteoprogenitor cells differentiate into osteoblasts and commence the assembly of osteoid (uncalcified bone matrix). This matrix will then mineralize side by side with vascular ingrowth to form woven bone that matures into lamellar bone. Similar observations were noted by Sennerby and his collaborates around titanium implants placed in rat cortical bone (104). Another important feature of the non-transformed osteoblast like cells is that they

demonstrate a well-defined inverse relationship between cell differentiation and proliferation (114). These unique characteristics make this osteogenic cell line an excellent model to study the interaction between the osteoblastic cell and the extracellular matrix (ECM) in vitro.

### **1.5. Role of cell adhesion in Osseointegration**

The cell adhesion to extracellular matrix (ECM) proteins and implant surface is a crucial and decisive step in peri-implant bone healing process. It is well documented that the cell adhesion to the ECM proteins controls complex biological processes, through specific and dynamic regulation of cell behavior (35, 40, 53). This critical step is important in implementing an appropriate cell response to the implanted material surfaces.

Biocompatibility of implanted materials is intimately related to the cell behavior in contact with them and mostly to cell adhesion to their surface (13). Many studies for example showed that the interactions of osteoblasts with their surrounding ECM are essential for skeletal development, homeostasis, and for the maintenance of mature osteoblastic phenotype (57, 82, 118, 120).

After the surgical placement of the endosseous implant, undifferentiated mesenchymal stem cells approach the implant material from the bone marrow lining as well as blood and tissue fluids. It is extremely critical for these cells to populate the implant surface and to continue to proliferate. Moreover, it is even more important for these cells to be committed to the osteoblastic lineage and to mature into functional osteoblast to ensure successful integration of the endosseous implants. Multiple mechanisms, growth factors, and transcriptional factors are involved in this process. However, it is well established that initial cell attachment and subsequent cell adhesion to the implant surface play a critical role in

these imperative mechanisms (63, 84, 121, 127). The attachment, adhesion and spreading of cells are considered the first phase of cell/material interactions and the quality of this phase will profoundly impact subsequent central processes such as cell proliferation, migration, and phenotypic differentiation(79).

Cell adhesion can be divided into two phases. The attachment phase and the adhesion phase. Cellular attachment occurs spontaneously with short-term events, like physicochemical linkages between the cell and the substrate. The adhesion phase occurs in the long term and it involves ECM proteins, cell membrane proteins (adhesion molecules), and cytoskeletal proteins. Cytoskeletal proteins are cellular proteins that mediate the interaction between the cell membrane receptors and the actin filaments that maintain the cell shape. Moreover, these proteins are involved in signal transduction (13, 107). The function of these proteins will be discussed in more details in the following section.

Cells do not adhere directly to the implant surface. The adhesion is mediated through certain proteins that adsorb to the surface. This process starts almost immediately after the placement of endosseous implants (97). The preparation of the implantation site will result in hematoma which will initiate the clotting cascade. Nevertheless, before the blood clot is formed, a number of extracellular matrix proteins will adsorb on the surface of the implant from the blood and interstitial tissue fluids at the wound site or from cellular activity at the peri-implant region later on (47, 90, 124). This layer of adsorbed proteins converts the foreign surface into a biological environment that the cells can sense and respond to. The composition of this layer is a key mediator to cell behavior. The presence of particular adsorbed proteins can stimulate a beneficial cell response, stimulating wound healing and tissue integration, whereas proteins in an unrecognizable state may signify a foreign

substance to be removed or isolated (124). As mentioned earlier most of the proteins composing this layer are adsorbed from the ECM. Examples of ECM proteins that mediate the adhesion of osteoblastic cells with biomaterial surfaces include: fibronectin, vitronectin, type 1 collagen, osteopontin, bone sialoprotein, and thrombospondin. These proteins have chemotactic or adhesive properties, notably because they contain a ligand sequence of three amino acids; Glycine, Aspartic acid, Arginine (Arg-Gly-Asp) that is commonly referred to as RGD sequence. This ligand is specific to the fixation of cell membrane receptors like integrin that has emerged as a central regulator of cell-biomaterial interactions (13, 47, 107, 124).

### **1.6. Integrins as central regulators of osteoblast biomaterial interactions**

Integrins are a large family of transmembrane receptors that bind specifically to ECM proteins. An individual integrin is composed of two non-covalently bonded subunits  $\alpha$  and  $\beta$ . Therefore they are categorized as being heterodimeric proteins (53). This transmembrane receptor family was first recognized by Hynes (55). Each subunit is a glycoprotein that has a relatively large extracellular domain and short cytoplasmic domain and a transmembranous domain.

**Table 1.4: Length range of the different domains of  $\alpha$  and  $\beta$  chains of the integrin receptors**

	<b>Length of extracellular domain</b>	<b>Length of cytoplasmic domain</b>	<b>Length of transmembranous domain</b>
<b>Alpha chain</b>	1008-1152 amino acids	22-32 amino acids	20-29 amino acids
<b>Beta chain</b>	770 amino acids	20-50 amino acids	26-29 amino acids

Table 1.4 presents the length range of the different domains of both  $\alpha$  and  $\beta$  chains of integrin receptors. The extracellular parts of the  $\alpha$  and the  $\beta$  chains interact with each other, creating a functional heterodimer. Both subunits contain disulfide bridges protecting them from proteolysis (107). Mammals contain 18  $\alpha$  and 8  $\beta$  subunits that combine to produce at least 24 distinct heterodimers that have been recognized up to date (41, 53). These proteins mediate the interaction between the cells and their surrounding ECM as well as the interaction between the cells with each other with the help of other transmembrane receptors like cadherins. Moreover, these receptors work as linker proteins to mediate the interaction and adhesion of the cells to biomaterial substrates. Integrins are versatile proteins. They span the cell membrane and act as an interfacier between intra- and extra- cellular compartments. They act as a bidirectional allosteric signaling machine that transmits inside-out and outside-in signals. They have the ability to translate the attachment of external ligands to internal information which induces vital cellular mechanisms. They interact with the ECM and the external environment through their extracellular domains, and with components of the cell cytoskeleton and signaling molecules through their intracellular domains. It is believed that this cross talking regulates important cellular functions, such as; cell adhesion, motility, shape, growth, apoptosis, proliferation and differentiation. (13, 36, 41, 54, 107). Figure 1.3 is a simple schematic representation of the integrin  $\alpha$  and  $\beta$  subunits and their interactions with ECM proteins through specific binding ligands and the subsequent signal transduction phenomenon that regulates cellular functions.

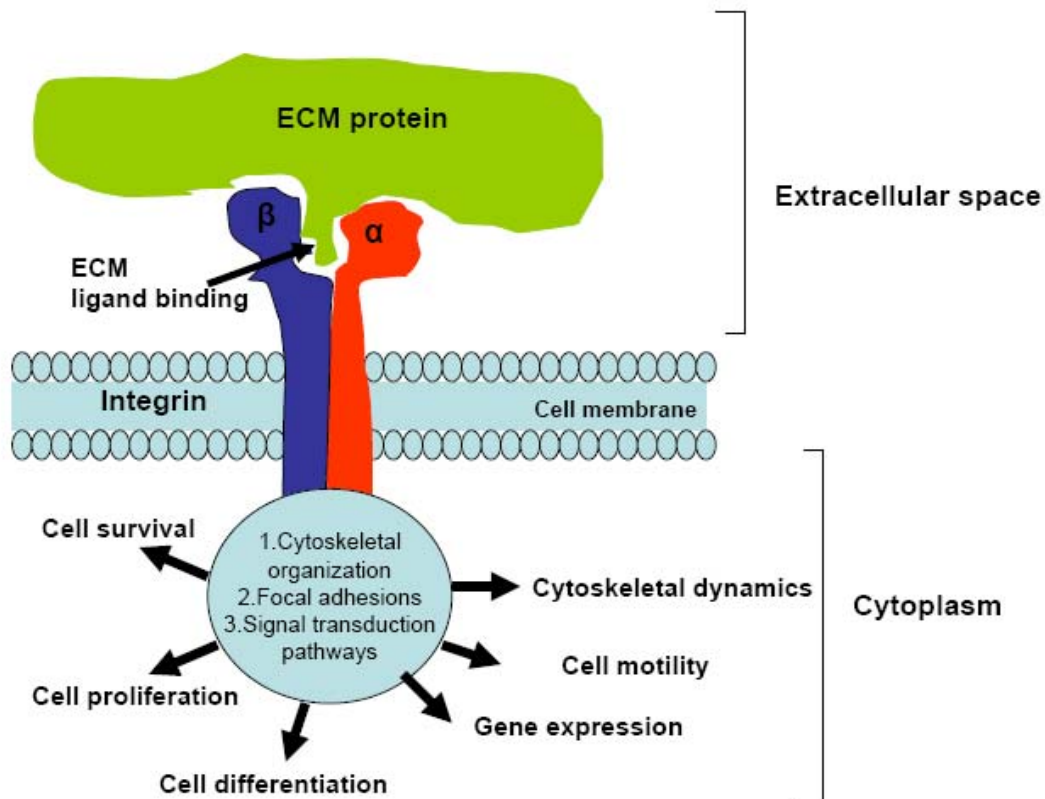


**Figure 1.3.: Schematic representation of integrin subunits and signal transduction:**

Integrins bind to specific ECM proteins through specific binding ligands. This activates the integrin. The cytoplasmic domain will activate special cytoskeletal structural proteins that are part of complex signaling network. These signal transduction pathways will dictate some of the vital mechanisms of cell life such as motility, proliferation, differentiation, and phenotypic gene expression.

The sites of adhesion between tissue culture cells and substrate surfaces are called focal contacts. Once the integrins are bound to their ligands they move laterally in the plane of the membrane to form these specialized clusters or the focal adhesions sites. The external faces of these contacts are formed by the integrins. On the internal face special cytoskeletal proteins are clustered they include; talin, paxillin, vinculin, and tensin. Many proteins will interact with these cytoskeletal components to form special attachment organelles and signaling centers. Protein kinases, in particular the focal adhesion kinase (FAK) and

phosphatases are crucial enzymes that mediate the phosphorylation of signaling molecules activating specific signaling pathways. FAK is a potent signaling molecule with important kinase activity. In osteoblast for instance, specific integrin activation results in clustering of FAK that starts a cascade of kinase dependant reactions ending in the activation of extracellular signal-related kinase (ERK), a mitogen-activated protein kinase (MAPK). MAPK is an enzyme that has been implicated in the control of osteoblast-specific gene expression and matrix mineralization (36, 99). Moreover, the activation of integrin also results in the organization of the cytoskeleton through rearrangement of actin filaments, subsequently affecting cell shape, spreading, adhesion and mobility (13, 41, 53, 107).

Regulation of integrin activity also depends on the ECM protein ligand. Signals from different ECM ligands will activate different signaling pathways (24). This mode of activity is referred to as outside- in signaling. Through this mode of regulation it is suggested that implant surface features have the potential to alter the signaling of an integrin receptor. Thus, blocking of the integrin function with specific antibodies or soluble peptides will inhibit the integrin function and have an impact on the cellular activities regulated through this receptor (82, 83, 116). Nevertheless, integrins can be present on cell the membrane in an inactive state where they do not bind ligands and do not signal. The activity of the integrin may depend upon the ligand, as well as on the integrin. For instance, ligand clustering and conformational changes might modulate integrin binding. Nevertheless, some integrins might require a second binding site (synergy site) for optimal function. The activation of the synergy site might be regulated by intracellular signaling pathways. This mode of integrin activation is referred to as inside-out signaling. Furthermore, integrins have the ability to cross-talk with other integrins on the cell surface as well as synergistically cooperating with growth factors

receptors. These synergistic mechanisms play a crucial role in regulation of cellular processes such as cycle progression and cell migration (36, 107). The complexity of integrin regulation and its diverse function make it a fascinating field of study for cell and molecular biologists. In osseointegration research for example, there are some findings that still lack a comprehensive explanation; particularly, the roles of integrins in osteoblast- implant interaction and its ability to mediate surface specific changes.

### **1.6.1. Integrins and osteoblast implant interactions**

It is well documented that the osteoblast interaction with material surfaces is of fundamental relevance and contributes to the clinical success of implants (29, 35, 50, 131). Certain implant surface characteristics have been attributed in modulating osteoblast behavior, mainly surface chemistry and topography. As discussed earlier, the osteoblast does not interact directly with the implant surface. This interaction process is mediated by a layer of adsorbed proteins on the surface and by the integrin transmembrane receptors on the cell surface. Nevertheless, the exact role that integrins play in mediating osteoblast adhesion to the implant surface and its effect on subsequent cell spreading, motility, proliferation, differentiation, and matrix mineralization is not completely understood. When examining the behavior of osteoblastic cells on surfaces with different roughness controversial results were reported. Differential integrin expression was noted on different substrate materials, topographies, and among different cell lines (67, 92, 109). It is hard to compare results from in vitro studies because of the lack of consensus on the proper representation of implant surface topography (28). Moreover, the use of different cell lines, and the use of different substrate materials are important factors that contradicts the comparison of in vitro studies results.

Many integrin subunits are expressed by osteoblasts. The literature shows that the osteoblast expresses integrin subunits  $\alpha 1$ ,  $\alpha 2$ ,  $\alpha 3$ ,  $\alpha 4$ ,  $\alpha 5$ ,  $\alpha 6$ ,  $\alpha v$ ,  $\beta 1$ ,  $\beta 3$ , and  $\beta 5$  (15, 34, 50, 109). However, integrin expression by osteoblasts is variable and can differ with the stage of development of the osteoblast as well as the cell source (107). Several integrin heterodimers are involved in osteoblast interaction with their experimental substrate. The main classes include  $\alpha 1\beta 1$ ,  $\alpha 2\beta 1$ ,  $\alpha 5\beta 1$ , and  $\alpha v\beta 3$  integrin heterodimers. The integrins  $\alpha 1\beta 1$ ,  $\alpha 2\beta 1$  are the main collagen binding integrins. Integrin  $\alpha 1\beta 1$  has higher affinity to the basement membrane type IV collagen. While, integrin  $\alpha 2\beta 1$  binds to type 1 collagen which is the dominant bone matrix protein. Gronthos and collaborates, documented that  $\beta 1$  integrins are the most predominant adhesion receptor utilized by osteoblast-like cells to adhere to the collagen matrix particularly  $\alpha 2\beta 1$  heterodimer(51). Moreover, several other studies indicated that the interaction of  $\alpha 2\beta 1$  with type I collagen is crucial for signal induction of osteoblastic differentiation and matrix mineralization (57, 82, 99, 118, 120, 128). On the other hand, the  $\alpha 5\beta 1$  pair is selective for fibronectin, and this interaction has also been identified as central to osteoblastic function (48, 83, 84, 116). The integrin pair  $\alpha v\beta 3$  can bind to multiple ligands including vitronectin, fibronectin, osteopontin, and bone sialoprotein (BSP) (13, 98, 107). The coordinated expression of  $\beta 3$  integrin with BSP which is a well documented determinant of osteoblast differentiation and bone formation gives the illusion that this selective  $\beta 3$ -integrin/BSP adhesion mediated signaling may play a significant role in osteoblast morpho-differentiation (32, 98). Nevertheless, unlike  $\beta 1$  integrin the role of  $\beta 3$  integrin in osteoblast biomaterial interaction has not been extensively investigated. The ability of certain integrin heterodimers to interact selectively with a certain protein ligands is a key factor in determining the cellular response to biomaterial interaction. The fact that there are multiple

integrin heterodimers mediating osteoblast substrate interaction provides the potential of regulating different cellular responses, depending on the integrin receptor expressed by the cell and the composition of the surrounding ECM.

The composition and the conformation of the extracellular adsorbed protein layer is thought to be the primary factor determining the cell response to biomaterial specification including surface chemistry, topography, charge, and wettability (13, 107, 124). Nonetheless, there is a growing evidence suggesting that substrate properties themselves are what determine the conformation and composition of the adsorbed protein layer, ECM production of adherent cells, and consequently the integrin receptor expressed (56, 63, 78, 102, 109). Besides, there is some evidence to show differential pattern of integrin expression at different stages of cellular maturation (15). Schneider and collaborates, for example, using a fetal bovine osteoblast culture model observed a restricted expression of  $\alpha v\beta 3$  integrin to days 3 and 5 in the cell culture in comparison to a generalized expression of  $\alpha 5\beta 1$  integrin over the 2 weeks culture period. (98). Therefore, understanding the basic role that integrin receptors play in osteoblast implant interaction and identifying the basic subunits that are involved in this process is fundamental for enhancing our understanding of osseointegration process. Another issue of critical importance is the ability to identify the particular ECM ligands for each integrin heterodimer, their mode of expression, and the cellular processes they mediate. A better understanding of these essential mechanisms will enhance our ability to engineer bioactive surfaces that can be used for biomedical and biotechnological purposes (46, 47)

The use of blocking antibodies against specific integrin subunits, or against a specific ECM protein ligand to disrupt cell substrate interaction and perturb integrin function, is a recommended procedure to analyze adhesive interactions to biomaterials. This procedure has

been utilized to identify specific integrin subunits and integrin-ligand pairs that mediate osteoblast adhesion to biomaterials and their influence on vital cellular mechanisms. (57, 82-84, 99, 108, 116, 128). This method will be used in this research project to evaluate the effect of  $\beta 1$  and  $\beta 3$  integrin subunits on the early interaction of osteoblast like cells (MC3T3-E1) with commercially pure titanium surfaces of different surface topographies.

### **1.7. Goals and specific aims**

Implant surface features affect bone formation and adherent cellular activities. The integrin transmembrane receptors particularly  $\beta 1$  and  $\beta 3$  receptors have emerged as central regulators of cell biomaterial interactions. Nevertheless, the exact role that these receptors play in modulating osteoblast behavior on different implant surfaces is not completely understood. The goals of this in vitro investigation are:

1. To examine the ability of  $\beta 1$ ,  $\beta 3$  integrin antibodies to disrupt cp Titanium surface-specific responses of MC3T3-E1 cells with particular emphasis on cell:
  - a. Adhesion
  - b. Spreading
  - c. Proliferation
  - d. Differentiation
2. To compare MC3T3-E1 early cell adhesion to cp titanium, and proliferation in the presence and absence of  $\beta 1$ ,  $\beta 3$  integrin function as a function of time and surface.
3. To quantify and compare the early expression of osteogenesis related genes with and without  $\beta 1$ ,  $\beta 3$  monoclonal antibody as a function of surface roughness.

## 1.8. Hypotheses

1. If  $\beta 1$  and or  $\beta 3$  integrins mediate surface-specific changes in osseointegration, then blocking of integrin interactions with implant surfaces will have surface-specific effects on cellular adhesion and osteoblast-specific gene expression.
2. Both  $\beta 1$  and  $\beta 3$  integrins have substantial effect on the early interaction between osteoblast like cells and implant surface in vitro.

## **CHAPTER 2**

### **MATERIALS AND METHODS**

#### **2.1. Commercially pure titanium surface preparation**

Commercially pure grade IV titanium (cpTi) disks were provided by the University of North Carolina (UNC) Dental Research Center, bone biology and implant therapy laboratory. The disks were 13 mm in diameter and 2 mm thick. Disks were randomly selected to prepare two different surface roughnesses, smooth (turned) and rough (sandblasted and hydrochloric acid etched). All disks were initially prepared by polishing using silicone carbide abrasive paper (3M, Saint Paul, MN). Disks were gradually polished by 200,400 and 600 grit carbide abrasive papers in a consecutive manner. While the disks were polished they were washed consequently with 70% ethanol to clean the debris and to minimize heat production. Afterwards, the disks were washed thoroughly using distilled water. The disks that were randomly selected to have smooth surface topography were ultrasonically cleaned using deionized distilled water (ddH<sub>2</sub>O). The disks went through 5 phases of ultrasonic cleaning for 5 minutes duration for each phase. The ddH<sub>2</sub>O was changed each time and the disks were further washed and rinsed thoroughly in ddH<sub>2</sub>O between phases.

The rough surface were prepared and passivated according to the preparation method proposed by Keller et al (62). Disks were further grit-blasted with 100 µm aluminum oxide Al<sub>2</sub>O<sub>3</sub> particles using a sandblasting machine (MicroBlaster, Comco Inc, Burbank, CA). Afterwards, sandblasted surfaces were washed with ddH<sub>2</sub>O, ultrasonically cleaned five

times, 5 minutes each time with ddH<sub>2</sub>O in a similar fashion to the smooth surfaces. Then the disks were acid etched with 5 mol/L hydrochloric acid (5N HCL) overnight. This procedure will result in grit blasted acid etched surface of the micron-scale level of roughness (4).

Finally, both smooth and rough surface disks were rinsed and washed thoroughly using ddH<sub>2</sub>O and passivated by soaking the disks 40% nitric acid for 5 minutes. After the passivation process, the disks were further washed by ddH<sub>2</sub>O and then were soaked in 70% alcohol for at least 24 hours. Prior to cell plating, the disks were exposed to ultraviolet light in a sterile tissue culture hood for 24 hours to dry and sterilize the disks.

## **2.2. Surface analysis**

To gain more detailed information regarding the prepared surfaces topography, a surface analysis was conducted using atomic force microscopy (AFM). Disks were subjected to AFM analysis (AFM; Auto Probe CP, Park Scientific Instruments, Sunnyvale, CA). The atomic force microscope uses a non-contacting stylus to image the surface of the disks and create a digitized image from which numerous surface parameters can be calculated. Scans (50 $\mu$ m X 50 $\mu$ m) were made for each surface, and three disks were analyzed for each individual surface. Packaged algorithms provided calculations for area statistics, which included average roughness (Ra) and root mean square roughness (RMS). Average roughness (Ra) is the most commonly reported surface parameter and it represents the arithmetic mean of deviations in the roughness profile from the mean line (91). On the other hand, RMS represents the standard deviation of the distribution of surface heights. It is important parameter to describe surface roughness by statistical methods.

### **2.3. Cells and cell culture**

The MC3T3-E1 osteogenic cell line (American type culture collection, Manassas, VA) was used in this project. The cells were maintained in Gibco Minimal Essential Medium Eagle, Alpha modification ( $\alpha$ -MEM) (Invitrogen Corporation, Carlsbad, CA). The medium was supplemented with 10% fetal bovine heat inactivated serum (FBS) (Invitrogen Corporation, Carlsbad, CA) and 1% antibiotics (penicillin/streptomycin) and antimicrobial agents (Sigma, Saint Louis, Missouri). The cells were cultured in a fully humidified atmosphere consisting of 95% air, 5% CO<sub>2</sub> at 37°C. The cells were passaged every third day. Cells at 90% confluent were removed by using Trypsin/EDTA reagent (Sigma, Saint Louis, Missouri). At the time of the experiments the cells were centrifuged at 1200 rpm for 4 minutes, suspended in complete medium counted and prepared for each experiment. Each experimental condition was performed in triplicate for statistical confidence.

### **2.4. Cell treatment with monoclonal antibodies and IgG control**

Before plating the cells on the disks for both the molecular and morphological studies, the cells were treated with either specific monoclonal antibodies for  $\beta$ 1 and  $\beta$ 3 integrin subunits or with control immunoglobulin G antibody (IgG). After the cells were trypsinized, counted, and centrifuged, they were resuspended in medium to provide the concentration of cells needed for the particular experiment. Afterwards, the cells were centrifuged again at 1200 rpm for 4 minutes and the medium was removed. The cell pellet was resuspended in media containing the specific monoclonal antibody or the IgG control at the defined concentration.

Monoclonal anti-mouse integrin  $\beta$ 1/ CD29 antibody (R&D systems, Minneapolis, MN) was used to block integrin  $\beta$ 1 function. The stock solution was diluted with 0.2 ml of ice cold 1X Phosphate buffered saline (PBS). This resulted in an antibody concentration of 500  $\mu$ g/ml. Moreover, monoclonal anti-  $\beta$ 3 CD61 mouse antibody (Fitzgerald industries international incorporation, Concord, MA) was used to block  $\beta$ 3 integrin function. The stock solution was reconstituted with 1 ml of ice cold 1X PBS that resulted in a concentration of 500  $\mu$ g/ml. Finally, for the control groups a Rat IgG isotype control antibody (R&D systems, Minneapolis, MN) was used. The stock solution was reconstituted with 1ml of ice cold PBS to produce a concentration of 500  $\mu$ g/ml. For each of the three reagents, 60  $\mu$ g was needed to treat one million cells. The cell pellet after centrifuging was washed twice with ice cold 1X PBS and was resuspended in the solution containing either the anti-  $\beta$ 1 monoclonal antibody, anti-  $\beta$ 3 monoclonal antibody, or the IgG isotype control. The tubes were kept in a cell culture incubator at 37°C with intermittent agitation. After one hour  $\alpha$ -MEM was added to produce a concentration of 20  $\mu$ g/ml for the three reagents in the RT<sup>2</sup> Profiler™ PCR Arrays experiment, and 8  $\mu$ g/ml for the SEM experiment. For both the molecular and the morphological studies cells were resuspended in 300  $\mu$ l media for plating on each disk. This resulted in final concentration of 6  $\mu$ g/ 100,000 cells for the molecular study and 2.4  $\mu$ g/40,000 cells for the morphological study.

### **2.5. Osteogenesis gene expression profiling with RT<sup>2</sup> Profiler™ PCR Arrays experiment**

After the completion of the cell treatment with anti-  $\beta$ 1 monoclonal antibody, anti-  $\beta$ 3 monoclonal antibody, or IgG isotype control and the addition of the required amount of  $\alpha$ -MEM medium, the cells were mixed thoroughly and were ready to be plated. This

experiment was performed twice; once the cells were treated with anti-  $\beta$ 1 monoclonal antibody in the test group and the second time cells were treated with anti- $\beta$ 3 monoclonal antibody in the test group. In both experimental conditions, cells in the control groups were treated with IgG isotype control. Having two different surface preparations (rough, smooth) and two different cell treatment protocols (anti  $\beta$ 1/  $\beta$ 3, Control) resulted in four different groups in each experimental condition (Figure 2.1).

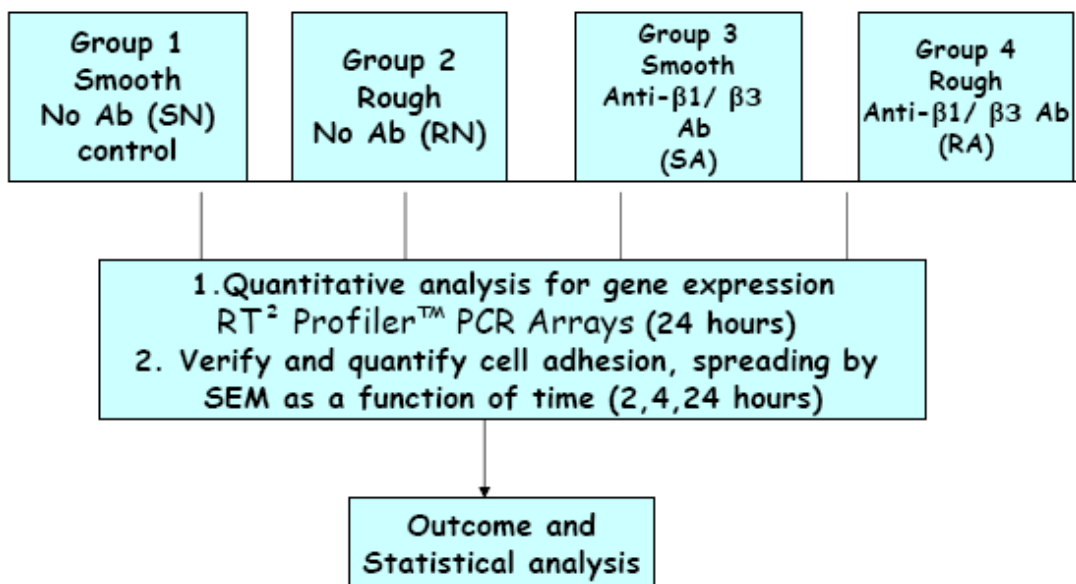


**Figure 2.1.: A flow chart representing the experimental design for The SEM and the RT<sup>2</sup> Profiler™ PCR Arrays experiments.**

The cells were seeded on the disks with a density of  $10^5$  cells/ disk in 300  $\mu$ l volume of medium. Seven disks were used for each group the disks were placed in cell culture plates and incubated in fully humidified atmosphere consisting of 95% air, 5% CO<sub>2</sub> at 37°C for 24 hours. The cells were allowed to attach initially to the surface for 3 hours and after 3 hours  $\alpha$ -MEM medium was added to cell culture plates until the disks were completely covered and

were placed back in the incubator for the remainder of the 24 hour culture period. After 24 hours, the cells were harvested using TRI REAGENT™ (Sigma, Saint Louis, Missouri). This reagent is a mixture of guanidine, thiocyanate, and phenol in a mono-phase solution. After the removal of the medium the disks were washed twice with ice cold 1X PBS, then the cells were harvested carefully using the TRI REAGENT™ and were ready for ribonucleic acid (RNA) isolation. After the cells were homogenized in TRI REAGENT, samples were stored at -70 °C till the time of RNA isolation less than a week after the completion of the experiment.

### **2.5.1. RNA isolation and first strand cDNA synthesis**

Total RNA was isolated from cell layers using TRI REAGENT™ (Sigma, Saint Louis, Missouri ), based on the single-step method described by Chomczynski and Sacchi (26).

1. The homogeneous mix sample was allowed to stand for 5 minutes at room temperature. Afterwards, 0.2 ml of chloroform was added per ml of TRI REAGENT used. The resulting mix was centrifuged at 12,000 x g for 10 minutes at 4 °C mix. Centrifugation separates the mixture into 3 phases: a red organic phase (containing protein), an interface (containing DNA), and a colorless upper aqueous phase (containing RNA).
2. The aqueous phase was transferred to fresh tube and 0.5 ml of isopropanol per ml of TRI REAGENT used in sample preparation. The resulting mixture was allowed to stand for 5-10 minutes at room temperature, and then it was centrifuged at 12,000 g for 10 minutes at 4°C. This step precipitated the RNA which formed a pellet on the side and bottom of the tube.

3. The supernatant was removed and the RNA pellet was washed with 75% ethanol per 1 ml of TRI REAGENT used in sample preparation. The mix was then shaken vigorously using Vortex and then it was centrifuged at 7,500 x g for 5 minutes at 4°C.
4. The RNA was air dried for 5-10 minutes without completely drying the pellet. Afterwards, the RNA was redissolved using 10-20µl of RNase free diethylpyrocarbonate (DEPC) water. To facilitate the dissolution, the liquid was mixed by repeated pipetting at 55-60 °C for 10-15 minutes.
5. The RNA was quantified by UV spectrophotometry (Beckmann DU-600). One µg of total RNA was needed to make cDNA using RT<sup>2</sup> first stand kit (SuperArray, Bioscience Corporation, Fredrick, MD) for each 96-well plate formats of RT<sup>2</sup> Profiler™ PCR Arrays.
6. For cDNA synthesis a genomic DNA elimination mixture was prepared by mixing total RNA with GE reagent (5x gDNA elimination buffer) and DPEC water. The mixture was incubated at 42 °C for 5 minutes and chilled immediately on ice. Afterwards 10 µl of the Reverse transcriptase (RT) cocktail was added to 10 µl of genomic DNA elimination mixture and they were mixed very well using a pipettor and were incubated at 42 °C for 15 minutes. Afterwards, they were heated to 95 °C for 5 minutes to degrade the RNA and to inactivate the reverse transcriptase. Finally, 91µl of ddH<sub>2</sub>O was added to each 20 µl of cDNA synthesis reaction. They were mixed well and the finished first strand cDNA was stored at -20 °C. The cDNA for each experimental group was equally divided into 3 samples to perform the PCR array in triplicate format.

### **2.5.2. Performing Real-Time PCR using RT<sup>2</sup>Profiler™ PCR Arrays**

To determine the relative differences in gene expression of osteogenesis specific genes the mouse osteogenesis RT<sup>2</sup>Profiler™ PCR Arrays system was used. This system brings together the quantitative performance of real-time PCR and the multiple gene profiling capability of microarrays. This PCR array profiles the expression of a panel of 84 genes related to osteogenic differentiation, skeletal development, bone and mineral metabolism, growth factors, cell adhesion and extracellular matrix molecules related to bone development, and genes mediating osteogenesis, cell proliferation, growth, and differentiation. The whole list of genes included in this array is represented in appendix A. The protocol for performing the PCR array took about two hours for each sample. The PCR was done in triplicate for each experimental or control group for statistical confidence. This resulted in 12 samples for the anti-  $\beta$ 1 experiment and another 12 samples for the anti-  $\beta$ 3 experiment.

For each sample (PCR plate) 102  $\mu$ l of diluted first strand cDNA was mixed with 1275  $\mu$ l of 2X superArray RT<sup>2</sup> qPCR master mix and 1173  $\mu$ l of ddH<sub>2</sub>O, this resulted in 2550  $\mu$ l of total volume. Equal aliquots of 25  $\mu$ l were added to the 96 wells containing the pre-dispensed gene-specific primer sets using a multi channel pipette and the wells were covered tightly with a plastic lid. PCR was performed using ABI prism 7000 real-time PCR thermocycler. The instrument's software was used to calculate the threshold cycle (C<sub>t</sub>) values for all genes on each PCR array. Five internal control genes presented in PCR array were used for normalization. A simple examination of C<sub>t</sub> value consistency of these internal control genes quickly indicated the proper normalization method. Fold changes in gene expression for pairwise comparison was calculated using comparative C<sub>t</sub> method ( $\Delta\Delta$  C<sub>t</sub> method). This method

was used to calculate the relative amount of the transcripts in the experimental sample and the control sample, both of which were normalized to the internal controls.  $\Delta Ct$  is the  $\log_2$  difference in Ct between the gene and internal controls,  $\Delta\Delta Ct = \Delta Ct (\text{experimental}) - \Delta Ct (\text{control})$  for biological RNA samples (69).

## **2.6. Cell binding experiment using scanning electron microscopy**

Evaluation of the effect of anti- $\beta 1$  and anti- $\beta 3$  monoclonal antibodies, time, and surface topography on MC3T3-E1 initial cell binding to Cp titanium surfaces as well as cell spreading were examined both quantitatively and qualitatively using SEM. The experimental design was similar to the PCR array experiment (figure 2.1). However, the effect of time on the initial cell binding and spreading was evaluated at 3 different time points for all different experimental groups (2 hours, 4 hours, and 24 hours). Unlike the PCR array experiment, anti- $\beta 1$  and anti- $\beta 3$  and control (IgG) were evaluated on both smooth and rough Cp titanium surfaces in the same experiment. This resulted in six different experimental groups that were evaluated at three different time points (figure 2.1). Two disks were used for each group at any single time point. The cells were treated with either anti- $\beta 1$  or anti- $\beta 3$  and IgG isotype control in a similar fashion to the PCR array experiment. However, only 40,000 cells in 300  $\mu\text{l}$  of medium were plated on each disk to decrease cell density and be able to identify individual cells when performing the SEM.

### **2.6.1. SEM preparation**

After plating the cells on the disk, adherent cells and disks at the particular time points were rinsed three times with ice cold 1X PBS and fixed for 60 minutes with 4 % Paraformaldehyde and left at room temperature for one hour, then they were refrigerated at -4 °C for at least 24 hours. For the 4 and 24 hour groups  $\alpha$ -MEM medium was added to cover the disks after 3 hours, then it was removed before washing the adherent cells and disks with 1X PBS and fixation with paraformaldehyde. After fixation for 24 hours the paraformaldehyde was removed and the disks were further washed three times with ice cold 1X for 15 minutes each time. Afterwards, the disks and adherent cells were dehydrated using graded ethanol solutions from 50% to 100% for 15 minutes each time in a 12 well-plate. The 100% ethanol step was repeated for 3 times. After the last 100% ethanol drying step, 2 ml of hexamethyldisilazane (HDMS) (Electron microscopy sciences, Fort Washington, PA) was added for each well and let to evaporate overnight under a fume hood for complete dehydration. Before performing the SEM imaging the samples were coated with conductive material according to SEM manufacturer recommendation. Hitachi S-4700 Scanning electron microscope (Hitachi High Technologies America, inc., Pleasanton, CA) was used to obtain SEM images for the different groups.

### **2.6.2. Quantitative and qualitative evaluation of osteoblast like cell adhesion, spreading and morphology on Cp titanium surfaces**

Cell adhesion was determined by averaging the number of the cells counted at low magnification (X 300) from three random areas per disk. Two disks were used for each group at any particular time point. The number of cells was counted three times by three different investigators working independently and who were blinded to the experimental group for

each sample. The investigators were calibrated before performing the cell counting process and inter-examiner reliability test showed a very good agreement among the three investigators (Kappa value 0.78). This protocol resulted in 18 readings for any experimental group at any particular time point. Descriptive statistics were calculated for each group using SPSS software (SPSS inc. Chicago, Illinois) and comparisons among groups and between particular groups were performed. Furthermore, the spreading of the cells was evaluated by using the presence of cell processes, elongation of the central cytoplasm region, cell diameter at its longest axis as criteria for spread cell to score the cell morphology manually. Cells that scored 20  $\mu\text{m}$  or more in its longest dimension as determined by the scale on SEM images, were considered as spread cells and the ones that scored less than 20  $\mu\text{m}$ , were considered as round cells. Data acquisition and analysis for round and spread cells were performed in identical fashion to total number of cells with three blind investigators counting cells independently.

SEM images at higher magnification (X 2000) for all experimental groups were made to evaluate cell shape, spreading and attachment for subjective comparison among different surfaces and treatment protocols.

## **2.7. Statistical analysis**

For the RT<sup>2</sup> Profiler™ PCR Arrays experiment, a specific data analysis web portal provided by the PCR arrays system was used to perform the data analysis. This web portal automatically performs calculations and interpretations of the control wells upon including threshold cycle data from the real-time PCR instrument. Statistical comparisons between fold

changes among any two groups were performed using T-test and any p-value less than 0.05 was considered statistically significant.

As for the quantitative analysis of cell adhesion and spreading using SEM, SPSS software was used to analyze the raw data. Descriptive statistics comparisons were performed for the different experimental groups. Moreover, factorial ANOVA was used to compare the mean number of total, spread, and round cells among the different experimental groups and at different time points and any P value less than 0.05 was considered statistically significant. For pair wise comparisons between individual groups post-hoc Tuckey test was used and any p value less than 0.05 was considered statistically significant.

## CHAPTER 3

### RESULTS

#### 3.1. Atomic force microscopy surface analysis

AFM analysis of the disks provided measures of average surface roughness (Ra) and root mean square roughness, for comparisons among individual surfaces (Table 3.1). Each surface displayed a unique topography (Figure 3.1). Smooth surfaces had relatively low peak-to-valley measurements compared to rough surfaces. Moreover, the Ra and RMS values were considerably greater for rough surfaces compared to smooth surfaces.

**Table 3.1: Surface parameter measurements as calculated by atomic force microscopy for smooth and rough surfaces.**

Surface	Ra	RMS
<b>Rough</b>	0.39 ( $\pm$ 0.019) $\mu\text{m}$	0.46 ( $\pm$ 0.027) $\mu\text{m}$
<b>Smooth</b>	0.036 ( $\pm$ 0.006) $\mu\text{m}$	0.047 ( $\pm$ 0.007) $\mu\text{m}$

Ra: average surface roughness, RMS: root mean square roughness. Data presented as the mean ( $\pm$  Standard error of the mean).

Atomic force microscopy representative images of 50  $\mu\text{m}$  X 50  $\mu\text{m}$  of the test surfaces for surface parameters analysis are presented in figure 3.1.

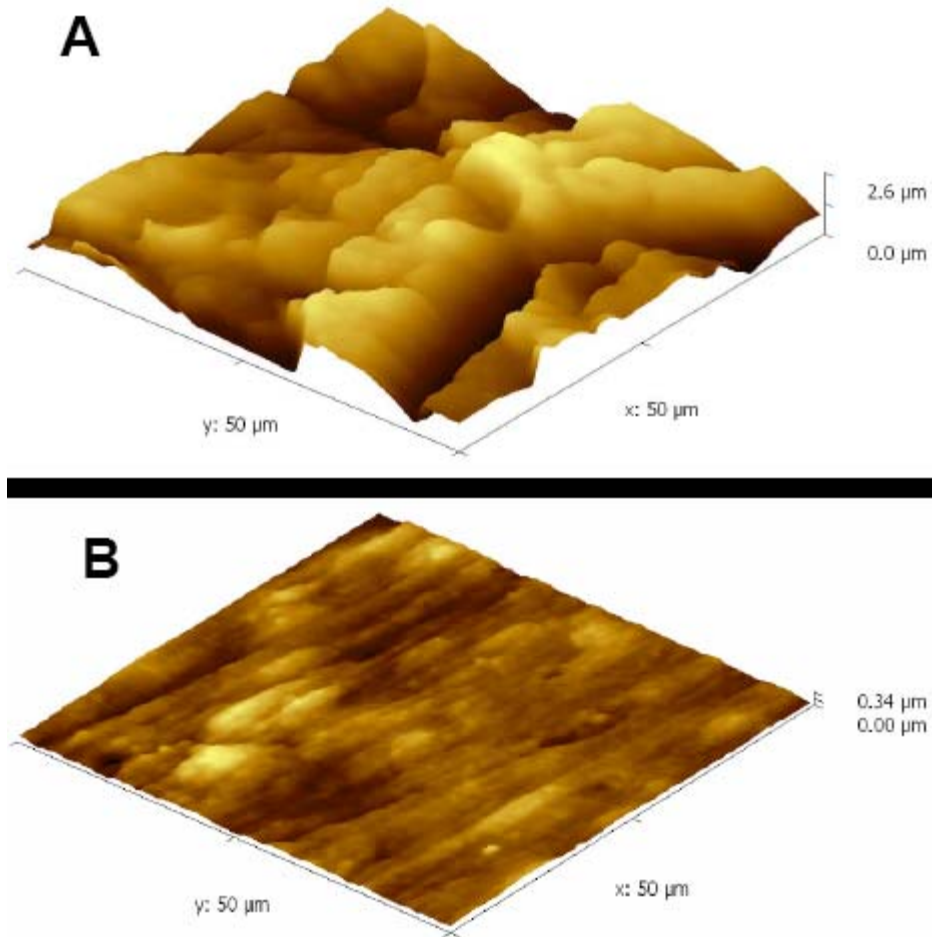


**Figure 3.1: Atomic force microscopy surface topography analyses representative of 50 μm X 50 μm areas of test surfaces ( A: Rough surface, B: Smooth surface).**

### **3.2. Initial cell attachment and total cell count**

The number of total cells per surface area was measured as a function of cell attachment to the cpTi surfaces. The input number of cells was held constant in this experiment. Mean number of adherent cells in the different experimental groups at three different time points on both smooth and rough surfaces are shown in figure 3.2.

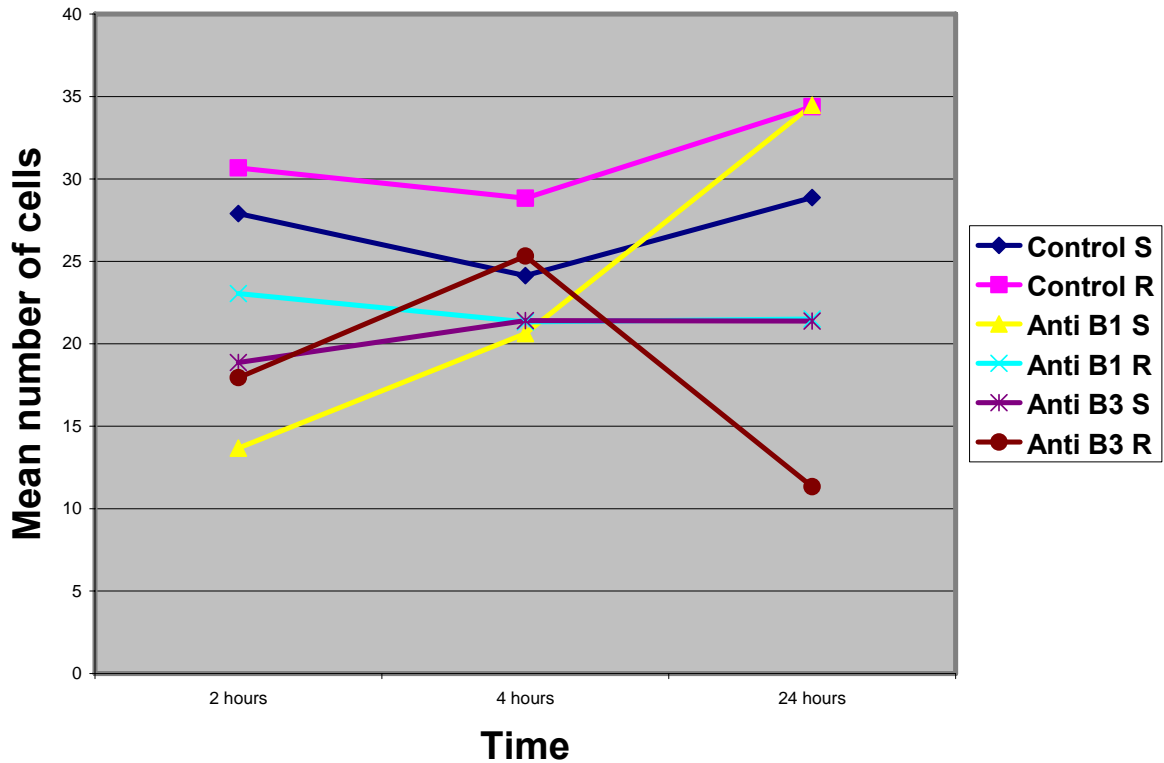


**Figure 3.2. : Mean number of cells at different time points among the different experimental groups on both smooth and rough surfaces.**

S: smooth surface, R: Rough surface

The number of cells in the control group is slightly higher on rough surface than smooth surface and they increase slightly at 24 hours in comparison to 2, 4 hours. Nevertheless, in the anti- $\beta 1$  and anti- $\beta 3$  groups the cell numbers initially at the 2 hours time point are less than the control group and they increase with time on the smooth surface particularly in the anti- $\beta 1$  group where cell numbers return to the level of the control group at 24 hours. On the other hand, cells decrease in number on rough surface between 4 and 24 hours in the anti- $\beta 3$  group and did not change in the anti- $\beta 1$  group. Nonetheless, when performing factorial ANOVA statistical test, the only factor which had a significant influence on number of cells was treatment (anti- $\beta 1$  Ab, anti- $\beta 3$  Ab, or IgG control). Figure 3.3 shows the mean number of cells at different time points among the different experimental groups on both surfaces.

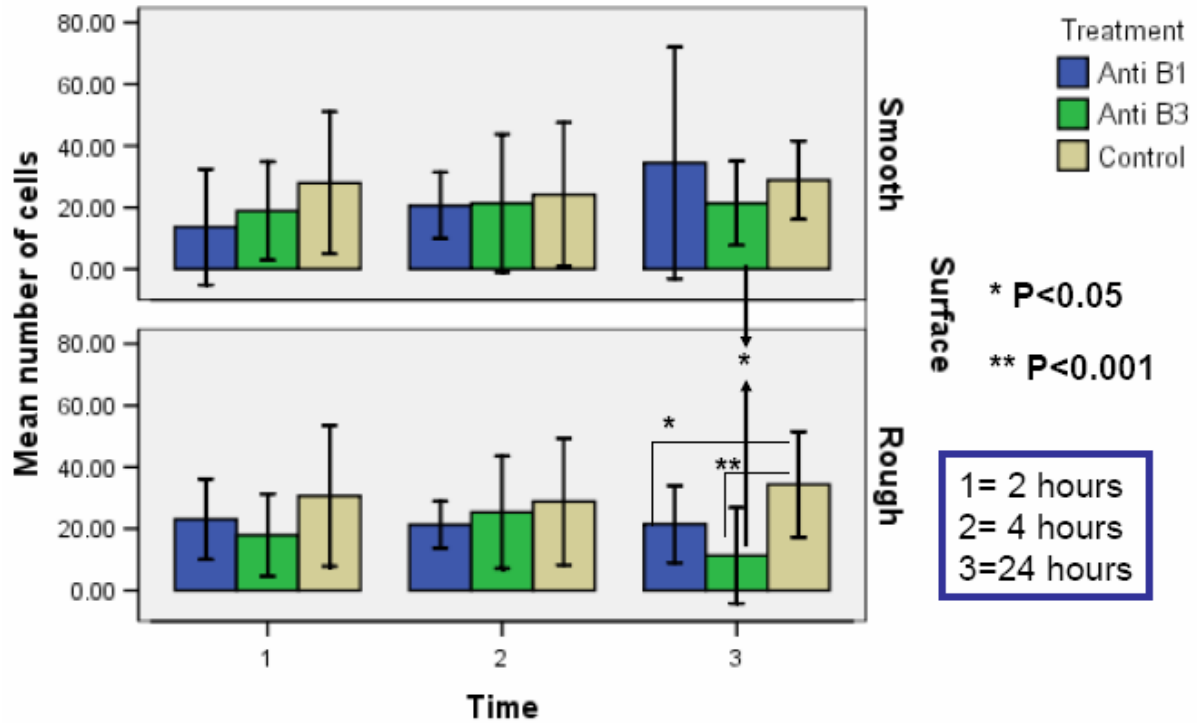


**Figure 3.3.: Clustered bar chart showing the mean number of cells among the different experimental groups on both smooth and rough surfaces.**

The control group had higher number of cells than the anti- $\beta$ 1 or the anti- $\beta$ 3 groups on both surfaces and at all time points except for the anti- $\beta$ 1 group at 24 hours on smooth surface. However, the difference was only statistically significant at 24 hours on rough surface as determined by post-hoc Tuckey test. Moreover, smooth surface has significantly higher number of adherent cells at 24 hours than rough surface in the anti- $\beta$ 3 group as determined by one way ANOVA statistical test.

### 3.3. Initial cell spreading and spread and round cell counts

Cell spreading was evaluated by measuring the number of spread cells versus round or spherical cells. The presence of cell processes the elongation of the cytoplasm and the ability of the cell to spread for more than 20  $\mu$ m as measured by the cell longest dimension were considered as surrogates for cell spreading. Figure 3.4 shows the mean number of spread

cells at different time points among the different experimental groups on both smooth and rough surfaces.

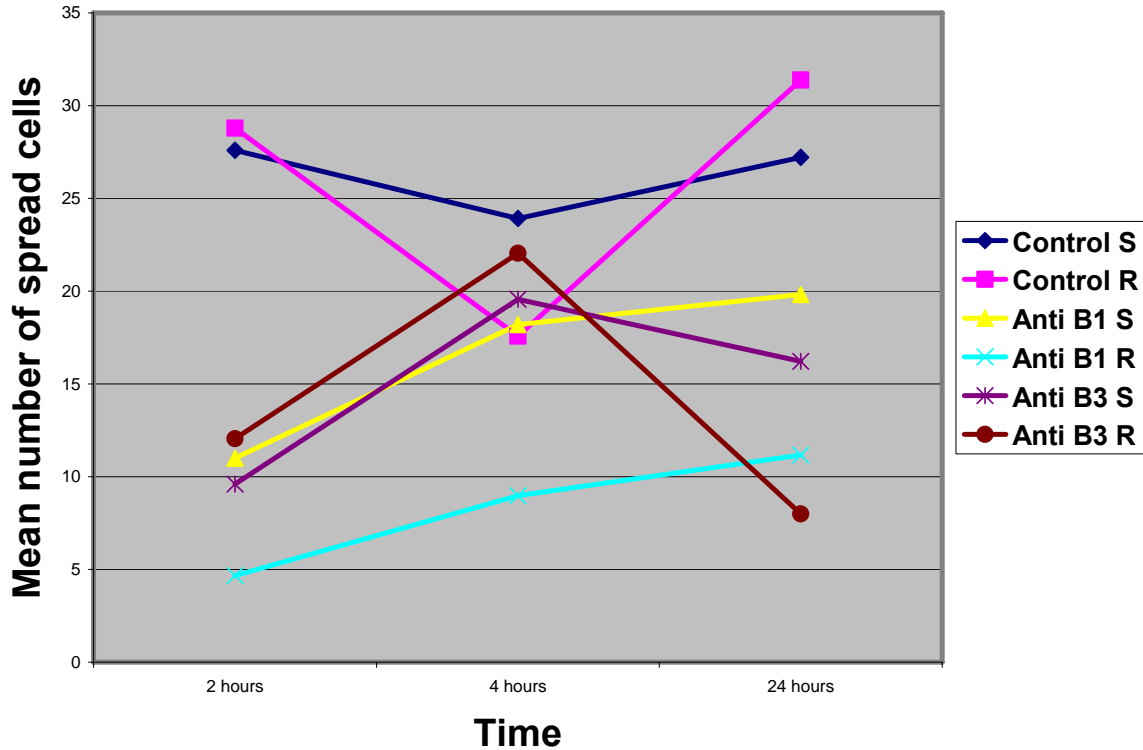


**Figure 3.4.: Mean number of spread cells at different time points among the different experimental groups on both smooth and rough surfaces.**  
 S: Smooth surface, R: Rough surface

In the control group numbers of spread cells on both surfaces were higher than for the anti- $\beta 1$  and the anti-  $\beta 3$  groups. However, cells in the control group adherent to the rough surface decreased from 2 to 4 hours then increased at the 24 hour mark. Notably, spread cells on smooth surface were higher than on rough surface. Similar finding was noted in the anti-  $\beta 1$  and anti-  $\beta 3$  groups with more spread cells in the anti-  $\beta 3$  group than anti-  $\beta 1$  group and more spread cells on smooth versus rough surface. Another finding was that cells slightly increased between the 4 and 24 hour time points in the anti-  $\beta 1$  group. On the other hand, they decreased in the anti-  $\beta 3$  group particularly on rough surface. Nonetheless, when

factorial ANOVA statistical test was performed, the only factor that had a significant influence on number of spread cells was treatment (anti-  $\beta$ 1 Ab, anti-  $\beta$ 3 Ab, or IgG control). Figure 3.5 shows the mean number of spread cells on both surfaces at the different time points among the different experimental groups.

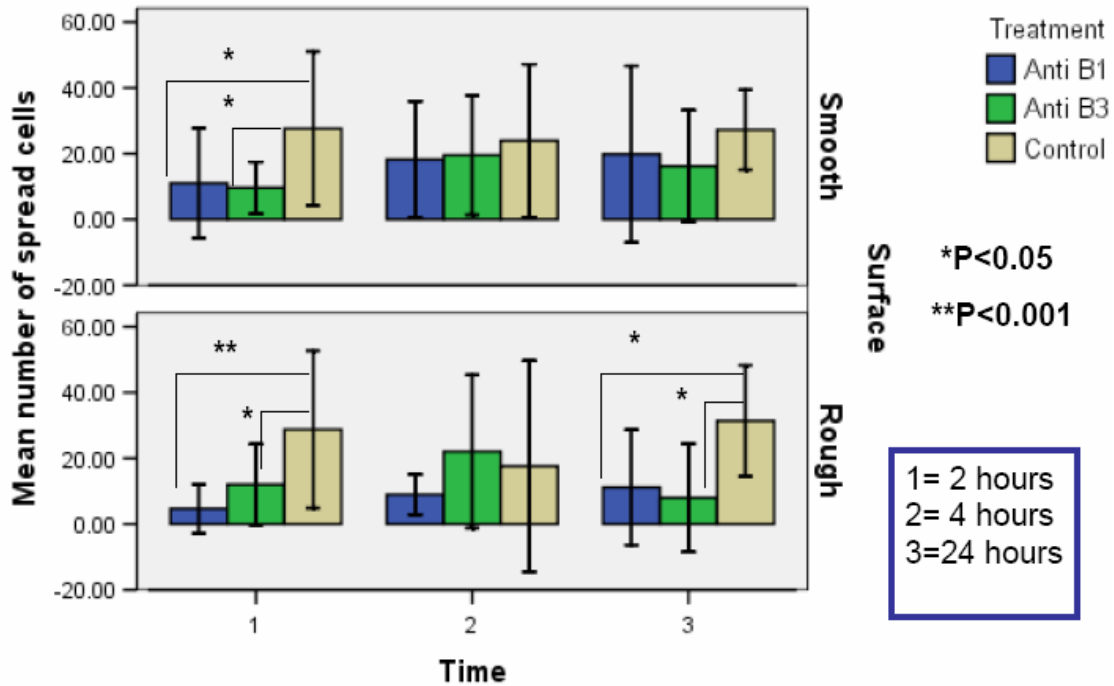


**Figure 3.5.: Clustered bar chart showing the mean number of spread cells among the different experimental groups on both smooth and rough surfaces.**

The control group had higher number of spread cells than anti-  $\beta$ 1 and anti-  $\beta$ 3 groups on both surfaces at all time points. Nevertheless, the difference was only significant at 2 hours on both surfaces and at 24 hours on rough surface only, as determined by post-hoc Tuckey test. The mean number of round or spherical cells at different time points among the different experimental groups are shown in figure 3.6.

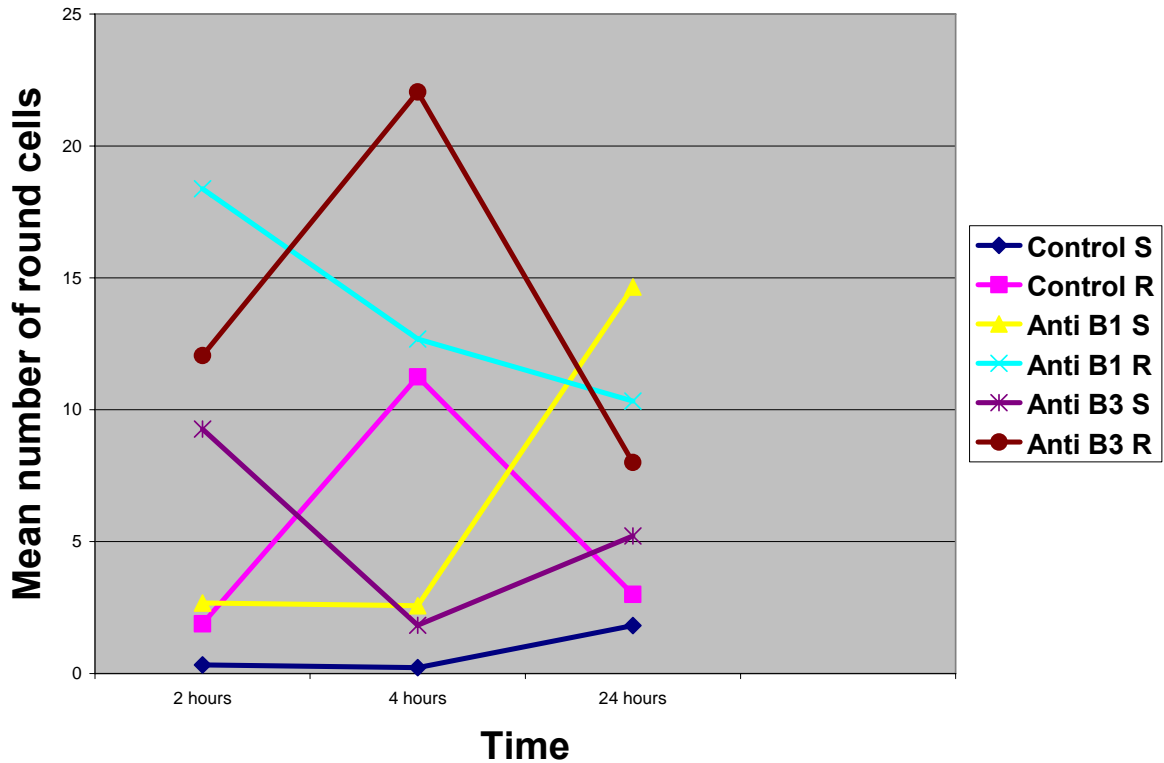


**Figure 3.6 .: Mean number of round cells at different time points among the different experimental groups on both smooth and rough surfaces.**

S: Smooth surface, R: Rough surface

This figure shows that the control group on both smooth and rough surfaces has less number of round cells in comparison to the anti- $\beta 1$  and the anti-  $\beta 3$  groups although round cell number on rough surface increased at the 4 hours mark on rough surface but they decreased on the 24 hours mark. Moreover, round cells were higher on rough surface in comparison to smooth surface. This observation was also noticed in the anti-  $\beta 1$  and the anti-  $\beta 3$  groups although at the 24 hour mark the highest number of round cells was measured at the smooth surface in the anti-  $\beta 1$  group. Another observation was that in both anti-  $\beta 1$  and anti-  $\beta 3$  groups round cell number decreased between the 4 and 24 hour time points on rough surface and increased on smooth surface.

When factorial ANOVA statistical test was performed the factors that had significant influence on number of round cells were treatment ( $P$  value $<0.0001$ ) and surface ( $p$  value $<0.05$ ). When post-hoc Tuckey test was performed for pair wise comparisons, anti- $\beta 1$  group had a significant higher number of round cells on rough surface than both anti- $\beta 3$  group and the control group at the 2 and 24 hours time points. Nevertheless, anti- $\beta 3$  had a significantly higher number of adherent round cells on smooth surface at the 2 hour time point than the anti- $\beta 1$  and the control groups. Furthermore, one way ANOVA statistical test was performed for pair wise comparisons of the different experimental groups on both surfaces. These comparisons showed that the anti- $\beta 1$  and the control groups had significantly higher number of round cells on rough surface than on smooth surface at the 2 and 4 hours time points (figure 3.7).

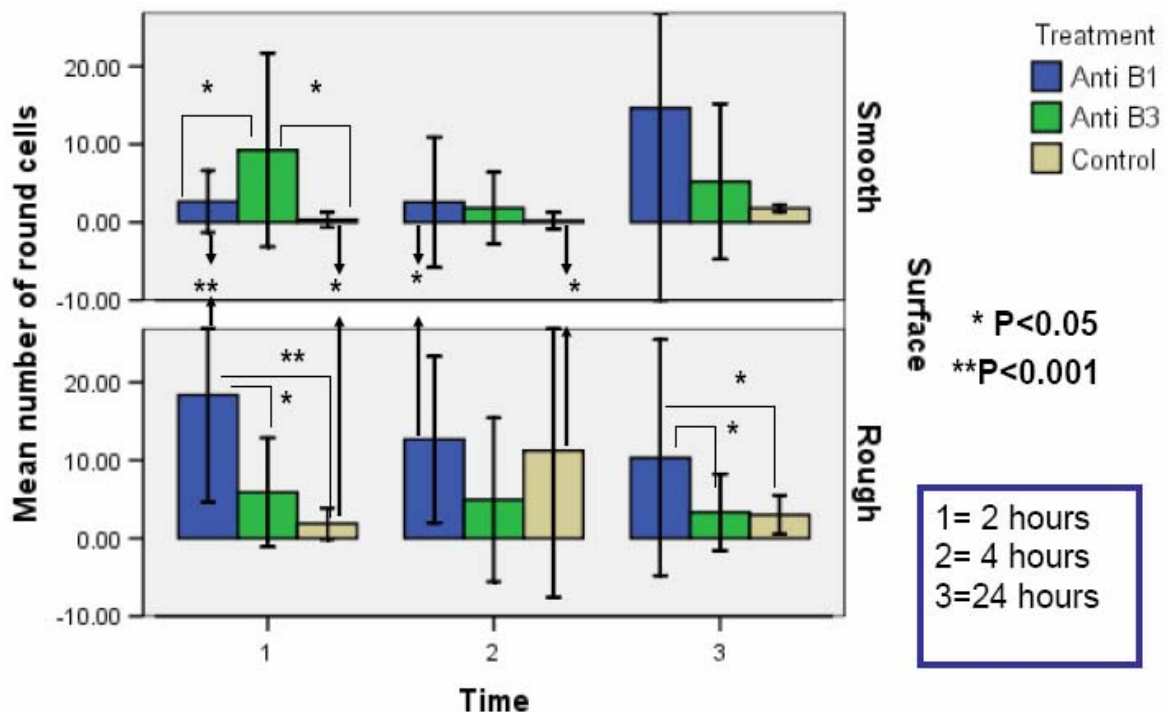
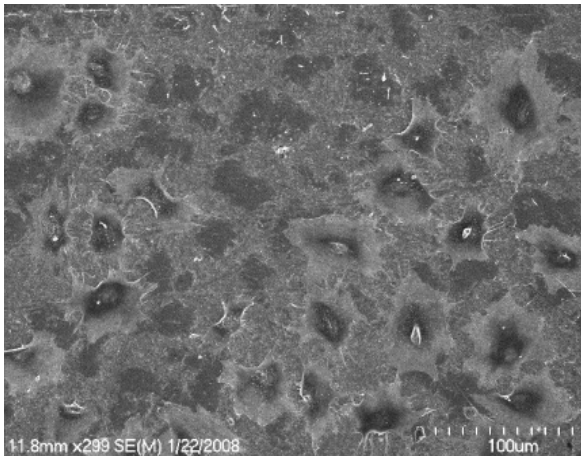
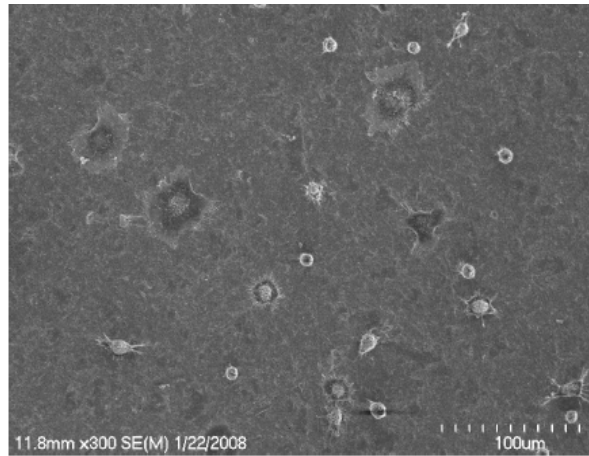


**Figure 3.7: Box plot graph showing the mean number of round cells among the different experimental groups on both smooth and rough surfaces.**

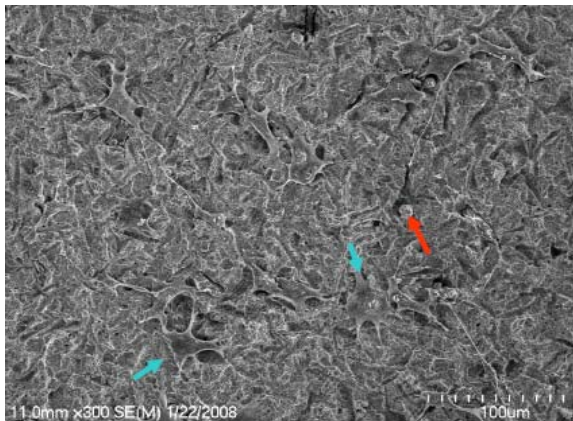
Different examples of SEM images that were used for counting the number of total, spread, and round cells are shown in figure 3.8. These sections show that the experimental groups anti- $\beta$ 1 and anti- $\beta$ 3 had less number of cells and higher number of round cells or cells that couldn't spread enough on the surface.



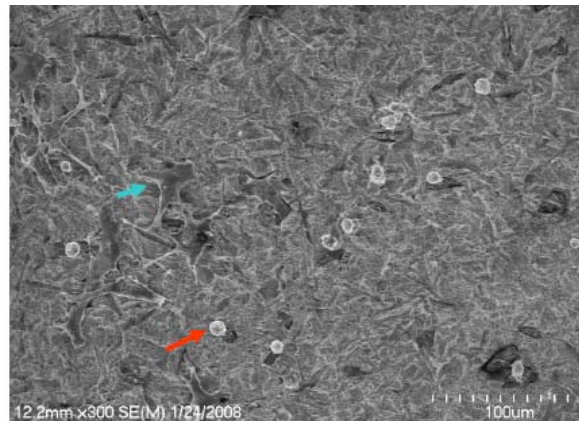
**Control at 2 hours  
Smooth surface**



**Anti  $\beta$ 3 at 2 hours  
Smooth surface**



**Control at 24 hours  
Rough surface**



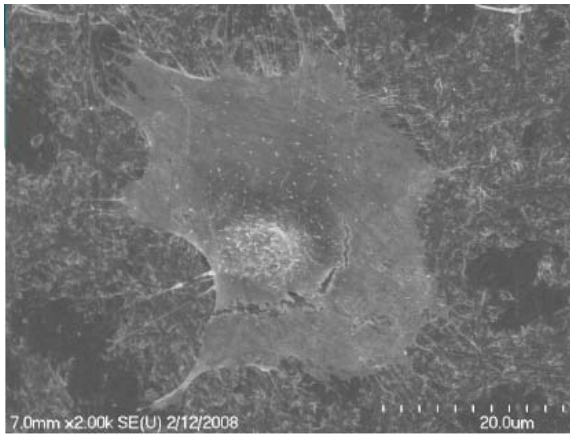
**Anti  $\beta$ 1 at 24 hours  
Rough surface**

**Figure 3.8.:** Examples of SEM images from different experimental groups and different time points that were used for data acquisition. Blue arrows: Spread cells. Red arrows: round cells

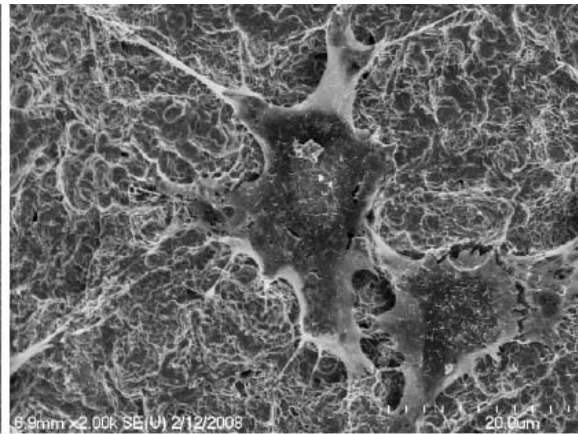
### 3.4. Subjective evaluation of SEM images at higher magnification

SEM images were made at higher magnification (X 2000) for subjective evaluation of the cell shape, spread, and interaction of the surface. Some examples of the SEM images are shown in figure 3.9. The highly magnified SEM images show that cells adhere differently on smooth and rough surfaces. By comparing images A and B the cells on both surfaces did spread over the surface. However, the cell on the smooth surface had still a round cytoplasm and less number of cell processes attaching the cell to the surface and it seems as if it is raised over the surface. On the other hand, cells on rough surface at the same time point had a more elongated cytoplasm and processes and they looked as if they were closely adapted to the configurations of the surface.

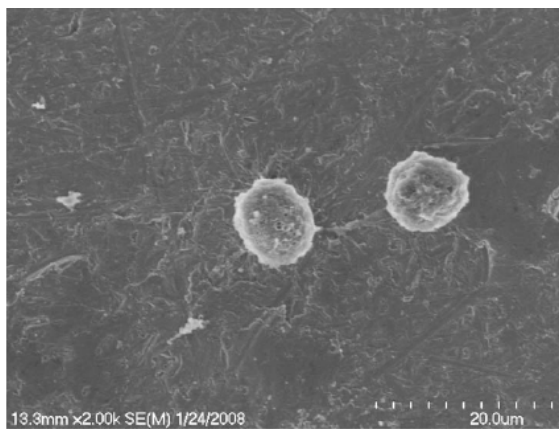
Similar findings can be observed when comparing images C and D. Cells on images C and D are round and couldn't spread over the surfaces. Nonetheless, these cells still could attach to the surface. Nevertheless, cells on the rough surface seem to have better ability to attach to the surface and to develop more cellular processes even earlier in the process. Image F shows cells that were treated with anti- $\beta 3$  antibody; both cells were round and didn't spread over the surface. However, one of the cells attached better to the surface (rough) with multiple processes and better adaptation to surface configurations. On the other hand, the other cell was probably only mechanically retained by the pits and irregularities produced by surface treatment. Finally, image E shows that cells were differentially affected by the anti- $\beta 3$  treatment. One cell could spread over the surface and the other did not. However, both of them developed some processes to attach them to the surface although the images show that they were less intimately attached to the smooth surface in comparison to the rough.



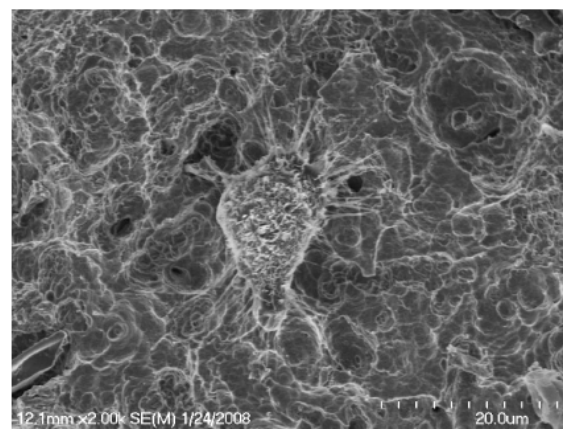
**(A) Control at 2 hours  
Smooth surface**



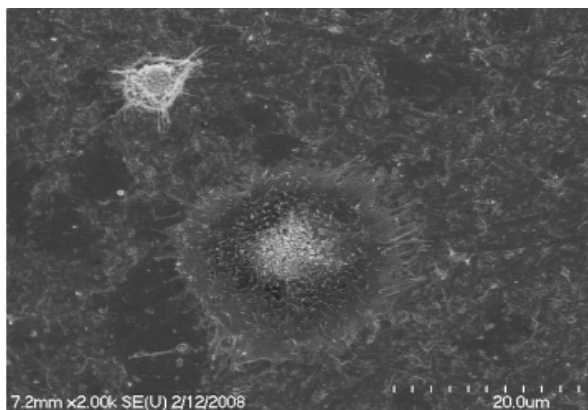
**(B) Control at 2 hours  
Rough surface**



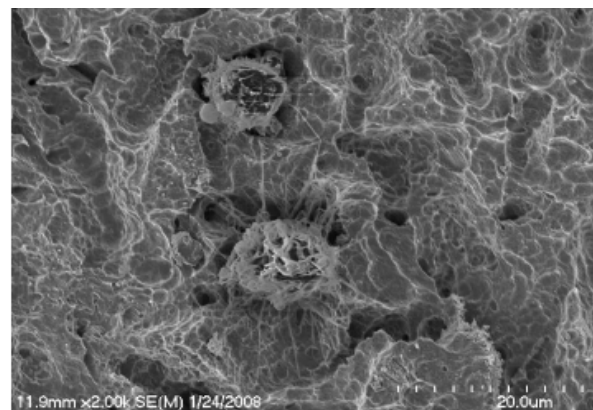
**(C) Anti  $\beta$ 1 at 24 hours  
Smooth surface**



**(D) Anti  $\beta$ 1 at 4 hours  
rough surface**



**(E) Anti  $\beta$ 3 at 4 hours  
Smooth surface**



**(F) Anti  $\beta$ 3 at 4 hours  
rough surface**

**Figure 3.9.: SEM images at higher magnification (X 2000).**

### 3.5. RT<sup>2</sup>Profiler™ PCR Arrays results

Mouse RT<sup>2</sup>Profiler™ PCR Arrays system was used to determine the relative differences in gene expression of a panel of 84 genes associated with the process of osteogenesis. This system profiles the expression of genes from different functional groups related to many cellular activities such as skeletal development, bone mineral metabolism, cell growth and differentiation, ECM proteins, cell adhesion molecules, collagen proteins, and transcriptional factors and regulators. A complete list of all genes available in this system is presented in appendix A. Nevertheless, for easier presentation of data, selective classes of functional genes will be considered in the data analysis. Table 3.2., presents the functional group of genes and the genes that showed significant changes among different experimental groups.

**Table 3.2: Functional group of genes and genes that presented significant changes among different experimental groups** (significant: either statistically significant or has more that 2 fold difference in mRNA expression).

Functional group of genes	Genes presented significant changes (anti-β1)	Genes presented significant changes (anti-β3)
Bone morphogenic protein superfamily	Tgfβ1, Bmp2, Bmp6	Gdf10, Bmp2, Bmp3, Bmp5, Bmp6
Bone matrix proteins	Ambn, Sost, Ahsg, ALP	Ambn, Sost, Ahsg, ALP
Integrin receptors	Itga2, Itgβ1, Itgav	
Growth factors	Vegfa, Vegfb, pdgfa, fgf3, Csf2, Csf3	Vegfa, Fgf2, Fgf3, Egf, Csf2, Csf3
Transcriptional factors	Smad4, Runx2, Msx1, Twist1	Msx1

In the following sections the fold difference in mRNA expression between the anti-β1/anti-β3 and the control group on both smooth and rough surfaces will be presented for

selective functional gene groups. Furthermore, the group of genes which are not presented in the following sections showed similar trends.

### 3.5.1. Bone morphogenic protein superfamily

The bone morphogenetic proteins (Bmps) are a family of secreted signaling molecules that can induce ectopic bone growth. Many Bmps are part of the transforming growth factor-beta (Tgf $\beta$ ) superfamily. Bmps were originally identified by an ability of demineralized bone extract to induce endochondral osteogenesis in vivo in an extraskeletal site. Figures 3.10 and 3.11 represent bar graph charts of fold difference in mRNA expression of Bmp superfamily genes between the anti- $\beta$ 1/anti- $\beta$ 3 and the control group on both smooth and rough surfaces.

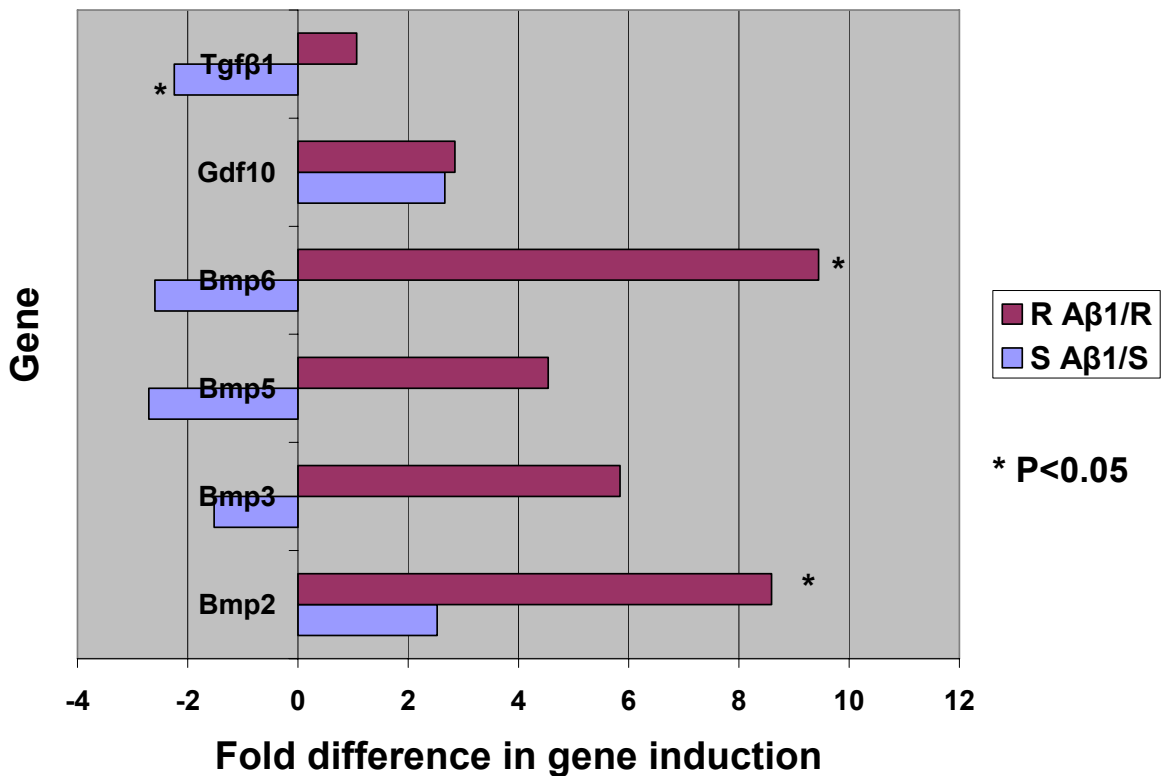


**Figure 3.10: Bar graph showing the difference in mRNA expression of Bmp superfamily genes between anti- $\beta$ 1 and control groups on both smooth and rough surfaces.**

R: rough surface, S: smooth surface.

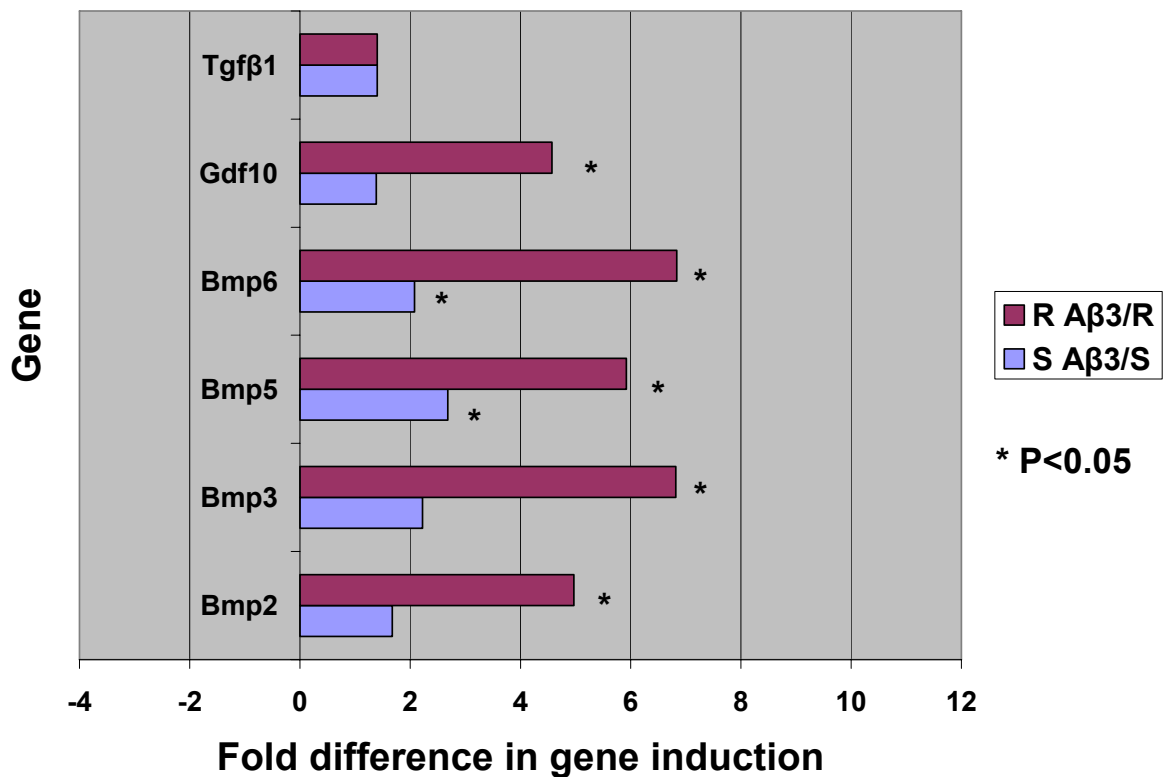


**Figure 3.11: Bar graph showing the difference in mRNA expression of Bmp superfamily genes between anti-β3 and control groups on both smooth and rough surfaces.**

R: rough surface, S: smooth surface.

The results show that there is a different trend in Bmp superfamily gene expression when β1 and β3 integrins were blocked with specific antibodies particularly on smooth surface (Figure 3.10, 3.11). Pre-treatment of MC3T3-E1 cells with anti-β1 antibody on smooth surface resulted in down regulation of the Bmp superfamily gene expression of about 2 folds, with the exception of Bmp2, and Gdf10 which were up-regulated. On the contrary, when cells were pretreated with anti-β3 antibody, all Bmp superfamily genes were up-regulated on smooth surface and Bmp5 and Bmp6 were significantly up-regulated. Nevertheless, on rough surface, Bmp superfamily gene expression show a similar trend, when cells were

pretreated with anti- $\beta$ 1 and anti-  $\beta$ 3 antibodies. All Bmp superfamily genes in the anti-  $\beta$ 1 group were up-regulated or rough surface with Bmp2 and Bmp6 significantly up regulated (more than 8 folds) and Bmp3 and Bmp5 with more that 4 folds of up-regulation . In the anti-  $\beta$ 3 group all Bmp superfamily genes were significantly up-regulated (over 4 folds) with the exception of Tgf $\beta$ .

### **3.5.2. Bone matrix proteins**

This group of genes contains some of the matrix proteins that are associated with osteogenesis and tissue development. Alkaline phosphatase (ALP) is a tetrameric glycoprotein found on the surface of osteoblast and is responsible for laying down matrix for bone. It is considered as a marker for early bone formation. Sclerostin (Sost) is a secreted glycoprotein that works as a Bmp antagonist. A mutation in the Sost gene is associated with an autosomal recessive disorder called sclerosteosis which causes progressive bone overgrowth. Alpha-2-HS-glycoprotein (Ahsg) is a glycoprotein that is present in serum and is involved in bone development and formation as well as development of other tissues. Finally, Biglycan (Bgn) is a cellular or peri-cellular proteoglycan, it is thought to function in connective tissue metabolism by binding to collagen fibrils and Tgf $\beta$ . Figures 3.12 and 3.13 represent bar graph charts of fold difference in mRNA expression of these bone matrix proteins between the anti- $\beta$ 1/anti- $\beta$ 3 and the control group on both surfaces.

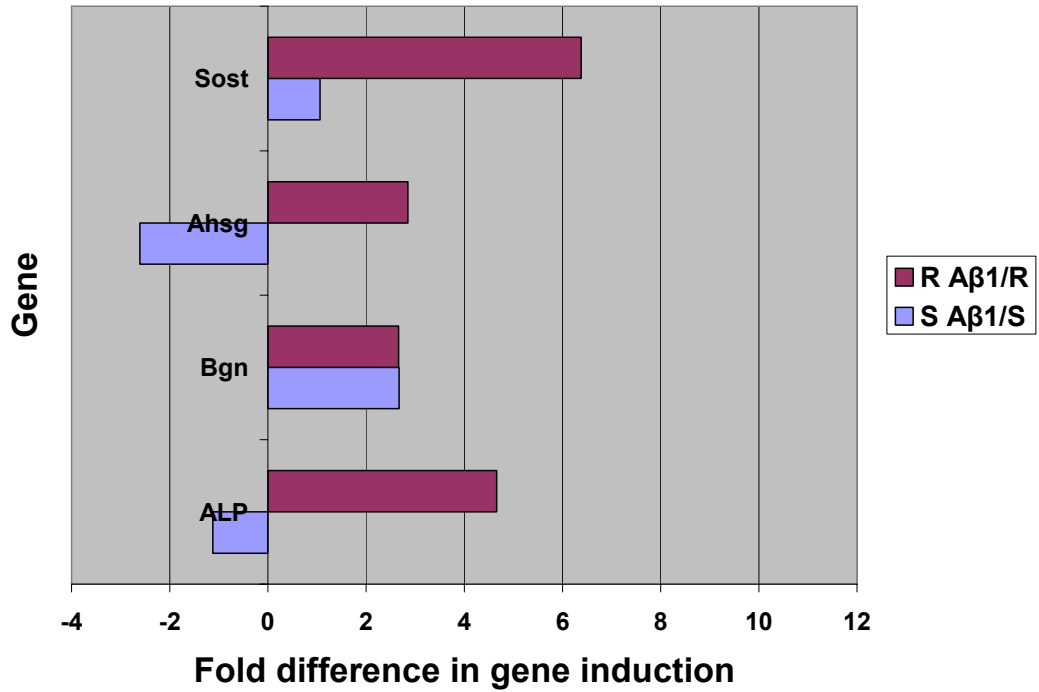


Figure 3.12: Bar graph showing the difference in mRNA expression of bone matrix proteins between anti-β1 and control groups on both smooth and rough surfaces.

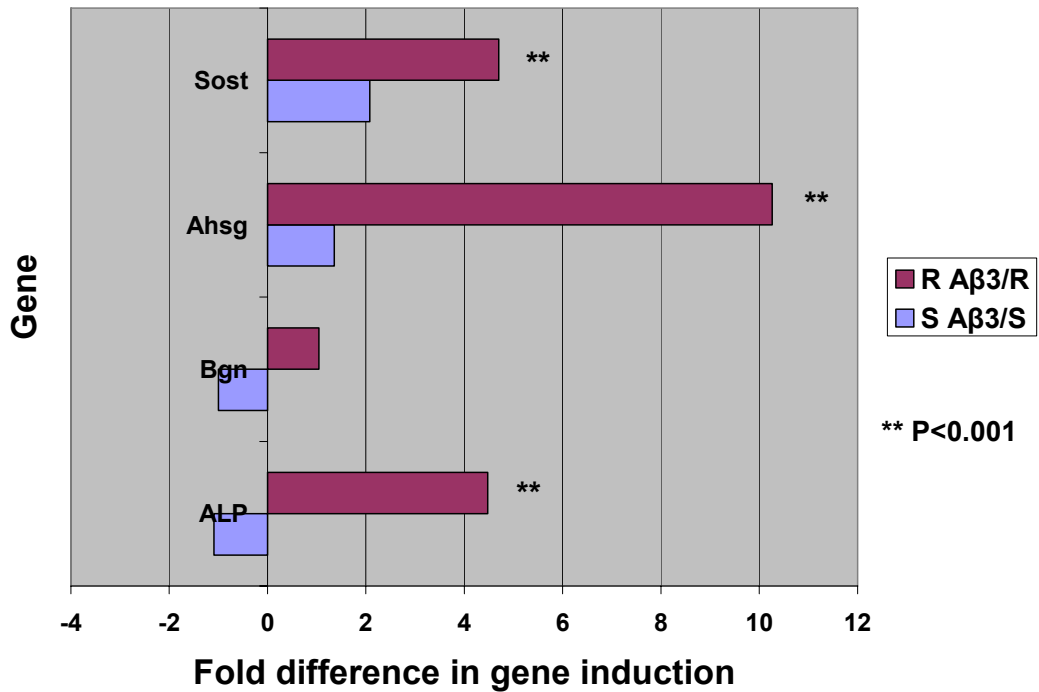


Figure 3.13: Bar graph showing the difference in mRNA expression of bone matrix proteins between anti-β3 and control groups on both smooth and rough surfaces.

Figures 3.12 and 3.13 show similar trends in bone matrix proteins gene expression in both anti-  $\beta$ 1 and anti-  $\beta$ 3 experiments. When MC3T3-E1 were pre-treated with anti-  $\beta$ 1 antibody bone matrix proteins gene expression were slightly down regulated on smooth surface with the exception of Sost and Bgn that were slightly up-regulated . Nevertheless, these differences were not statistically significant. On the contrary, on rough surfaces all bone matrix proteins showed up regulation in gene expression specifically Sost, and ALP that had at least 4 or more fold increase in gene expression (figure 3.12). Likewise, when MC3T3-E1 cells were pre-treated with anti-  $\beta$ 3 antibody similar findings were noted. On smooth surface, bone matrix proteins were not regulated without any significant changes in gene expression except for Sost that had 2 fold increase in gene expression. Yet, on rough surface the difference was more pronounced and bone matrix proteins gene expression show a highly significant up regulation with 4 fold or more with the exception of Bgn which didn't show a marked difference in gene expression (figure 3.13).

### **3.5.3. Growth factors**

This group of genes includes multiple growth factors that are associated with growth and development of many tissues and cells. Vascular endothelial growth factors (Vegfa, Vegfb) are important factors in increasing vascular permeability and promoting angiogenesis and cell migration. The colony stimulating factors (Csf2, Csf3) are cytokines that controls the function and differentiation of macrophages and granulocytes. Platelet derived growth factor alpha (Pdgf $\alpha$ ) is an important mitogenic factor for cells from mesenchymal origin. Epidermal growth factor (Egf) is another mitogenic factor that has a potent effect on the differentiation of variety of cells from ectodermal and mesodermal origin. Finally the fibroblast growth factor family (Fgf) is a family of growth factors that have broad mitogenic and angiogenic

activities which play an important role in tissue repair, cell growth, and morphogenesis.

Figures 3.14 and 3.15 represent bar graph charts of fold difference in mRNA expression of these growth factors between the anti- $\beta$ 1/anti- $\beta$ 3 and the control group on both surfaces.

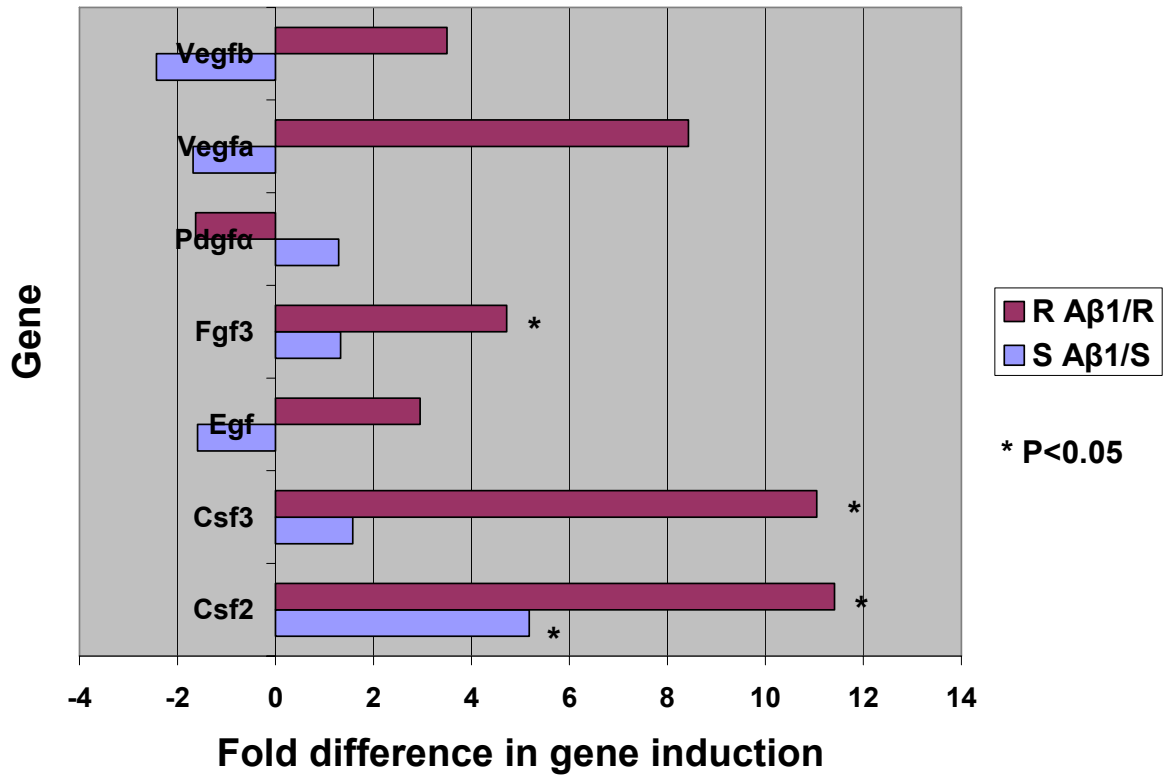


**Figure 3.14: Bar graph showing the difference in mRNA expression of selective growth factors between anti- $\beta$ 1 and control groups on both smooth and rough surfaces.**

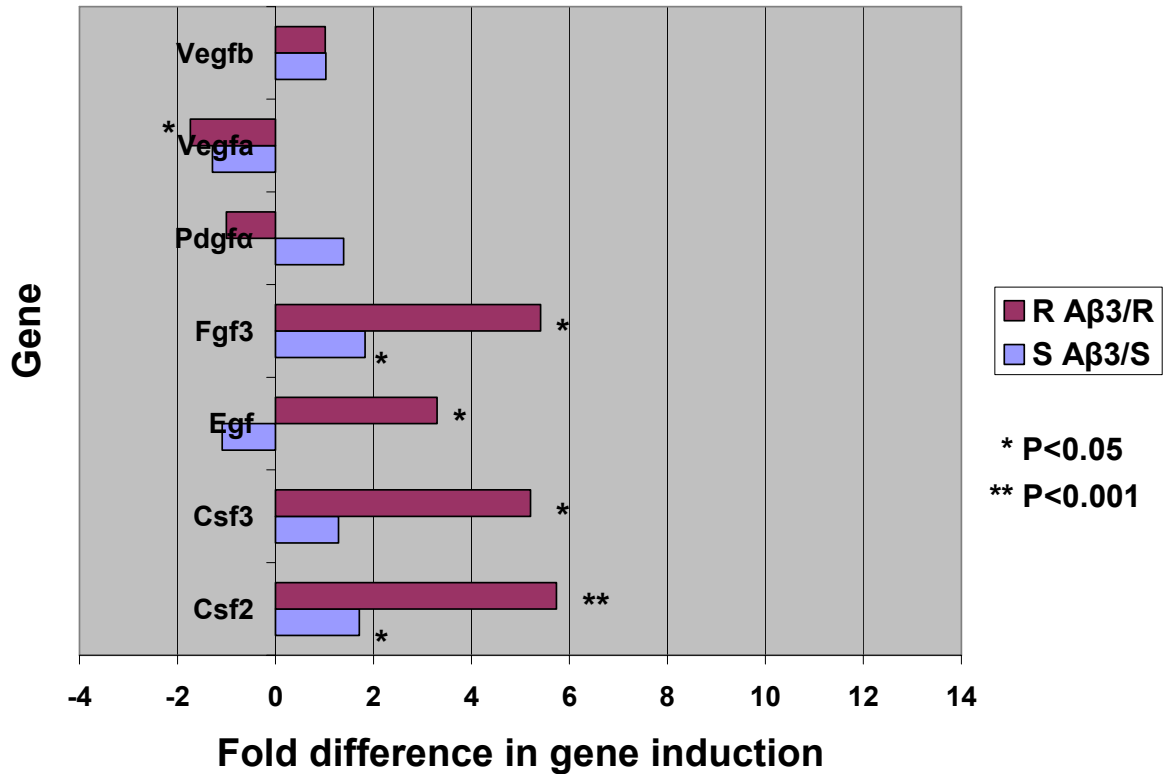


**Figure 3.15: Bar graph showing the difference in mRNA expression of selective growth factors between anti-β3 and control groups on both smooth and rough surfaces.**

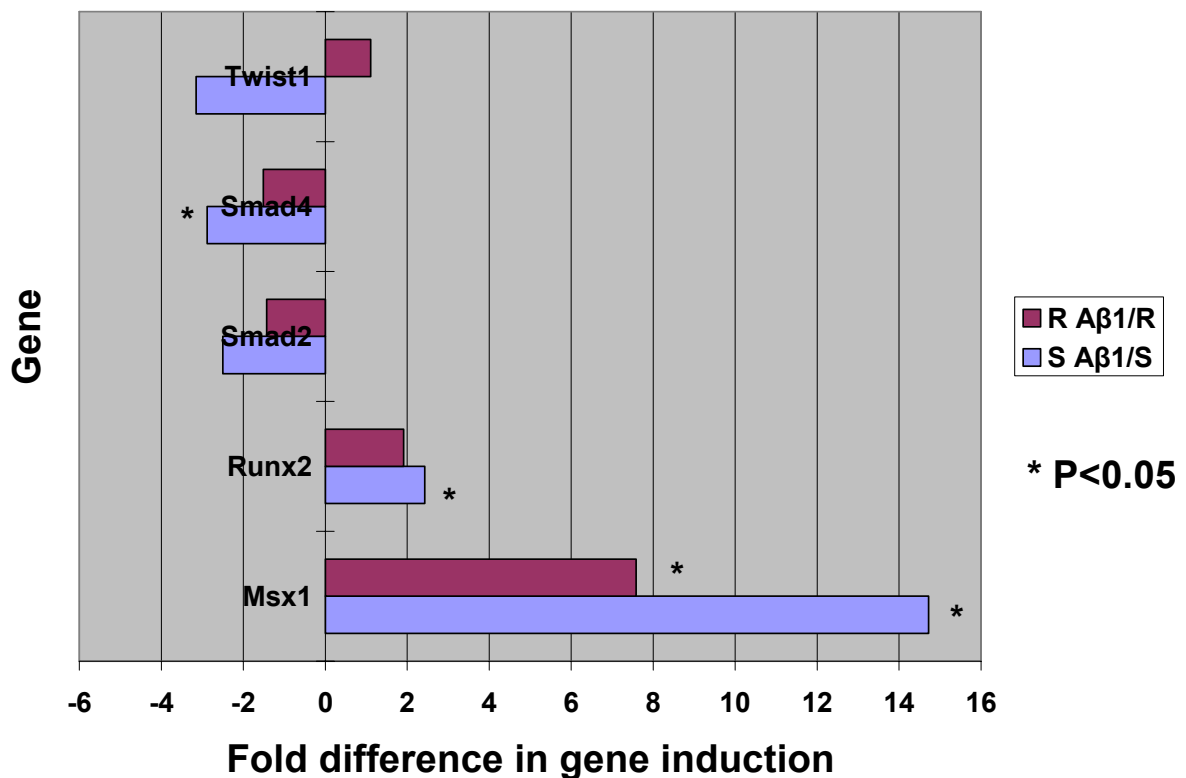
Figure 3.14 shows that when MC3T3-E1 cells were pre-treated with anti-β1 antibody prior to plating on smooth surfaces, vegfa, pdgfa, Fgf3, Egf, Csf3 were not regulated with less than 2 folds increase or decrease in gene expression. Nevertheless, Vegfb was down regulated with over two folds and csf2 on the contrary had over five fold increase in gene expression which was statistically significant. However, on rough surface all growth factors showed up regulation of gene expression when cells were pre-treated with anti- β1 antibody with the exception of pdgfa which was not regulated. The fold increase in gene induction of Csf2, and Csf3 was pronounced with over 10 folds increase which was statistically significant. Moreover, Fgf3 showed over 4 fold increase in gene induction which was statistically significant as well.

Figure 3.15 shows the relative difference in gene induction of the growth factors family when MC3T3-E1 cells were pretreated with anti- $\beta$ 3 antibody before plating on both experimental surfaces. The key difference in comparison to the anti-  $\beta$ 1 group was the relative expression of the Vegf family. Vegfa did not show much change on both surfaces while Vegfa was down regulated for about two folds on rough surfaces although it was up regulated for more that 8 folds in the anti-  $\beta$ 1 experiment. Other growth factors showed similar trends in gene induction to the anti-  $\beta$ 1 experiment, with Fgf3, Egf, Csf2, Csf3 being significantly up regulated on rough surface when cells were pretreated with anti-  $\beta$ 3 antibody before plating.

#### **3.5.4. Transcriptional factors**

This group of genes includes some transcription factors that are important for osteoblastic differentiation, cell lineage determination, and signal transduction. Twist homolog 1 (Twist1) is a transcriptional factor that has been implicated in cell lineage determination and differentiation. Smad proteins are signal transducers and transcription modulators that mediate multiple signaling pathways. Smad 2 mediates Tgf $\beta$  signal and it is associated with Smad4 protein which plays an important role in the translocation of Smad2 into the nucleus, where it binds to target promoters and forms a transcription repressor complex. Runt related transcription factor 2 (Runx2) is essential for osteoblastic differentiation and skeletal morphogenesis. It acts as a scaffold for nucleic acids and regulatory factors involved in skeletal gene expression. Mutations in this gene are associated with cleidocranial dysplasia (130). Finally, Msh homeobox1 (Msx1) plays an important role in limb-pattern formation and craniofacial development particularly odontogenesis besides it role in embryogenesis. Figures 3.16 and 3.17 represent bar graph charts of fold difference in mRNA expression of

these transcriptional factors between the anti- $\beta$ 1/anti- $\beta$ 3 and the control group on both surfaces. Figure 3.16 and figure 3.17 show that most of the transcriptional factors didn't show dramatic changes in relative gene expression in both experimental conditions. Nevertheless, Msx1 levels show statistically significant up regulation of gene expression in the anti-  $\beta$ 1 experiment on both smooth and rough surface. However, the expression was more pronounced on the smooth surface. Moreover, Smad4 gene showed more than two folds down regulation on smooth surface in the anti-  $\beta$ 1 experiment and Runx2 showed more than two folds up regulation on the smooth surface in anti-  $\beta$ 1 experiment. All the other transcriptional factors in both experiments were not regulated with relative gene induction of less than 2 folds.



**Figure 3.16:** Bar graph showing the difference in mRNA expression of selective transcriptional factors between anti- $\beta$ 1 and control groups on both smooth and rough surfaces.

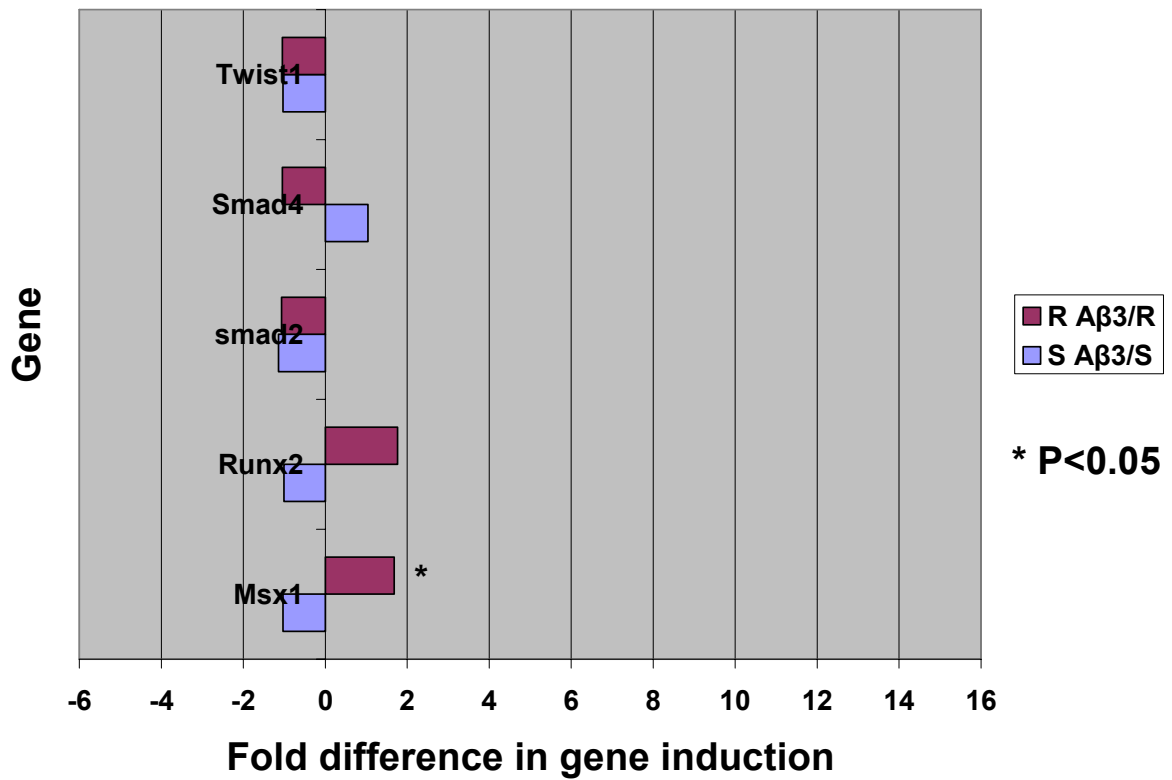


**Figure 3.17:** Bar graph showing the difference in mRNA expression of selective transcriptional factors between anti-β3 and control groups on both smooth and rough surfaces.

## **CHAPTER 4**

### **DISCUSSION**

The success of endosseous implants is determined by the integration of the biomaterial substances with the surrounding tissues and the formation of direct bone to implant contact (6, 8, 18). The peri-implant bone healing is a complex and synchronized process that involves multiple cellular and molecular mechanisms which ends in bone formation and wound healing (104). The initial adhesion and spreading of osteoblast-like cells on the implant surface is crucial in implementing an appropriate cell response to the surface and is related to the skeletal development, homeostasis and maturation of osteoblastic phenotype(57, 79, 82, 118).

There is growing evidence suggesting that implant surface features affect bone formation and related adherent cellular activities (56, 61, 101). Integrin transmembrane receptor has emerged as a central regulator of cell biomaterial interactions. Moreover, the ability of the osteoblast-like cells to sense and react to different surface characteristics has been attributed to the integrin receptors particularly specific heterodimers containing  $\beta 1$  and  $\beta 3$  integrin subunits (63, 71, 108, 122). Nonetheless, the exact role that integrins play in mediating osteoblast adhesion to the implant surface and its effect on subsequent cell spreading, motility, proliferation, differentiation, and matrix mineralization is not completely understood. Thus, this project was conducted to compare and contrast the effects of  $\beta 1$  and

$\beta 3$  integrins on early osteoblast implant interactions and their ability to mediate surface specific changes.

#### **4.1. Experimental model**

A cell culture model utilizing the mouse osteoblast like MC3T3-E1 cells was used in this project. Cell culture models have proved to be a very successful and valuable in investigating the aspects of bone formation and osteoblast implant interactions (30, 31, 39). In addition, MC3T3-E1 cells are a good model for this project taking into consideration their ability of showing different stages of growth and development under cell culture conditions (79). Commercially pure grade IV titanium disks were prepared using two different protocols to produce surfaces with different roughness topographies (turned or machined versus micro-rough surface), to investigate the cell behavior on different surface topographies and the ability of  $\beta 1$  and  $\beta 3$  integrins to mediate surface specific changes. The AFM surface analysis showed that the rough surface has an average surface roughness values that are compatible with minimally rough surfaces, which reflects the spectrum of micro-rough implant surfaces. Moreover, the Ra values for rough surface were considerably greater than the smooth surface. Similar results were documented with Abron and collaborates who used similar protocol for surface preparation (4).

Functional perturbation of  $\beta 1$  and  $\beta 3$  integrin subunits using integrin-specific monoclonal antibodies was used to evaluate the role of these transmembrane receptors in mediating osteoblast implant interactions. This procedure has been utilized to identify specific integrin subunits and integrin-ligand pairs that mediate osteoblast adhesion to biomaterials and their influence on mediating vital cellular mechanisms (82-84, 108, 116). Furthermore, in order to offset any IgG non-specific effects an isotype IgG control was used in the control groups in

the same concentration as the monoclonal antibodies. In a similar experimental protocol, Siebers and collaborates examined the influence of integrin subunit- $\beta 1$  and subunit-  $\beta 3$  on the behavior of primary osteoblast-like cells (rat bone marrow cells), cultured on calcium phosphate coated and non-coated titanium. They treated the cells with specific monoclonal antibodies in a similar fashion to this project. Nevertheless, they didn't use isotype IgG control to match nonspecific IgG effects. Besides, in their experiment they treated the cells with antibody concentration of 50 $\mu$ g/ml which is very likely a saturating concentration that could possibly have had some inhibitory effect on cell adhesion. Nevertheless, their results showed that cell adhesion was only slightly affected by pre-treatment with anti- $\beta 3$  antibody. However, their molecular data showed that pretreatment with either anti- $\beta 1$  or anti-  $\beta 3$  resulted in decrease of ALP expression (108).

Another important factor in blocking the integrin subunits with specific monoclonal antibodies is the timing of the antibody treatment. In our protocol, cells were treated with the antibody one hour before the experiment and no serum was added to the cells. Cells, PBS, antibody or IgG mixture was incubated in cell culture incubator at 37 °C for one hour before the cells were plated on the titanium disks. This protocol, gives the antibody the chance to block integrins on all surfaces of the cells. Furthermore, no serum was added to avoid competitive binding of the antibodies with serum proteins. Other investigators performed the blocking protocol by adding the antibodies to the cell culture medium after the cells were initially attached (64, 116, 122). The problem with such protocol is that integrins are also expressed on non-binding surfaces of the cells, thus the effect of the antibody will be through integrin not involved in cell substrate interaction and this will influence only the cell signaling without affecting the cell adhesion as cells had already adhered. Moreover, the

initial cell adhesion before the antibody blocking changes integrin expression. Other inherent problems with antibody blocking experiments include binding affinities, as well as the variable expression levels between the two integrins. More conclusive studies could be performed to compare the functions of these two integrins. Examples include, using knock-out animals or silencing of the integrin subunits. Such studies not only encompass transcription, but also, can be complemented by experiments verifying the integrin protein expression changes.

Three variables that influence initial cell adhesion and spreading (the effect of anti-body treatment ( $\beta 1$ ,  $\beta 3$ ), surface, and time), were explored using SEM. The numbers of total, spread, and round cells were counted in three random areas on each disk. Two disks were used for each group at each particular time point. Three calibrated and blinded investigators counted the number of cells separately to decrease any risk of bias in the results. SEM images at higher magnification were done for subjective evaluation of cell shape, spread and interaction with the respective surface. A specific criteria regarding the elongation of the cell cytoplasm, the presence of cell processes, as well the diameter of the cell at its longest dimension were utilized as guide lines for cell spreading. This method provides the ability to evaluate initial cell adhesion as well as spreading both quantitatively and qualitatively in the same experimental setting. Nevertheless, there are some inherent disadvantages with this method including:

1. Cells with different stages of maturation might present with different sizes and shapes.
2. The differential cell density on different sites of the disks depending on cell plating uniformity and accuracy.

To overcome these potential problems, semi confluent cells of passage 6 or less were used in the experiments and three random areas were selected for each disk. These random areas were replicated in each disk to account for plating imperfections. Other investigators measured cell number on various substrates when cells were treated with specific monoclonal antibodies, or by silencing integrin  $\beta 1$ . The cell count was performed by detaching the cells using trypsin and counting the cells with a cell counter (108, 122). This method doesn't provide the ability to evaluate cell shape and spread in the same experimental setting. Additionally, other methods for evaluation of cell adhesion and spreading had been reported in the literature such as; using cell adhesion assays, cell spreading assays, confocal microscopic analysis, immunofluorescence assays, and cell staining. Some of these methods were used to evaluate cell adhesion as a function of focal contacts distribution, cytoskeletal proteins organization, and staged cell spreading (71, 96). These methods can be very valuable in future studies to verify cell adhesion and spreading in a more characteristic fashion regarding the organization, distribution of integrin receptors, focal adhesion contacts, and cytoskeletal proteins. Furthermore, developing a cell adhesion assay model where mean cell surface area can be calculated as a guide line for cell spreading is recommended. This method would provide a more objective mechanism for evaluating cell spreading.

In order to further investigate the effect  $\beta 1$  and  $\beta 3$  integrin subunits and surface roughness on osteogenesis, the relative differences in gene expression of osteogenesis specific genes were quantified using the mouse osteogenesis RT<sup>2</sup>Profiler™ PCR Arrays system. This system brings together the quantitative performance of real-time PCR and the multiple gene profiling capability of microarrays. This PCR array profiles the expression of a panel of 84 genes related to osteogenesis. Thus, it provides a unique opportunity to survey these

multifunctional genes and investigate the effect of integrin-ligand blocking on multiple cellular mechanisms as well as the effect of increased surface roughness on cellular adhesion, and osteoblastic differentiation. RT<sup>2</sup>Profiler™ PCR Arrays system was utilized for a variety of molecular biology applications such as; toxicology, oncology, and immunology research and proved to be a reliable and accurate tool of analyzing the expression of a focused panel of genes(95, 129).

#### **4.2. Cell adhesion**

The initial cellular attachment as measured by cell count showed similar number of cells on both surfaces in the control group. Nevertheless, numbers of cells were slightly higher on rough surface in comparison to the smooth surface and they slightly increase from 4 to 24 hours as expected. Although, these differences were not statistically significant, they still support the hypothesis that micro- rough surfaces support early cellular adhesion. Moreover, by careful observation of SEM images with higher magnification we can clearly see that cells on rough surface developed more cellular processes and adopted more irregular elongated shape and spanned across the pits on the surface. On the contrary, cells on smooth surface were more spherical, flattened, had fewer cellular processes, and seem to be differently adhered to the surface (figure 3.9 (A, B)). These observations are consistent with the findings of other investigators who found direct correlation between cell attachment and increased roughness on the micron-scale level (61, 85). Nevertheless, the literature shows that greater cellular adhesion is not necessarily associated with more adherent cell numbers. Keselowsky and collaborates found out that  $\alpha 5\beta 1$  integrin binding and FAK phosphorylation was directly related to surface roughness. Nonetheless, their results also showed that surface roughness

was inversely related to adherent cell numbers (64). Similarly, other investigators documented the presence of fewer numbers of cells on rough surfaces in comparison to smooth titanium surfaces. Kim and collaborators using titanium alloy and MG63 cells, found that after 3 days of cell culture proliferation was inhibited by 17% on sandblasted and acid etched surface in comparison to smooth surface(65). Wang and collaborators, using MG63 cells and grade 2 unalloyed titanium, found after 24 hours in culture, that cell numbers on sandblasted and acid etched surfaces and titanium plasma- sprayed (TPS) surfaces were less than cell numbers on smooth titanium surfaces and plastic surfaces, which had similar number of cells(122). However, in a similar study design Martin and collaborators, found that micro- rough surfaces had higher number of cells in comparison to TPS surfaces and similar number to smooth surfaces(74).

When MC3T3-E1 cells were pre-treated with anti- $\beta$ 1 or anti-  $\beta$ 3 monoclonal antibodies, the numbers of adherent cells on both smooth and rough surfaces were reduced. Nevertheless, the difference was only statistically significant on the rough surface at the 24 hour time point among the experimental and the control groups. An interesting finding was that at the 24- hour time point the difference in cell numbers among the experimental groups was higher on smooth surfaces versus rough surfaces with a significant difference in the anti- $\beta$ 3 group. Moreover, cell numbers in the anti-  $\beta$ 3 group were less than the anti-  $\beta$ 1 group, where cell numbers returned to the control levels on smooth surfaces. These findings may suggest that either the cells plated on smooth surfaces had better ability to overcome the inhibitory effects of the function-blocking antibodies over time, or that function-blocking antibodies had a more pronounced effect on cells plated on rough surfaces. In addition, these findings may also suggest that  $\beta$ 3 integrins are more active later in the process (24 hours) of

cell binding, in comparison to  $\beta 1$  integrin, which might be more active at earlier stages. Our results agree with results from other studies. Wang collaborates using MG63 cells found out that integrin  $\beta 1$  silencing resulted in 40% decrease in cell numbers after 24 hours on 5 different surfaces including plastic, polished smooth titanium surface, sandblasted/ acid etched titanium surface, and TPS surface. Moreover, their results showed the presence of more adherent cells at 24 hours on smooth surfaces versus rough surfaces (122). Keselowsky and collaborates reported that cell number on smooth and TPS surfaces were reduced at 3 days when MG63 cells were pre-treated with anti- $\alpha 5$  antibody to block  $\alpha 5\beta 1$  integrin function(64). On the otherhand, Siebers and collaborates using rat bone marrow cells found out that cell binding was affected differently on calcium phosphate ( CaP) coated surfaces versus bare titanium surfaces, when cells were pretreated with anti-  $\beta 1$  and anti-  $\beta 3$  antibodies. On CaP-coated surfaces, they found that cell numbers decreased around 20-30% after pre-treatment with anti-  $\beta 1$ . This decrease in cell numbers was significant from 30 minutes up to 1 day after plating. On the other hand, cell numbers decreased on CaP- coated surfaces around 40-50% when cells were pre-treated with anti-  $\beta 3$  antibody. This decrease was significant from 30 minutes up to 3 days after plating. Nonetheless, their results on bare titanium surfaces did not show significant decrease in cell numbers in the anti-  $\beta 1$  group. But, pre-treatment with anti-  $\beta 3$  showed 30% decrease in cell number after 30 and 60 minutes of plating on the bare titanium surfaces (108). These results show clearly that cell binding is not only integrin dependent but also, surface dependent. Moreover, their results on CaP-coated surfaces might suggest that  $\beta 3$  integrin is more important later in the process of cell binding (1-3 days) in comparison to  $\beta 1$  integrin.

### 4.3. Cell spreading

One of the aims of this investigation was to evaluate the importance of  $\beta 1$  and  $\beta 3$  integrins as well as, surface topography in mediating cell spreading. Cell spreading on substrate surface, is one of the parameters frequently reported in cell biomaterial interaction research, due to its relation to cell migration, growth, and differentiation (13, 124). Nevertheless, cell spreading evaluation methods are not standardized. Some investigators used a special software to calculate mean cell surface area as an indication of cell spreading (71, 85). On the other hand, Lumbikanonda and Sammons developed a model to classify cell attachment/spreading into four stages depending on morphological criteria (70, 96). In the current investigation cell spreading was evaluated as a dichotomous variable where cells were classified as spread or round depending on specific criteria related to cell morphology and dimensions(3).

Our results showed that pre-treatment with anti- $\beta 1$  and anti-  $\beta 3$  antibodies, reduced the number of spread cells on both surfaces. This reduction was statistically significant on both surfaces at the 2 hour time point and on rough surface at the 24 hour time point. Moreover, the results showed that, at the 24 hour time point there were more spread cells on smooth surfaces in comparison to rough surfaces in both anti-  $\beta 1$  and anti-  $\beta 3$  groups. This observation might indicate that either the cells had better ability to overcome the inhibitory effects of function-blocking antibodies on smooth surface, or that surface roughness modulates antibody function. Although, our results didn't show significant difference between number of spread cells on rough and smooth surfaces in the control groups, yet they are consistent with observations made by other investigators. Several studies reported an inverse relationship between cell spreading as measured by mean surface area, and surface

roughness as well as cellular adhesion (64, 71, 85). Woodruff and collaborators, stated that cell adhesion is not indicative of how supportive a substrate is to cell spreading which doesn't correlate with focal contact formation(126). On the contrary, Sammons and collaborators, reported that rough surfaces of porous microstructure may enhance the rate of cell spreading. Nevertheless, their observations were based on morphological criteria rather than the mean cell surface area (96). These observations agree with our subjective results using highly magnified SEM that showed more morphological variation in cell shape on rough surfaces in comparison to smooth surfaces.

The mean numbers of round cells in the different experimental groups confirm our findings that both integrin  $\beta 1$  and  $\beta 3$  are involved in cell spreading. Furthermore, these results show that the anti-  $\beta 1$  group had significantly higher number of round cells in comparison to the anti-  $\beta 3$  group on rough surface. These results are consistent with observations made by Luthen and collaborators, who reported that  $\beta 1$  integrins are more involved in the formation of fibrillar adhesion than  $\beta 3$  integrins, which is affected by the surface roughness of titanium (71).

#### **4.4. Relative expression of osteogenesis genes**

The effect of  $\beta 1$  and  $\beta 3$  integrin on the relative expression of a panel of osteogenesis related genes, was evaluated using RT<sup>2</sup> Profiler™ PCR Arrays. Several functional group of genes related to osteogenesis were examined using this method (appendix A). Nevertheless, for simplicity purposes only the results of specific functional groups of genes were presented in this thesis and will be discussed accordingly.

#### 4.4.1. Bone morphogenic protein superfamily

Our results show differential relative expression of Bmp superfamily proteins when cells were pre-treated with anti- $\beta$ 1 antibody versus anti- $\beta$ 3 antibody. Pre-treatment of MC3T3-E1 cells with anti- $\beta$ 1 antibody before cell plating, resulted generally in slight down regulation of Bmp superfamily genes on smooth surface. On the contrary when MC3T3-E1 cells were pre-treated with anti- $\beta$ 3 antibody before cell plating, the Bmp superfamily gene expression were slightly up-regulated on smooth surface. Nevertheless, the expressions of Bmp superfamily genes on rough surfaces in both experimental groups were similar. They were pronouncedly up-regulated particularly Bmp2 and Bmp6. This differential expression might suggest that the effect of the surface on Bmp superfamily gene expression is beyond the effect of  $\beta$ 1 and  $\beta$ 3 integrins. Moreover, it might suggest that the cells respond to integrin blocking by compensatory effect through other integrin and non-integrin signals. Another explanation of this finding could be that the antibody it self creates signals that is reflected in up regulation of Bmp superfamily gene expression. Nonetheless, these results still show that both  $\beta$ 1 and  $\beta$ 3 integrins might be involved in mediating surface specific changes, which is evident in the differential expression of Bmp superfamily proteins on rough versus smooth surfaces.

These results agree with observations from previous studies which show that Tgf $\beta$  superfamily and Bmps particularly Bmp2 are correlated and work closely in mediating cell adhesion. Nissinen and collaborates showed that human recombinant Bmp2, regulate cell matrix interactions by modifying the expression of integrin  $\alpha$ 3 $\beta$ 1 that mediates cell adhesion to laminin-5(86). On the other hand, Shah and collaborates reported that pre-treatment of primary human osteoblastic cells with Bmp-2 for 12 hours before plating on titanium alloy, resulted in increased expression of  $\alpha$ 5 and  $\beta$ 1 integrin subunits, fibronectin, and focal

adhesion kinase expressions. In addition, they showed that this increased expression was associated with stimulated cell adhesion and proliferation of osteoblastic cells, which was reflected on long term mineralization (105). Similarly, Lai and Su documented that Bmp2 up-regulates the expression of  $\alpha\nu\beta$  integrins which in turn, play a critical role in Bmp2 osteoblastic function (66).

#### **4.4.2. Bone matrix proteins**

For this group of genes the results were similar when the cells were pre-treated with anti- $\beta$ 1 or anti- $\beta$ 3 antibodies particularly for ALP and Sost genes. On smooth surface there was slight down-regulation of ALP and slight up-regulation of Sost. However, there was a significant up-regulation of both genes expression on rough surface. An interesting observation was the up-regulation of Sost gene expression, when cells were pre-treated with either anti- $\beta$ 1 or anti- $\beta$ 3 antibodies. This gene is a Bmp antagonist, and it is associated with reduction of the expression of proteins associated with osteoblastic differentiation, proliferation, and matrix mineralization (125). These results may indicate that  $\beta$ 1 and  $\beta$ 3 integrins are involved in mediating osteoblastic differentiation in a surface dependent manner.

The ALP relative gene expression was surface dependent with slight down- regulation on smooth surfaces and significant up-regulation on rough surfaces. These observations agree and disagree with observations made by other investigators in similar study designs. Wang and collaborates reported that blocking  $\beta$ 1 integrin function with specific antibody, resulted in reduction of ALP expression in Mg63 cells. Moreover they observed that this decrease in gene expression was dependent on time of antibody treatment, dose of antibody, and

substrate on which the cells were plated (122). Similarly, Siebers and collaborates reported that pre-treatment of rat bone marrow cells with either anti-  $\beta 1$  or anti-  $\beta 3$  antibodies before plating, resulted in surface dependent decrease in ALP gene expression(108). Although, it is difficult to compare these contradictory results, due to differences in cell types, substrates, and experimental conditions, yet, they all agree that blocking  $\beta 1$  and  $\beta 3$  integrin function resulted in substrate dependent change in ALP gene expression.

#### **4.4.3. Growth factors**

The relative gene expressions of several growth factors were evaluated. The results were similar in both the anti-  $\beta 1$  and anti-  $\beta 3$  groups with the exception of the vascular endothelial growth factors. These results further confirm the observation that blocking  $\beta 1$  and  $\beta 3$  function with specific monoclonal antibodies resulted in surface dependent change in growth factors gene expression. These results are similar to observations made with other functional group of genes and the same explanations may be applied. Nevertheless, the differential expression of the Vegf genes, particularly Vegfa among the anti-  $\beta 1$  and anti-  $\beta 3$  experimental groups was of interest. In the anti-  $\beta 1$  group, Vegfa was slightly down regulated on smooth surface and up regulated on rough surface. Nevertheless, in the anti-  $\beta 3$  group it was down regulated on both surfaces with more down regulation on the rough surface. It is well documented that integrins  $\beta 1$ ,  $\beta 3$ , and  $\beta 5$  are expressed in endothelial cells and are involved in the process of angiogenesis through their effect on Vegf (12, 72). Nevertheless, integrin  $\beta 3$  particularly  $\alpha v\beta 3$  has the most potent effect on angiogenesis. Mahabeleshwar and collaborates showed that inhibition of  $\beta 1$ ,  $\beta 3$ , and  $\beta 5$  integrin expression in endothelial cells resulted in down regulation of endothelial cell adhesion and migration. Moreover, they

reported that inhibition of  $\beta 3$  integrin resulted in the most potent reduction in capillary growth stimulated by Vegf. Our results agree with these observations reported in relation to endothelial cells. Further investigation of the correlated effect of integrins particularly  $\beta 3$  and Vegf in osteoblasts is of interest, since angiogenesis is a crucial process in peri-implant bone healing.

#### **4.4.4. Transcriptional factors**

The results in this group of genes surprisingly did not show much difference in the relative expression among the different experimental groups on both surfaces, with the exception of Msx1 gene in the anti-  $\beta 1$  group. Nevertheless, an interesting finding was that the Smad proteins were down regulated in the anti-  $\beta 1$  group for more than two folds on smooth surface. This correlates with the fact that these proteins work as signaling molecules, and are part of the downstream signaling mechanism of Tgf $\beta$  and Bmps(45). This might further indicate the involvement of  $\beta 1$  integrin in modulating osteoblastic differentiation. The other interesting observation was the significant up-regulation of Msx1 gene expression when cells were pre-treated with anti- $\beta 1$  antibodies particularly on smooth surface. There is no known connection between this gene and integrins. This observation might suggest that the effect of the surface is complex and goes beyond the integrin transmembrane receptor. Moreover, there is a possibility that the blocking antibody, might un-mask key non-integrin signals. Nevertheless, it is interesting to further explore the possibility of having a correlation between  $\beta 1$  integrin function and Msx1 gene expression in osteoblasts.

#### 4.5. Summary of findings and future recommendations

The findings of this in-vitro study can be summarized as following:

1. Both  $\beta 1$  and  $\beta 3$  integrins are involved in mediating osteoblast implant surface interactions. They have a direct effect on initial cell adhesion and spreading in a surface and time dependant manner.
2. Integrin  $\beta 1$  and  $\beta 3$  seem to be active at different stages of cell adhesion, with  $\beta 1$  being more active early in the process in comparison to  $\beta 3$  which has more potent effect later in the process.
3. Function blocking of both integrin subunits resulted in variable and surface dependant differences in gene expression of multiple genes related to osteogenesis.  
Nevertheless, function blocking antibodies seem to initiate signals that translate in up-regulation of multiple genes.
4. The molecular results might suggest that, cell biomaterial interaction is a complex process, which can be further mediated by other integrin and non-integrin molecules.
5. It seems like osteoblast like cells have the ability to compensate to a great extent for the blocking strategy applied in this investigation.
6. More conclusive comparative studies are recommended. These studies should be performed at different time points, and involve innovative techniques to knock out the integrin subunits such as; knock- out animals or RNA silencing (siRNA). Such designs can result in more precise evaluation of the effect of integrin receptors on cell biomaterial interaction and provide better insight on the long term effect of these interactions.

## **CHAPTER 5**

### **CONCLUSIONS**

Within the limitations of this in-vitro investigation we can make the following conclusions:

1. Blocking integrin- $\beta$ 1 and integrin-  $\beta$ 3 subunits with antibodies has an inhibitory effect on osteoblast like cell binding, and spreading to commercially pure titanium surfaces in vitro.
2. Beta one and beta three integrin mediation of initial cell adhesion and spreading is both time and surface dependent.
3. Both beta one and beta three integrins are involved in mediating surface specific changes, that modulate osteogenesis related gene expression. However, other integrin and non-integrin molecules might be involved in this process.
4. Function-blocking antibodies (that block cell binding) may activate signaling which result in a substrate dependent temporal expression of osteogenesis related genes.

## APPENDIX A

### Functional Gene Grouping

#### 1. Skeletal Development:

Bone Mineralization: Ahsg, Ambn, Enam, Fgfr2, Smad1, Tuft1.

Cartilage Condensation: Bmpr1b, Col11a1, Col2a1, Sox9.

Ossification: Ahsg, Ambn, Dmp1, Enam, Phex, Sost, Tfip11, Tuft1.

Osteoclast Differentiation: Tnf.

Other Skeletal Development Genes: Bmp2, Bmp4, Bmp5, Bmp6, Runx2, Tgfb1, Vdr.

#### 2. Bone Mineral Metabolism:

Calcium Ion Binding and Homeostasis: Anxa5, Bmp1, Cdh11, Comp, Egf, Mmp2, Mmp8, Vdr.

Phosphate Transport: Bmp5, Col10a1, Col11a1, Col12a1, Col14a1, Col1a1, Col1a2, Col2a1, Col3a1, Col4a1, Col4a2, Col5a1, Col6a1, Col6a2, Col7a1.

#### 3. Cell Growth and Differentiation:

Regulation of Cell Cycle: Fgf1, Fgf2, Fgf3, Itgb1, Pdgfa, Tgfb1, Tgfb2, Tgfb3, Vegfa, Vegfb.

Cell Proliferation: Fgf1, Fgf2, Fgf3, Fgfr2, Pdgfa, Smad3, Tgfb1, Tgfb2, Tgfb3, Tgfb2, Vegfa, Vegfb.

Growth Factors and Receptors: Bmp1, Bmp2, Bmp3, Bmp4, Bmp5, Bmp6, Bmpr1a, Bmpr1b, Csf2, Csf3, Egf, Fgf1, Fgf2, Fgf3, Fgfr1, Flt1, Gdf10, Igf1, Igf1r, Pdgfa, Scarb1, Tgfb1, Tgfb2, Tgfb3, Tgfb1, Tgfb2, Tgfb3, Vdr, Vegfa, Vegfb.

Cell Differentiation: Bmp2, Bmp4, Bmp6, Csf2, Fgf2, Igf1, Runx2, Smad2, Sox9, Tfip11, Tgfbr2, Twist1.

#### **4. Extracellular Matrix (ECM) Proteins:**

Basement Membrane Constituents: Col4a1, Col4a2.

Collagens: Col11a1, Col1a1, Col1a2, Col2a1, Col3a1, Col4a1, Col4a2, Col5a1, Col6a1, Col6a2.

ECM Protease Inhibitors: Ahsg, Col7a1, Serpinh1.

ECM Proteases: Bmp1, Ctsk, Mmp10, Mmp2, Mmp8, Mmp9, Phex.

Structural Constituents of Tooth Enamel: Ambn, Enam, Tuft1.

Other ECM Molecules: Akp2, Bgn, Bmp2, Bmp4, Bmp5, Bmp6, Bmpr1a, Col10a1, Col12a1, Col14a1, Comp, Csf2, Csf3, Dmp1, Egf, Fgf2, Fgf3, Fgfr1, Fgfr2, Fgfr3, Flt1, Fn1, Gdf10, Igf1, Igf1r, Itga2, Itga2b, Itgam, Itgb1, Pdgfa, Sost, Tfip11, Tgfb1, Tgfb2, Tgfb3, Tgfbr1, Tgfbr3, Vcam1, Vegfa, Vegfb.

#### **5. Cell Adhesion Molecules:**

Cell-cell Adhesion: Cdh11, Icam1, Vcam1.

Cell-matrix Adhesion: Itga2, Itga2b, Itga3, Itgam, Itgav, Itgb1.

Other Cell Adhesion Molecules: Cd36, Col11a1, Col12a1, Col14a1, Col5a1, Col6a1, Col6a2, Comp, Fn1, Scarb1.

#### **6. Transcription Factors and Regulators:**

Msx1, Nfkb1, Runx2, Smad1, Smad2, Smad3, Smad4, Sox9, Twist1, Vdr.

## REFERENCES

1. **The glossary of prosthodontic terms.** *J Prosthet Dent* 94: 10-92, 2005.
2. **The Japanese market for dental implants: executive summary.** *Implant Dent* 11: 103-106, 2002.
3. **Akimoto H and Cooper LF.** *Un published thesis: Biological Modification of Titanium Surfaces Using Bifunctional Peptides.* 2007.
4. **Abron A, Hopfensperger M, Thompson J and Cooper LF.** Evaluation of a predictive model for implant surface topography effects on early osseointegration in the rat tibia model. *J Prosthet Dent* 85: 40-46, 2001.
5. **Albrektsson T.** Hydroxyapatite-coated implants: a case against their use. *J Oral Maxillofac Surg* 56: 1312-1326, 1998.
6. **Albrektsson T, Branemark PI, Hansson HA and Lindstrom J.** Osseointegrated titanium implants. Requirements for ensuring a long-lasting, direct bone-to-implant anchorage in man. *Acta Orthop Scand* 52: 155-170, 1981.
7. **Albrektsson T and Johansson C.** Osteoinduction, osteoconduction and osseointegration. *Eur Spine J* 10 Suppl 2: S96-101, 2001.
8. **Albrektsson T and Sennerby L.** Direct bone anchorage of oral implants: clinical and experimental considerations of the concept of osseointegration. *Int J Prosthodont* 3: 30-41, 1990.
9. **Albrektsson T and Wennerberg A.** The impact of oral implants - past and future, 1966-2042. *J Can Dent Assoc* 71: 327, 2005.
10. **Albrektsson T and Wennerberg A.** Oral implant surfaces: Part 1--review focusing on topographic and chemical properties of different surfaces and in vivo responses to them. *Int J Prosthodont* 17: 536-543, 2004.
11. **Albrektsson TO, Johansson CB and Sennerby L.** Biological aspects of implant dentistry: osseointegration. *Periodontol* 2000 4: 58-73, 1994.
12. **Alghisi GC and Ruegg C.** Vascular integrins in tumor angiogenesis: mediators and therapeutic targets. *Endothelium* 13: 113-135, 2006.
13. **Anselme K.** Osteoblast adhesion on biomaterials. *Biomaterials* 21: 667-681, 2000.
14. **Barrere F, van der Valk CM, Meijer G, Dalmeijer RA, de Groot K and Layrolle P.** Osseointegration of biomimetic apatite coating applied onto dense and porous metal implants in femurs of goats. *J Biomed Mater Res B Appl Biomater* 67: 655-665, 2003.

15. **Bennett JH, Carter DH, Alavi AL, Beresford JN and Walsh S.** Patterns of integrin expression in a human mandibular explant model of osteoblast differentiation. *Arch Oral Biol* 46: 229-238, 2001.
16. **Biesbrock AR and Edgerton M.** Evaluation of the clinical predictability of hydroxyapatite-coated endosseous dental implants: a review of the literature. *Int J Oral Maxillofac Implants* 10: 712-720, 1995.
17. **Boyan BD, Lohmann CH, Dean DD, Sylvia VL, Cochran DL and Schwartz Z.** Mechanisms involved in osteoblast response to implant surface morphology. *Annu. Rev. Mater. Res.* 31: 357-371, 2001.
18. **Branemark PI.** Osseointegration and its experimental background. *J Prosthet Dent* 50: 399-410, 1983.
19. **Branemark PI, Hansson BO, Adell R, Breine U, Lindstrom J, Hallen O and Ohman A.** Osseointegrated implants in the treatment of the edentulous jaw. Experience from a 10-year period. *Scand J Plast Reconstr Surg Suppl* 16: 1-132, 1977.
20. **Brunette DM.** In vitro models of biological responses to implants. *Adv Dent Res* 13: 35-37, 1999.
21. **Buser D, Brogini N, Wieland M, Schenk RK, Denzer AJ, Cochran DL, Hoffmann B, Lussi A and Steinemann SG.** Enhanced bone apposition to a chemically modified SLA titanium surface. *J Dent Res* 83: 529-533, 2004.
22. **Buser D, Schenk RK, Steinemann S, Fiorellini JP, Fox CH and Stich H.** Influence of surface characteristics on bone integration of titanium implants. A histomorphometric study in miniature pigs. *J Biomed Mater Res* 25: 889-902, 1991.
23. **Caetano-Lopes J, Canhao H and Fonseca JE.** Osteoblasts and bone formation. *Acta Reumatol Port* 32: 103-110, 2007.
24. **Carvalho RS, Kostenuik PJ, Salih E, Bumann A and Gerstenfeld LC.** Selective adhesion of osteoblastic cells to different integrin ligands induces osteopontin gene expression. *Matrix Biol* 22: 241-249, 2003.
25. **Caulier H, van der Waerden JP, Wolke JG, Kalk W, Naert I and Jansen JA.** A histological and histomorphometrical evaluation of the application of screw-designed calciumphosphate (Ca-P)-coated implants in the cancellous maxillary bone of the goat. *J Biomed Mater Res* 35: 19-30, 1997.
26. **Chomczynski P and Sacchi N.** Single-step method of RNA isolation by acid guanidinium thiocyanate-phenol-chloroform extraction. *Anal Biochem* 162: 156-159, 1987.
27. **Cochran DL.** A comparison of endosseous dental implant surfaces. *J Periodontol* 70: 1523-1539, 1999.

28. **Cooper LF.** A role for surface topography in creating and maintaining bone at titanium endosseous implants. *J Prosthet Dent* 84: 522-534, 2000.
29. **Cooper LF.** Biologic determinants of bone formation for osseointegration: clues for future clinical improvements. *J Prosthet Dent* 80: 439-449, 1998.
30. **Cooper LF, Masuda T, Whitson SW, Yliheikkila P and Felton DA.** Formation of mineralizing osteoblast cultures on machined, titanium oxide grit-blasted, and plasma-sprayed titanium surfaces. *Int J Oral Maxillofac Implants* 14: 37-47, 1999.
31. **Cooper LF, Masuda T, Yliheikkila PK and Felton DA.** Generalizations regarding the process and phenomenon of osseointegration. Part II. In vitro studies. *Int J Oral Maxillofac Implants* 13: 163-174, 1998.
32. **Cooper LF, Yliheikkila PK, Felton DA and Whitson SW.** Spatiotemporal assessment of fetal bovine osteoblast culture differentiation indicates a role for BSP in promoting differentiation. *J Bone Miner Res* 13: 620-632, 1998.
33. **Cooper LF, Zhou Y, Takebe J, Guo J, Abron A, Holmen A and Ellingsen JE.** Fluoride modification effects on osteoblast behavior and bone formation at TiO<sub>2</sub> grit-blasted c.p. titanium endosseous implants. *Biomaterials* 27: 926-936, 2006.
34. **Cowles EA, Brailey LL and Gronowicz GA.** Integrin-mediated signaling regulates AP-1 transcription factors and proliferation in osteoblasts. *J Biomed Mater Res* 52: 725-737, 2000.
35. **Damsky CH.** Extracellular matrix-integrin interactions in osteoblast function and tissue remodeling. *Bone* 25: 95-96, 1999.
36. **Damsky CH and Ilic D.** Integrin signaling: it's where the action is. *Curr Opin Cell Biol* 14: 594-602, 2002.
37. **Davies JE.** Understanding peri-implant endosseous healing. *J Dent Educ* 67: 932-949, 2003.
38. **Davies JE.** Mechanisms of endosseous integration. *Int J Prosthodont* 11: 391-401, 1998.
39. **Davies JE.** In vitro modeling of the bone/implant interface. *Anat Rec* 245: 426-445, 1996.
40. **De Arcangelis A and Georges-Labouesse E.** Integrin and ECM functions: roles in vertebrate development. *Trends Genet* 16: 389-395, 2000.
41. **Docheva D, Popov C, Mutschler W and Schieker M.** Human mesenchymal stem cells in contact with their environment: surface characteristics and the integrin system. *J Cell Mol Med* 11: 21-38, 2007.

42. **Ducy P, Schinke T and Karsenty G.** The osteoblast: a sophisticated fibroblast under central surveillance. *Science* 289: 1501-1504, 2000.
43. **Ellingsen JE, Johansson CB, Wennerberg A and Holmen A.** Improved retention and bone-to-implant contact with fluoride-modified titanium implants. *Int J Oral Maxillofac Implants* 19: 659-666, 2004.
44. **Esposito M, Murray-Curtis L, Grusovin MG, Coulthard P and Worthington HV.** Interventions for replacing missing teeth: different types of dental implants. *Cochrane Database Syst Rev* (4): CD003815, 2007.
45. **Funaba M and Mathews LS.** Identification and characterization of constitutively active Smad2 mutants: evaluation of formation of Smad complex and subcellular distribution. *Mol Endocrinol* 14: 1583-1591, 2000.
46. **Garcia AJ and Keselowsky BG.** Biomimetic surfaces for control of cell adhesion to facilitate bone formation. *Crit Rev Eukaryot Gene Expr* 12: 151-162, 2002.
47. **Garcia AJ and Reyes CD.** Bio-adhesive surfaces to promote osteoblast differentiation and bone formation. *J Dent Res* 84: 407-413, 2005.
48. **Globus RK, Doty SB, Lull JC, Holmuhamedov E, Humphries MJ and Damsky CH.** Fibronectin is a survival factor for differentiated osteoblasts. *J Cell Sci* 111 ( Pt 10): 1385-1393, 1998.
49. **Goene RJ, Testori T and Trisi P.** Influence of a nanometer-scale surface enhancement on de novo bone formation on titanium implants: a histomorphometric study in human maxillae. *Int J Periodontics Restorative Dent* 27: 211-219, 2007.
50. **Gronowicz G and McCarthy MB.** Response of human osteoblasts to implant materials: integrin-mediated adhesion. *J Orthop Res* 14: 878-887, 1996.
51. **Gronthos S, Stewart K, Graves SE, Hay S and Simmons PJ.** Integrin expression and function on human osteoblast-like cells. *J Bone Miner Res* 12: 1189-1197, 1997.
52. **Hahn J and Vassos DM.** Long-term efficacy of hydroxyapatite-coated cylindrical implants. *Implant Dent* 6: 111-115, 1997.
53. **Hynes RO.** Integrins: bidirectional, allosteric signaling machines. *Cell* 110: 673-687, 2002.
54. **Hynes RO.** Integrins: versatility, modulation, and signaling in cell adhesion. *Cell* 69: 11-25, 1992.
55. **Hynes RO.** Integrins: a family of cell surface receptors. *Cell* 48: 549-554, 1987.

56. **Jayaraman M, Meyer U, Buhner M, Joos U and Wiesmann HP.** Influence of titanium surfaces on attachment of osteoblast-like cells in vitro. *Biomaterials* 25: 625-631, 2004.
57. **Jikko A, Harris SE, Chen D, Mendrick DL and Damsky CH.** Collagen integrin receptors regulate early osteoblast differentiation induced by BMP-2. *J Bone Miner Res* 14: 1075-1083, 1999.
58. **Johansson CB, Han CH, Wennerberg A and Albrektsson T.** A quantitative comparison of machined commercially pure titanium and titanium-aluminum-vanadium implants in rabbit bone. *Int J Oral Maxillofac Implants* 13: 315-321, 1998.
59. **Joos U, Wiesmann HP, Szuwart T and Meyer U.** Mineralization at the interface of implants. *Int J Oral Maxillofac Surg* 35: 783-790, 2006.
60. **Kasemo B.** Biocompatibility of titanium implants: surface science aspects. *J Prosthet Dent* 49: 832-837, 1983.
61. **Keller JC, Schneider GB, Stanford CM and Kellogg B.** Effects of implant microtopography on osteoblast cell attachment. *Implant Dent* 12: 175-181, 2003.
62. **Keller JC, Stanford CM, Wightman JP, Draughn RA and Zaharias R.** Characterizations of titanium implant surfaces. III. *J Biomed Mater Res* 28: 939-946, 1994.
63. **Keselowsky BG, Collard DM and Garcia AJ.** Surface chemistry modulates focal adhesion composition and signaling through changes in integrin binding. *Biomaterials* 25: 5947-5954, 2004.
64. **Keselowsky BG, Wang L, Schwartz Z, Garcia AJ and Boyan BD.** Integrin alpha(5) controls osteoblastic proliferation and differentiation responses to titanium substrates presenting different roughness characteristics in a roughness independent manner. *J Biomed Mater Res A* 80: 700-710, 2007.
65. **Kim HJ, Kim SH, Kim MS, Lee EJ, Oh HG, Oh WM, Park SW, Kim WJ, Lee GJ, Choi NG, Koh JT, Dinh DB, Hardin RR, Johnson K, Sylvia VL, Schmitz JP and Dean DD.** Varying Ti-6Al-4V surface roughness induces different early morphologic and molecular responses in MG63 osteoblast-like cells. *J Biomed Mater Res A* 74: 366-373, 2005.
66. **Lai CF and Cheng SL.** Alphavbeta integrins play an essential role in BMP-2 induction of osteoblast differentiation. *J Bone Miner Res* 20: 330-340, 2005.
67. **Lange R, Luthen F, Beck U, Rychly J, Baumann A and Nebe B.** Cell-extracellular matrix interaction and physico-chemical characteristics of titanium surfaces depend on the roughness of the material. *Biomol Eng* 19: 255-261, 2002.
68. **Le Guehennec L, Soueidan A, Layrolle P and Amouriq Y.** Surface treatments of titanium dental implants for rapid osseointegration. *Dent Mater* 23: 844-854, 2007.

69. **Livak KJ and Schmittgen TD.** Analysis of relative gene expression data using real-time quantitative PCR and the 2(-Delta Delta C(T)) Method. *Methods* 25: 402-408, 2001.
70. **Lumbikanonda N and Sammons R.** Bone cell attachment to dental implants of different surface characteristics. *Int J Oral Maxillofac Implants* 16: 627-636, 2001.
71. **Luthen F, Lange R, Becker P, Rychly J, Beck U and Nebe JG.** The influence of surface roughness of titanium on beta1- and beta3-integrin adhesion and the organization of fibronectin in human osteoblastic cells. *Biomaterials* 26: 2423-2440, 2005.
72. **Mahabeleshwar GH, Chen J, Feng W, Somanath PR, Razorenova OV and Byzova TV.** Integrin affinity modulation in angiogenesis. *Cell Cycle* 7: 335-347, 2008.
73. **Marie PJ.** Transcription factors controlling osteoblastogenesis. *Arch Biochem Biophys* 2008.
74. **Martin JY, Schwartz Z, Hummert TW, Schraub DM, Simpson J, Lankford J, Jr, Dean DD, Cochran DL and Boyan BD.** Effect of titanium surface roughness on proliferation, differentiation, and protein synthesis of human osteoblast-like cells (MG63). *J Biomed Mater Res* 29: 389-401, 1995.
75. **Masaki C, Schneider GB, Zaharias R, Seabold D and Stanford C.** Effects of implant surface microtopography on osteoblast gene expression. *Clin Oral Implants Res* 16: 650-656, 2005.
76. **Massaro C, Rotolo P, De Riccardis F, Milella E, Napoli A, Wieland M, Textor M, Spencer ND and Brunette DM.** Comparative investigation of the surface properties of commercial titanium dental implants. Part I: chemical composition. *J Mater Sci Mater Med* 13: 535-548, 2002.
77. **Masuda T, Yliheikkila PK, Felton DA and Cooper LF.** Generalizations regarding the process and phenomenon of osseointegration. Part I. In vivo studies. *Int J Oral Maxillofac Implants* 13: 17-29, 1998.
78. **Matsuzaka K, Walboomers XF, Yoshinari M, Inoue T and Jansen JA.** The attachment and growth behavior of osteoblast-like cells on microtextured surfaces. *Biomaterials* 24: 2711-2719, 2003.
79. **Meyer U, Buchter A, Wiesmann HP, Joos U and Jones DB.** Basic reactions of osteoblasts on structured material surfaces. *Eur Cell Mater* 9: 39-49, 2005.
80. **Millennium Research Group.** European markets for dental implants and final abutments 2004: executive summary. *Implant Dent* 13: 193-196, 2004.
81. **Millennium Research Group.** U.S. markets for dental implants 2001: executive summary. *Implant Dent* 10: 234-237, 2001.

82. **Mizuno M, Fujisawa R and Kuboki Y.** Type I collagen-induced osteoblastic differentiation of bone-marrow cells mediated by collagen- $\alpha$ 2 $\beta$ 1 integrin interaction. *J Cell Physiol* 184: 207-213, 2000.
83. **Moursi AM, Damsky CH, Lull J, Zimmerman D, Doty SB, Aota S and Globus RK.** Fibronectin regulates calvarial osteoblast differentiation. *J Cell Sci* 109 ( Pt 6): 1369-1380, 1996.
84. **Moursi AM, Globus RK and Damsky CH.** Interactions between integrin receptors and fibronectin are required for calvarial osteoblast differentiation in vitro. *J Cell Sci* 110 ( Pt 18): 2187-2196, 1997.
85. **Nebe JG, Luethen F, Lange R and Beck U.** Interface interactions of osteoblasts with structured titanium and the correlation between physicochemical characteristics and cell biological parameters. *Macromol Biosci* 7: 567-578, 2007.
86. **Nissinen L, Pirila L and Heino J.** Bone morphogenetic protein-2 is a regulator of cell adhesion. *Exp Cell Res* 230: 377-385, 1997.
87. **Oreffo RO and Triffitt JT.** In vitro and in vivo methods to determine the interactions of osteogenic cells with biomaterials. *J Mater Sci Mater Med* 10: 607-611, 1999.
88. **Orsini G, Piattelli M, Scarano A, Petrone G, Kenealy J, Piattelli A and Caputi S.** Randomized, controlled histologic and histomorphometric evaluation of implants with nanometer-scale calcium phosphate added to the dual acid-etched surface in the human posterior maxilla. *J Periodontol* 78: 209-218, 2007.
89. **Pearce AI, Richards RG, Milz S, Schneider E and Pearce SG.** Animal models for implant biomaterial research in bone: a review. *Eur Cell Mater* 13: 1-10, 2007.
90. **Puleo DA and Nanci A.** Understanding and controlling the bone-implant interface. *Biomaterials* 20: 2311-2321, 1999.
91. **Puleo DA and Thomas MV.** Implant surfaces. *Dent Clin North Am* 50: 323-38, v, 2006.
92. **Raz P, Lohmann CH, Turner J, Wang L, Poythress N, Blanchard C, Boyan BD and Schwartz Z.**  $1\alpha,25(\text{OH})_2\text{D}_3$  regulation of integrin expression is substrate dependent. *J Biomed Mater Res A* 71: 217-225, 2004.
93. **Remes A and Williams DF.** Immune response in biocompatibility. *Biomaterials* 13: 731-743, 1992.
94. **Roberts WE.** Bone tissue interface. *Int J Oral Implantol* 5: 71-74, 1988.
95. **Ross JS, Linette GP, Stec J, Clark E, Ayers M, Leschly N, Symmans WF, Hortobagyi GN and Pusztai L.** Breast cancer biomarkers and molecular medicine: part II. *Expert Rev Mol Diagn* 4: 169-188, 2004.

96. **Sammons RL, Lumbikanonda N, Gross M and Cantzler P.** Comparison of osteoblast spreading on microstructured dental implant surfaces and cell behaviour in an explant model of osseointegration. A scanning electron microscopic study. *Clin Oral Implants Res* 16: 657-666, 2005.
97. **Schneider G and Burrige K.** Formation of focal adhesions by osteoblasts adhering to different substrata. *Exp Cell Res* 214: 264-269, 1994.
98. **Schneider GB, Whitson SW and Cooper LF.** Restricted and coordinated expression of beta3-integrin and bone sialoprotein during cultured osteoblast differentiation. *Bone* 24: 321-327, 1999.
99. **Schneider GB, Zaharias R and Stanford C.** Osteoblast integrin adhesion and signaling regulate mineralization. *J Dent Res* 80: 1540-1544, 2001.
100. **Schwartz Z, Lohmann CH, Oefinger J, Bonewald LF, Dean DD and Boyan BD.** Implant surface characteristics modulate differentiation behavior of cells in the osteoblastic lineage. *Adv Dent Res* 13: 38-48, 1999.
101. **Schwartz Z, Nasazky E and Boyan BD.** Surface microtopography regulates osteointegration: the role of implant surface microtopography in osteointegration. *Alpha Omegan* 98: 9-19, 2005.
102. **Scotchford CA, Ball M, Winkelmann M, Voros J, Csucs C, Brunette DM, Danuser G and Textor M.** Chemically patterned, metal-oxide-based surfaces produced by photolithographic techniques for studying protein- and cell-interactions. II: Protein adsorption and early cell interactions. *Biomaterials* 24: 1147-1158, 2003.
103. **Sela J, Gross UM, Kohavi D, Shani J, Dean DD, Boyan BD and Schwartz Z.** Primary mineralization at the surfaces of implants. *Crit Rev Oral Biol Med* 11: 423-436, 2000.
104. **Sennerby L, Thomsen P and Ericson LE.** Early tissue response to titanium implants inserted in rabbit cortical bone, Part I: Light microscopic observations. *J.Mater.Sci.Mater.Med.* 4: 240-250, 1993.
105. **Shah AK, Lazatin J, Sinha RK, Lennox T, Hickok NJ and Tuan RS.** Mechanism of BMP-2 stimulated adhesion of osteoblastic cells to titanium alloy. *Biol Cell* 91: 131-142, 1999.
106. **Shalabi MM, Gortemaker A, Van't Hof MA, Jansen JA and Creugers NH.** Implant surface roughness and bone healing: a systematic review. *J Dent Res* 85: 496-500, 2006.
107. **Siebers MC, ter Brugge PJ, Walboomers XF and Jansen JA.** Integrins as linker proteins between osteoblasts and bone replacing materials. A critical review. *Biomaterials* 26: 137-146, 2005.

108. **Siebers MC, Walboomers XF, van den Dolder J, Leeuwenburgh SC, Wolke JG and Jansen JA.** The behavior of osteoblast-like cells on various substrates with functional blocking of integrin-beta1 and integrin-beta3. *J Mater Sci Mater Med* 2007.
109. **Sinha RK and Tuan RS.** Regulation of human osteoblast integrin expression by orthopedic implant materials. *Bone* 18: 451-457, 1996.
110. **Stanford CM and Brand RA.** Toward an understanding of implant occlusion and strain adaptive bone modeling and remodeling. *J Prosthet Dent* 81: 553-561, 1999.
111. **Stanford CM and Keller JC.** The concept of osseointegration and bone matrix expression. *Crit Rev Oral Biol Med* 2: 83-101, 1991.
112. **Steflik DE, Corpe RS, Lake FT, Young TR, Sisk AL, Parr GR, Hanes PJ and Berkery DJ.** Ultrastructural analyses of the attachment (bonding) zone between bone and implanted biomaterials. *J Biomed Mater Res* 39: 611-620, 1998.
113. **Steflik DE, Sisk AL, Parr GA, Lake FT and Hanes PJ.** Experimental studies of the implant-tissue interface. *J Oral Implantol* 19: 90-4; discussion 136-7, 1993.
114. **Stein GS, Lian JB, Gerstenfeld LG, Shalhoub V, Aronow M, Owen T and Markose E.** The onset and progression of osteoblast differentiation is functionally related to cellular proliferation. *Connect Tissue Res* 20: 3-13, 1989.
115. **Steinemann SG.** Titanium--the material of choice? *Periodontol* 2000 17: 7-21, 1998.
116. **Stephansson SN, Byers BA and Garcia AJ.** Enhanced expression of the osteoblastic phenotype on substrates that modulate fibronectin conformation and integrin receptor binding. *Biomaterials* 23: 2527-2534, 2002.
117. **Sudo H, Kodama HA, Amagai Y, Yamamoto S and Kasai S.** In vitro differentiation and calcification in a new clonal osteogenic cell line derived from newborn mouse calvaria. *J Cell Biol* 96: 191-198, 1983.
118. **Suzawa M, Tamura Y, Fukumoto S, Miyazono K, Fujita T, Kato S and Takeuchi Y.** Stimulation of Smad1 transcriptional activity by Ras-extracellular signal-regulated kinase pathway: a possible mechanism for collagen-dependent osteoblastic differentiation. *J Bone Miner Res* 17: 240-248, 2002.
119. **Sykaras N, Iacopino AM, Marker VA, Triplett RG and Woody RD.** Implant materials, designs, and surface topographies: their effect on osseointegration. A literature review. *Int J Oral Maxillofac Implants* 15: 675-690, 2000.
120. **Takeuchi Y, Suzawa M, Kikuchi T, Nishida E, Fujita T and Matsumoto T.** Differentiation and transforming growth factor-beta receptor down-regulation by collagen-alpha2beta1 integrin interaction is mediated by focal adhesion kinase and its downstream signals in murine osteoblastic cells. *J Biol Chem* 272: 29309-29316, 1997.

121. **Tamura Y, Takeuchi Y, Suzawa M, Fukumoto S, Kato M, Miyazono K and Fujita T.** Focal adhesion kinase activity is required for bone morphogenetic protein--Smad1 signaling and osteoblastic differentiation in murine MC3T3-E1 cells. *J Bone Miner Res* 16: 1772-1779, 2001.
122. **Wang L, Zhao G, Olivares-Navarrete R, Bell BF, Wieland M, Cochran DL, Schwartz Z and Boyan BD.** Integrin beta1 silencing in osteoblasts alters substrate-dependent responses to 1,25-dihydroxy vitamin D3. *Biomaterials* 27: 3716-3725, 2006.
123. **Wennerberg A and Albrektsson T.** Suggested guidelines for the topographic evaluation of implant surfaces. *Int J Oral Maxillofac Implants* 15: 331-344, 2000.
124. **Wilson CJ, Clegg RE, Leavesley DI and Percy MJ.** Mediation of biomaterial-cell interactions by adsorbed proteins: a review. *Tissue Eng* 11: 1-18, 2005.
125. **Winkler DG, Sutherland MK, Geoghegan JC, Yu C, Hayes T, Skonier JE, Shpektor D, Jonas M, Kovacevich BR, Staehling-Hampton K, Appleby M, Brunkow ME and Latham JA.** Osteocyte control of bone formation via sclerostin, a novel BMP antagonist. *EMBO J* 22: 6267-6276, 2003.
126. **Woodruff MA, Jones P, Farrar D, Grant DM and Scotchford CA.** Human osteoblast cell spreading and vinculin expression upon biomaterial surfaces. *J Mol Histol* 38: 491-499, 2007.
127. **Xiao G, Jiang D, Thomas P, Benson MD, Guan K, Karsenty G and Franceschi RT.** MAPK pathways activate and phosphorylate the osteoblast-specific transcription factor, Cbfa1. *J Biol Chem* 275: 4453-4459, 2000.
128. **Xiao G, Wang D, Benson MD, Karsenty G and Franceschi RT.** Role of the alpha2-integrin in osteoblast-specific gene expression and activation of the Osf2 transcription factor. *J Biol Chem* 273: 32988-32994, 1998.
129. **Yamamoto T, Kikkawa R, Yamada H and Horii I.** Investigation of proteomic biomarkers in in vivo hepatotoxicity study of rat liver: toxicity differentiation in hepatotoxicants. *J Toxicol Sci* 31: 49-60, 2006.
130. **Yoshida T, Kanegane H, Osato M, Yanagida M, Miyawaki T, Ito Y and Shigesada K.** Functional analysis of RUNX2 mutations in Japanese patients with cleidocranial dysplasia demonstrates novel genotype-phenotype correlations. *Am J Hum Genet* 71: 724-738, 2002.
131. **Zinger O, Zhao G, Schwartz Z, Simpson J, Wieland M, Landolt D and Boyan B.** Differential regulation of osteoblasts by substrate microstructural features. *Biomaterials* 26: 1837-1847, 2005.